



**SYNTHESIS OF BILATERALLY THIADIAZOLE
SUBSTITUTED *vic*-DIOXIME LIGANDS AND
INVESTIGATION OF THEIR POLYMERIC METAL
COMPLEXES**

**2024
MASTER THESIS
CHEMISTRY**

Omar Khalid Abdulkareem AL-QARAGHULI

**Thesis Advisor
Prof. Dr. Şaban UYSAL**

**SYNTHESIS OF BILATERALLY THIADIAZOLE SUBSTITUTED *vic*-
DIOXIME LIGANDS AND INVESTIGATION OF THEIR POLYMERIC
METAL COMPLEXES**

Omar Khalid Abdulkareem AL-QARAGHULI

**Thesis Advisor
Prof. Dr. Şaban UYSAL**

**T.C.
Karabuk University
Institute of Graduate Programs
Department of Chemistry**

**Prepared as
Master Thesis**

**KARABUK
March 2024**

I certify that, in my opinion the thesis submitted by Omar Khalid Abdulkareem AL-QARAGHULI titled “SYNTHESIS OF BILATERALLY THIADIAZOLE SUBSTITUTED *vic*-DIOXIME LIGANDS AND INVESTIGATION OF THEIR POLYMERIC METAL COMPLEXES” is fully adequate in scope and quality as a thesis for the degree of Master of Science.

Prof. Dr. Şaban UYSAL

Thesis Advisor, Department of Chemistry

This thesis is accepted by the examining committee with a unanimous vote in the Department of Chemistry as a Master of Science Thesis. 15/03/2024

Examining Committee Members (Institutions)

Signature

Chairman : Prof. Dr. Ziya Erdem KOÇ (SU)

Member : Prof. Dr. Şaban UYSAL (KBU)

Member : Prof. Dr. Hakan TAHTACI (KBU)

The degree of Master of Science by the thesis submitted is approved by the Administrative Board of the Institute of Graduate Programs, Karabuk University.

Assoc. Prof. Dr. Zeynep ÖZCAN

Director of the Institute of Graduate Programs



“I declare that all the information within this thesis has been gathered and presented in accordance with academic regulations and ethical principles and I have according to the requirements of these regulations and principles cited all those which do not originate in this work as well.”

Omar Khalid Abdulkareem AL-QARAGHULI

ABSTRACT

M. Sc. Thesis

SYNTHESIS OF BILATERALLY THIADIAZOLE SUBSTITUTED vic-DIOXIME LIGANDS AND INVESTIGATION OF THEIR POLYMERIC METAL COMPLEXES

Omar Khalid Abdulkareem AL-QARAGHULI

**Karabuk University
Institute of Graduate Programs
Department of Chemistry**

Thesis Advisor:

Prof. Dr. Şaban UYSAL

March 2024, 72 pages

In this study, three novels substituted 1,3,4-thiadiazole-derived vic-dioxime ligands and their corresponding polymeric transition metal (Co^{2+} and Ni^{2+}) complexes were synthesized and their structural characterizations were performed. For this purpose, 4,4'-bis(chloroacetyldiphenyl) ether (OKS1) was obtained from the reaction of diphenyl ether with chloroacetyl chloride at a 1:2 molar ratio with the help of the Friedel-Crafts reaction. Our first starting oxime compound “2,2'-(oxybis(4,1-phenylene))bis(N-hydroxy-2-oxoacetimidoyl chloride (OKS2)” was obtained from the reaction of this compound with butyl nitrite at a 1:2 molar ratio under the catalysis of HCl gaz. Then, our final starting vic-dioxime compound “2,2'-(oxybis(4,1-phenylene))bis(N-hydroxy-2-(hydroxyimino) acetimidoyl chloride) (OKS3)” was obtained from the reaction of OKS2 and hydroxylamine hydrochloride in ethanol media at 40 °C. Then, our original target vic-dioxime compounds were synthesized

from the reaction of substituted 2-amino-1,3,4-thiadiazole compounds synthesized according to the literature with OXS3. Structural characterizations of all synthesized organic compounds were made using elemental analysis, FTIR, ^1H and ^{13}C NMR and mass spectroscopy methods. Target complexes were obtained from the reaction of all ligands with $\text{MCl}_2 \cdot n\text{H}_2\text{O}$ (M: Co^{2+} and Ni^{2+}) salts, and their structures were elucidated using FTIR, magnetic susceptibility, thermogravimetric analysis, elemental analysis, and ICP-AES spectroscopy methods.

Keywords : *vic*-Dioxime; 1,3,4-Thiadiazole; Transition Metal Complex; Diphenyl Ether

Science Code : 20103

ÖZET

Yüksek Lisans Tezi

İKİ TARAFLI TİYADİAZOL SUBTİTUE *vic*-DİOKSİM LİGANDLARININ SENTEZİ VE POLİMERİK METAL KOMPLEKSLERİNİN İNCELENMESİ

Omar Khalid Abdulkareem AL-QARAGHULI

Karabük Üniversitesi
Lisansüstü Eğitim Enstitüsü
Kimya Anabilim Dalı

Tez Danışmanı:
Prof. Dr. Şaban UYSAL
Mart 2024, 72 sayfa

Bu çalışmada üç yeni sübtitüe 1,3,4-tiadiazol türevli *vic*-dioksim ligandı ve bunların polimerik geçiş metali (Co^{2+} ve Ni^{2+}) kompleksleri sentezlendi ve yapısal karakterizasyonları yapıldı. Bu amaçla Friedel-Crafts reaksiyonu yardımıyla difenil eterin kloroasetil klorür ile 1:2 mol oranındaki reaksiyonundan “4,4'-bis(kloroasetildifenil) eter (OKS1)” elde edildi. İlk başlangıç oksim bileşiğimiz olan “2,2'-(oksibis(4,1-fenilen))bis(N-hidroksi-2-oksoasetimidoil klorür (OKS2)”, bu bileşiğin bütül nitrit ile 1:2 mol oranındaki reaksiyonuyla HCl gaz katalizörlüğünde elde edildi. Daha sonra son başlangıç *vic*-dioksim bileşiğimiz “2,2'-(oksibis(4,1-fenilen))bis(N-hidroksi-2-(hidroksiimino)aseti-midoil klorür) (OKS3)”, OKS2 ve hidroksilamin hidroklorürün etanol ortamındaki reaksiyonundan 40 °C da elde edildi. Daha sonra literatüre uygun olarak sentezlenen sübtitüe 2-amino-1,3,4-tiyadiazol bileşiklerinin OKS3 ile reaksiyonundan orijinal hedef *vic*-dioksim bileşiklerimiz sentezlendi. Sentezlenen tüm organik bileşiklerin yapısal karakterizasyonları elementel analiz, FTIR, 1H ve ^{13}C

NMR ve kütle spektroskopisi yöntemleri kullanılarak yapıldı. Tüm ligandların $MCl_2 \cdot nH_2O$ (M: Co^{2+} ve Ni^{2+}) tuzları ile reaksiyonundan hedef kompleksler elde edilmiş ve yapıları FTIR, manyetik duyarlılık, termogravimetrik analiz, element analizi ve ICP-AES spektroskopi yöntemleri kullanılarak aydınlatılmıştır.

Anahtar Kelimeler : *vic*-Dioksim; 1,3,4-Tiyadiazol; Geçiş Metali Kompleksi; Difenil

Eter

Bilim Kodu : 20103



ACKNOWLEDGEMENT

To the one who led the hearts and minds of humanity to a haven, the first teacher of humanity, Muhammad (Peace be upon him)

To my supporters throughout my academic life, my dear father, Prof. Dr. Khalid, and to my dear mother, Dr. Itimad, to the one who was my shadow when I was tired, my devoted wife, the seed of my heart and hope for tomorrow, my beloved children, Mesk and Reem, to my dear sister and my brother's soul. To my teacher, inspiration, and light of my way throughout my master's studies, Prof. Dr. Şaban UYSAL, your sharp intelligence, precise guidance, and enthusiasm sparked my initial curiosity and nurtured it into a burning flame. Your constant encouragement and unwavering belief in my potential pushed me during moments of doubt and ignited a fire within me to strive for excellence. Prof. Dr. Ahmet COSKUN and Prof. Dr. Hakan TAHTACI thank you. And the fragrance of friendship, and the rose of love to the brothers with whom I am connected in the field of work, Mojahid Salah and Ahmed Hamdi. To every hand and heart that has walked with me on the path of achievement. And to all of them I dedicate this study, hoping from God that it will be a window to knowledge and the energy of knowledge.

Their assistance has enabled me to focus on my research and achieve my goals, and the KBU-BAP unit for supporting this study with BAP project no: KBÜBAP-23-YL-075. With deepest gratitude and enduring affection.

CONTENTS

	<u>Page</u>
APPROVAL	ii
ABSTRACT	iv
ÖZET	vi
ACKNOWLEDGEMENT	viii
LIST OF FIGURES.....	xii
SYMBOLS AND ABBREVIATIONS INDEX	xv
PART 1	1
INTRODUCTION	1
1.1. OXIME.....	1
1.1.1. Synthesis of Oximes	2
1.1.2. Properties of Oximes	4
1.1.2.1. Stability And Formation.....	4
1.1.2.2. Analytical Applications.....	4
1.1.2.3. Tautomerism.....	4
1.1.2.4. Reactivity	5
1.1.2.5. Biological Activity	5
1.1.3. Oxime Derivatives	5
1.1.3.1. Hydroxamic Acids Are Compounds That Function as Inhibitors of Histone Deacetylase.....	5
1.1.3.2. Derivatives of Oxime Ether as Antimicrobial Agents.....	5
1.1.3.3. Metal Ion Oxime-Based Chelators.....	6
1.1.3.4. Oxime Derivatives as Photo Stabilizers.....	6
1.1.3.5. Oxime Derivatives as Reactivators of Cholinesterase	6
1.1.3.6. Prodrugs For Drug Delivery That Contain Oxime	6
1.2. DIOXIME.....	6
1.2.1. Synthesis of Dioxime.....	7

	<u>Page</u>
1.2.1.1. Synthesis from Ketone	7
1.2.1.2. Synthesis from Diamine.....	8
1.2.3. Dioxime Applications	10
1.3. THIADIAZOLE	10
1.3.1. Thiadiazole Derivatives	11
1.3.2. Uv Properties Of Thiadiazole Compounds.....	14
1.3.3. Thiadiazole Synthesis	14
1.3.4. Thiadiazole Applications	15
1.4. TRANSITION METAL COMPLEXES	16
1.4.1. Applications of The Transition Metal Complexes	16
 PART 2	 19
LITERATURE REVIEW	19
 PART 3	 35
EXPERIMENTAL SECTION.....	35
3.1. DEVICES USED IN THIS STUDY	35
3.2. CHEMICALS USED IN THIS STUDY	35
3.3. THE FORMULA OF SYNTHESIZED LIGANDS IN THIS STUDY	36
3.4. SYNTHESIS METHODS OF ALL COMPOUNDS	37
3.4.1. Synthesis Methods of Starting Compound	37
3.4.1.1. Synthesis of 1,1'-(Oxybis(4,1-phenylene))bis(2-chloroethane) [OKS1].....	37
3.4.1.2. Synthesis Methods of (2,2'-(Oxybis(4,1-phenylene))bis(N-hydroxy- 2-oxoacetimidoyl Chloride) (OKS2)	38
3.4.1.3. Synthesis Methods of 4,4'-Oxybis (phenylglyoxylohydroxymoyl Chloride) (OKS3)	39
3.4.1.4. General Synthesis Procedure of Ligands (OKL1-OKL3).....	40
3.4.1.5. General Synthesis Procedure of Co(II) and Ni(II) Complexes of The Ligands (OKL1-OKL).....	42

	<u>Page</u>
PART 4	44
RESULTS AND DISCUSSION.....	44
4.1. CHEMICAL EVALUATION OF ALL COMPOUNDS.....	44
4.2. PHYSICAL EVALUATION OF ALL COMPOUNDS	50
4.2.1. Evaluation of Magnetic Susceptibility Data.....	50
4.2.2. Evaluation of Electrospray Ionization Mass Spectrometry (ESI-MS) Data of All Ligands	51
4.2.3. Evaluation of Thermogravimetric Analysis Results.....	53
 PART5	56
CONCLUSION AND RECOMMENDATIONS	56
 REFERENCES.....	58
 APPENDIX A.	68
FTIR SPECTRA OF COMPLEXES.....	68
 RESUME	72

LIST OF FIGURES

	<u>Page</u>
Figure 1.1. Oxime structure.	1
Figure 1.2. The prevalent structural categories of oxime-metal complexes.	2
Figure 1.3. General synthesis of oximes from ketones and aldehydes.	2
Figure 1.4. General synthesis of oximes by oxidation of primary amines.	3
Figure 1.5. The most common methods for oxime synthesis.	3
Figure 1.6. Synthesis of di-oximes by isomerization.	3
Figure 1.7. Synthesis of oximes from aldehydes or ketones.	4
Figure 1.8. Synthesis of 1,3-di-oximes from ketone.	7
Figure 1.9. Synthesis di-oximes from mono ketone.	7
Figure 1.10. Synthesis cyclic di-oximes 2,1-(hydroxyamino) ethyl) cyclohexan-1-one oxime).	8
Figure 1.11. Synthesis of 2,6-dioximinocyclohexanone.	8
Figure 1.12. Synthesis of 4,9-diaza-3,3,10,10-tetramethyldodecan-2,11-dione di- oxime.	8
Figure 1.13. Synthesis of 4,9-Diaza-3,10-dimethyldodecan 2,11-dione di-oxime.	9
Figure 1.14. General reaction of diamine with 4-Methylpent-3-en-2-one.	9
Figure 1.15. The compound 1,3,4-thiadiazole and derivatives (1-8).	11
Figure 1.16. Some compound 1,3,4-thiadiazole derivatives.	12
Figure 1.17. Steele and Suzuki reactions.	12
Figure 1.18. Subjecting the thiadiazole derivative (1) to a range of isoselenocyanates.	14
Figure 1.19. Synthesis of novel 1,3,4-thiadiazole derivatives.	15
Figure 1.20. Deferent medical drug that contains thiadiazole.	16
Figure 2.1. Synthesis of ligands MICO and MIPMO and their complexes {Zn(MICO) ₂ Cl ₂ } (I) and {Zn(MIPMO) ₂ Cl ₂ } (II).	19
Figure 2.2. Synthesis of complexes I and II.	20
Figure 2.3. Synthesized nano-phenolic oxime complexes and transition metal complexes.	20

	<u>Page</u>
Figure 2.4. Synthesis of mixed ligand complexes [ML(phe)(H ₂ O) ₂] (M:Co(II), Ni(II), Cu(II)).....	21
Figure 2.5. Synthesis of trinuclear Schiff Base-Oxime.....	22
Figure 2.6. Synthesis of keto oxime and glyoxime with some transition metals.....	22
Figure 2.7. <i>Syn</i> - and <i>anti</i> - isomer forms of the synthesized ligands.	23
Figure 2.8. Structures of platinum complexes.	24
Figure 2.9. Expected ligand complexes with predetermined structures [L ¹ H ₂], [L ² H ₂], [L ³ H ₂].....	25
Figure 2.10. The configuration of the suggested <i>vic</i> -dioxime metal compounds M(LH) ₂].....	26
Figure 2.11. Synthesis of <i>vic</i> -dioximes 1 and 2	27
Figure 2.12. Synthesis of the ligand (LH ₂).....	28
Figure 2.13. Synthesis protocol for Fe(III) complexes of [H ₂ LSalen/Saloph].....	29
Figure 2.14. Synthesis of some complexes with <i>vic</i> -dioxime.....	30
Figure 2.15. Synthesis of complexes of thiadiazole derivatives.	31
Figure 2.16. Synthesis of disubstituted Imidazole and 1,3,4-thiadiazole derivatives.....	31
Figure 2.17. Synthesis of hetero-ligand complexes with some transition metal.....	32
Figure 2.18 Synthesis of a complex ligand with some transition metal.....	32
Figure 2.19. Preparation of 1,3,4-thiadiazole derivatives and their complexes with some transition metal.	33
Figure 2.20. 1,3,4-Thiadiazole synthesis.....	34
Figure 3.1. The formula of synthesized ligands in this study.....	36
Figure 3.2. The formula of synthesized complexes in this study.	37
Figure 3.3. Synthesis reaction of “OKS1” coded compound.....	37
Figure 3.4. Synthesis reaction of “OKS2” coded compound.....	36
Figure 3.5. Synthesis reaction of “OKS3” coded compound.....	39
Figure 3.6. General synthesis reaction of target ligands (OKL1-OKL3).....	40
Figure 3.7. General synthesis reaction of Co(II) and Ni(II) complexes of target ligands.	42
Figure 4.1. Synthetic route of all ligands and complexes.....	45
Figure 4.2. ¹ H NMR Spectrum of OKL1.	46
Figure 4.3. ¹³ C NMR Spectrum of OKL1.	46

	<u>Page</u>
Figure 4.4. ^1H NMR Spectrum of OKL2.	47
Figure 4.5. ^{13}C NMR Spectrum of OKL2.	47
Figure 4.6. ^1H NMR Spectrum of OKL3.	48
Figure 4.7. ^{13}C NMR Spectrum of OKL3.	48
Figure 4.8. FTIR Spectrum of OKL1.	49
Figure 4.9. FTIR Spectrum of OKL2.	49
Figure 4.10. FTIR Spectrum of OKL3.	50
Figure 4.11: ESI-MS spectrum of OKL1.	52
Figure 4.12: ESI-MS spectrum of OKL2.	52
Figure 4.13: ESI-MS spectrum of OKL3.	53
Figure 4.14. TGA-DTA curve of $[\text{Ni}(\text{OKL1})]_n$ complex.	54
Figure 4.15. TGA-DTA curve of $[\text{Ni}(\text{OKL3})]_n$ complex.	55
Figure A.1. FTIR Spectrum of $[\text{Co}(\text{OKL1})]_n$ complex.	69
Figure A.2. FTIR Spectrum of $[\text{Ni}(\text{OKL1})]_n$ complex.	69
Figure A.3. FTIR Spectrum of $[\text{Co}(\text{OKL2})]_n$ complex.	70
Figure A.4. FTIR Spectrum of $[\text{Ni}(\text{OKL2})]_n$ complex.	70
Figure A.5. FTIR Spectrum of $[\text{Co}(\text{OKL3})]_n$ complex.	71
Figure A.6. FTIR Spectrum of $[\text{Ni}(\text{OKL3})]_n$ complex.	71

SYMBOLS AND ABBREVIATIONS INDEX

°C	: Degree Centigrede
g	: Gram
δ	: Chemical shift
^{13}C -NMR	: Carbon-13 nuclear magnetic resonance
^1H -NMR	: Proton nuclear magnetic resonance
FTIR	: Fourier-transform infrared spectroscopy on microscopy
TGA	: Thermo gravimetric analysis
s	: Singlet
d	: Doublet
m	: Multiples
ppm	: Part per million
mmol	: Mili mol
Dec.	: Decomposition
D.P.	: Decomposition Point
B.M.	: Bohr Magnetton
MA	: Molecular Weight
ICP-AES	: Inductively Coupled Plasma Atomic Emission Spectroscopy

PART 1

INTRODUCTION

1.1. OXIME

An oxime is a chemical molecule classified as an imine, Figure 1.1 show an oxime is defined by the general formula ($R^1R^2C=NOH$), where R^1 is a chemical substituent and R^2 might be hydrogen, forming an aldoxime, or another organic group., leading to the formation of a ketoxime. the term "oxime" originates from the 19th century and is a combination of the words "oxygen" and "imine" [1].

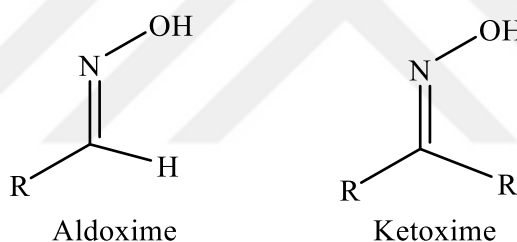


Figure 1.1. Oxime structure.

Oximes are frequently employed in the domain of organic chemistry for various applications. There are a range of molecules that incorporate the divalent $C=NOH$ group, primarily synthesized through the reaction of hydroxylamine with aldehydes and ketones. Analytical reagents are used to facilitate the process of identifying and quantifying aldehydes and ketones. Furthermore, oximes play a crucial role as essential constituents in the synthesis of several chemical compounds [2–5]. Oximes are of great significance in diverse domains, including analytical chemistry, biochemistry, antifungal and antibacterial studies, as well as their notable efficacy in extracting heavy metals. Additionally, their application as dyes has garnered considerable attention [6–8]. Oximes are widely used in research, pharmaceutical synthesis, and large-scale organic chemical manufacture, such as in the fabrication of caprolactam [9] Significant attention is given to analyzing the structural characteristics

b. Oxidative synthesis of primary amines

Primary amines can be oxidized to oximes using hydrogen peroxide and a sodium tungstate catalyst [20].

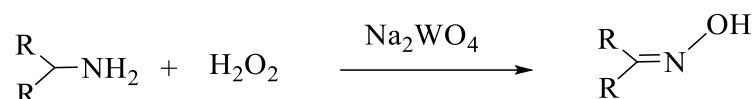


Figure 1.4. General synthesis of oximes by oxidation of primary amines.

There are various methods available for the manufacture of oximes, with two often employed techniques being discussed in this research. The first method involves the oximation of carbonyl compounds, while the second method involves the nitrosation of active methylene compounds. These two methods are widely recognized as the most prominent approaches for the synthesis of oximes [21].

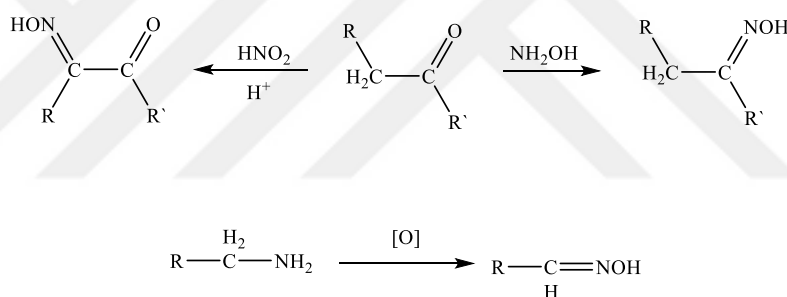


Figure 1.5. The most common methods for oxime synthesis.

Isomerization reactions are recognized as one of the established approaches to produce oximes. An example of this is the thermal rearrangement of pseudometeorites (2-nitronitroso dimers) to α -nitrooximes [21,22].

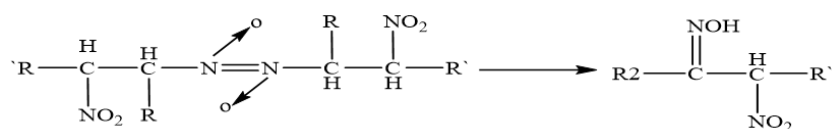


Figure 1.6. Synthesis of di-oximes by isomerization.

1.1.2. Properties of Oximes

Oximes are acidic (OH) Because of the hydroxyl group. The combination of bases and oximes results in oxime salts. In addition to forming connections with hydroxyl and amine groups, it can also form hydrogen bonds with other substances that contain hydrogen atoms [23,24].

Oximes are valuable chemicals in organic chemistry because they possess several significant characteristics. The following are among oxime's main characteristics:

1.1.2.1. Stability And Formation

Oximes are stable substances that are simple to make when aldehydes or ketones combine with hydroxylamine. Adding hydroxylamine to the carbonyl group (C=O) results in the production of the nitrogen-carbon double bond and the hydroxyl group, which is how oximes are created [24].

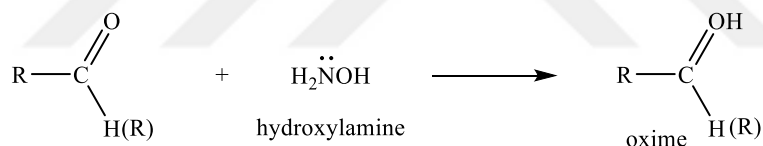


Figure 1.7. Synthesis of oximes from aldehydes or ketones.

1.1.2.2. Analytical Applications

Oximes are frequently employed as analytical tools for identifying and measuring aldehydes and ketones. They combine with carbonyl chemicals to create stable derivatives that are simple to characterize using various spectroscopic and chromatographic methods [25].

1.1.2.3. Tautomerism

Oximes can take on various tautomeric configurations, including the keto and enol tautomers. In contrast to the enol form, which has the C-OH=N structure, the keto form

has the C=NOH structure. The characteristics and reactivity of oximes can be affected by tautomerism [26].

1.1.2.4. Reactivity

Oximes can go through a variety of reactions to produce various functional groups, including rearrangements, condensations, and reductions. These reactions can be used to create a variety of organic molecules [27].

1.1.2.5. Biological Activity

Certain chemicals' oxime derivatives can display noteworthy biological activity, such as antibacterial, antiviral, and anticancer effects. The development of pharmaceuticals and medicinal chemistry is interested in these substances [28, 29].

1.1.3. Oxime Derivatives

Oxime derivatives are used extensively in many different disciplines, such as medical chemistry, material science, and chemical synthesis. The following are some examples of oxime derivatives, with citations for more information:

1.1.3.1. Hydroxamic Acids Are Compounds That Function as Inhibitors of Histone Deacetylase

As a class of oxime derivative known as a histone deacetylase inhibitor (HDACi), hydroxamic acid derivatives have received substantial research. HDAC inhibitors have shown promise in the treatment of several malignancies and can modify gene expression [30].

1.1.3.2. Derivatives of Oxime Ether as Antimicrobial Agents

It has been created and tested for the antibacterial activity of oxime ether derivatives. These compounds may be used in the creation of fresh antibiotics to treat bacterial illnesses that are resistant to current antibiotics [31].

1.1.3.3. Metal Ion Oxime-Based Chelators

Oxime derivatives have been employed as metal ion complexing ligands. These chelators have uses in various domains, including environmental remediation and imaging in medicine [32].

1.1.3.4. Oxime Derivatives as Photo Stabilizers

Oxime derivatives have been studied as photostabilizers to prevent the fading of dyes and pigments caused by exposure to light [33].

1.1.3.5. Oxime Derivatives as Reactivators of Cholinesterase

Organophosphates, which are frequently present in nerve agents, inhibit acetylcholinesterase. Oxime derivatives are utilized as reactivators of this enzyme. They may be used as medicinal defenses against chemicals used in chemical warfare [34].

1.1.3.6. Prodrugs For Drug Delivery That Contain Oxime

Targeted drug delivery using oxime-containing prodrugs has been developed, in which the prodrug is activated through circumstances in the target tissue, releasing the active drug [35].

1.2. DIOXIME

A dioxime is a chemical molecule that can be represented by the general formula $R_2C=N-OH$, where R denotes an organic moiety. The nomenclature "di-oxime" is assigned because of two oxime ($R-C=N-OH$) functional groups within the compound. Oximes are chemical substances that are generated through the interaction between an aldehyde or ketone and hydroxylamine (NH_2OH). The first di-oxime metal complex, bis methylglyoximatonickel (II) was discovered in 1897 by Tschugaeff [36]. Vicinal di-oximes and their derivatives constitute a highly significant class of ligands. Numerous experiments have been conducted on a wide range of transition metal complexes, including these ligands, mostly motivated by the intriguing coordination

chemistry displayed by vicinal di-oximes [37, 38]. The utilization of *vic*-dioximes, a class of organic chemical compounds, as viable sensing elements for the detection and quantification of organophosphates through the implementation of chemical gas sensors [39]. *vic*-dioxime has been identified as a potential antidote for nerve agents such as soman and tabun [40].

1.2.1. Synthesis of Dioxime

1.2.1.1. Synthesis from Ketone

- a. To make 1,3-dioxime, 1,3-dicarbonyl compounds are mixed with hydroxylamine hydrochloride while pyridine is present [41–44].

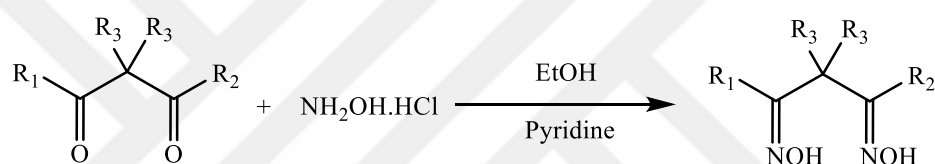


Figure 1.8. Synthesis of 1,3-di-oximes from ketone.

- b. The process involves adding NOCl to α -methyl ketone, creating 1-chloro-1,2-dione-1-oxime, purifying it with hydroxylamine hydrochloride, and adding an amine compound to create the desired di-oxime complex [45].

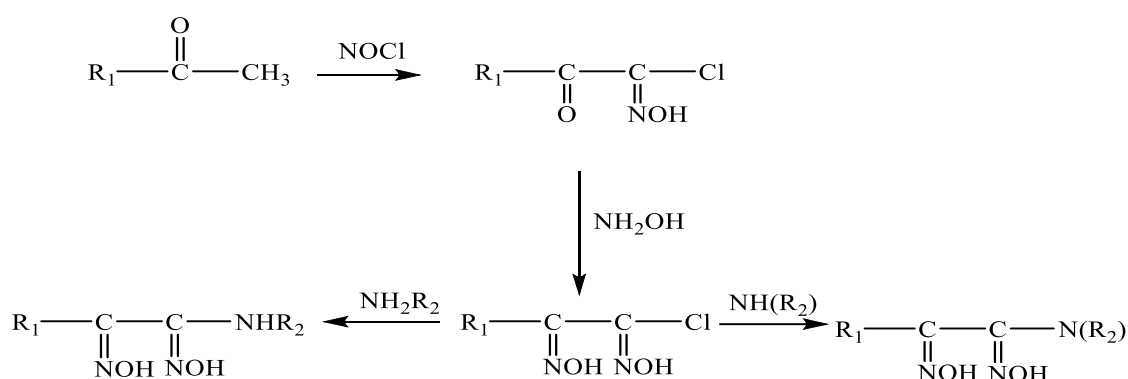


Figure 1.9. Synthesis di-oximes from mono ketone.

- c. Other examples; Cyclic di-oximes are formed by reacting the suitable di-carbonyl compound with hydroxylamine hydrochloride (ClH_4NO) and potassium carbonate (CK_2O_3) in an aqueous solution [46].

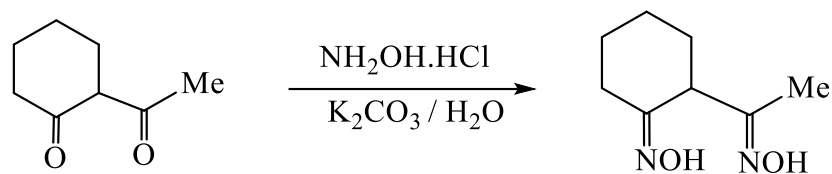


Figure 1.10. Synthesis cyclic di-oximes 2,1-(hydroxyamino) ethyl) cyclohexan-1-one oxime).

The synthesis of 2,6-dioximinocyclohexanone the di-oxime yield was obtained by subjecting cyclohexanone to methyl nitrite (CH_3NO_2) in the presence of hydrochloric acid (HCl) [47–49].

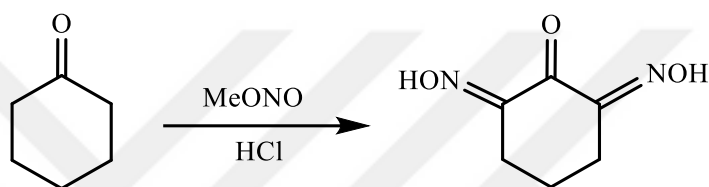


Figure 1.11. Synthesis of 2,6-dioximinocyclohexanone.

1.2.1.2. Synthesis from Diamine

- Using 2-chloro-3-nitrosobutane ($\text{C}_4\text{H}_8\text{ClNO}$) The compound 2-chloro-2-methyl-3-nitrosobutane ($\text{C}_5\text{H}_{10}\text{ClNO}$) was combined with 1,4-diaminobutane ($\text{C}_4\text{H}_{12}\text{N}_2$) in a controlled procedure, leading to the creation of 4,9-diaza-3,3,10,10-tetramethyldodecan-2,11-dione di-oxime ($\text{C}_{16}\text{H}_{30}\text{N}_4\text{O}_2$) [50].

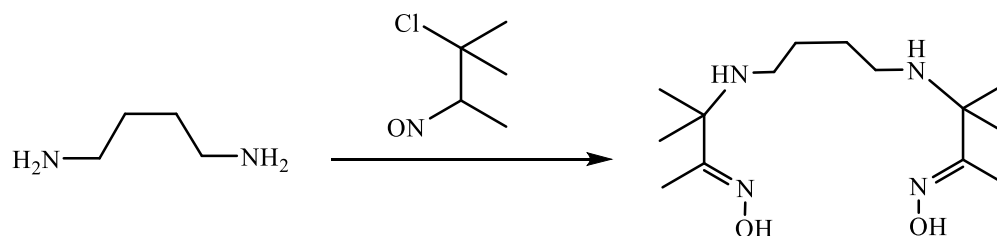


Figure 1.12. Synthesis of 4,9-diaza-3,3,10,10-tetramethyldodecan-2,11-dione di-oxime.

b. With Butan-2,3-dione mono oxime

Butan-2,3-dione mono-oxime solution was slowly added drop by drop to a solution of 1,4-diaminobutane. The resulting product was isolated and subsequently subjected to further reduction using NaBH₄, leading to the synthesis of 4,9-Diaza-3,10-dimethyldodecan 2,11-dione di-oxime (C₁₆H₃₀N₄O₂). Another step in the reaction involved the addition of a solution containing 2-chloro-2-methyl-3-nitrosobutane (C₅H₁₀ClNO) to 1,4-diaminobutane (C₄H₁₂N₂), conducted under controlled conditions. This reaction yielded the formation of 4,9-diaza-3,3,10,10-tetramethyldodecan-2,11-dione di-oxime (C₁₆H₃₀N₄O₂) [50].

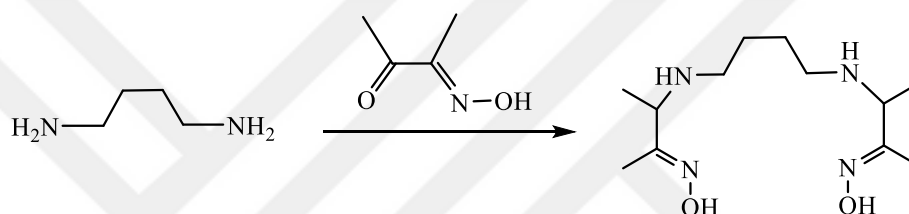


Figure 1.13. Synthesis of 4,9-Diaza-3,10-dimethyldodecan 2,11-dione di-oxime.

c. With 4-Methylpent-3-en-2-one (C₆H₁₀O)

The compound 4-Methylpent-3-en-2-one was introduced into a reaction mixture containing 1,3-diaminopropane, following the experimental procedure outlined in the studies conducted by Archer and Schlemper [50, 51].

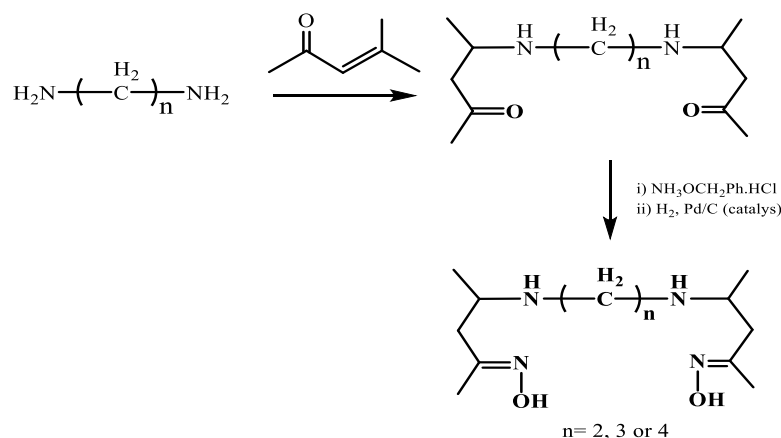


Figure 1.14. General reaction of diamine with 4-Methylpent-3-en-2-one.

1.2.3. Dioxime Applications

Anticancer Agents: Several di-oxime-metal complexes have exhibited favorable anticancer effects. These complexes have the capability to selectively target cancer cells and Trigger cell death through many ways, including halting DNA replication. or disrupting physiological processes [52].

Antimicrobial Agents: Extensive research has been conducted to evaluate the efficacy of di-oxime-metal complexes as antibacterial agents targeting bacterial, fungal, and viral infections. These complexes have the potential to inhibit microbial development through their interaction with crucial macromolecules or by disrupting essential cellular processes [10, 53].

Metalloenzyme Inhibition: Many in-depth studies have been done to investigate the possibility of metal di-oxime complexes as inhibitors of metalloenzymes, with the goal of treating a wide range of health problems. Scientists have developed therapeutic strategies to treat neurodegenerative conditions like Alzheimer's disease and Parkinson's disease, where metal ions affect the aggregation of proteins. These interventions have been mostly centered around targeting specific enzymes involved in disease processes [54–56].

1.3. THIADIAZOLE

The compound 1,3,4-thiadiazole and its derivatives remain a subject of significant interest among numerous researchers. A search was conducted on the Chemical Abstracts database spanning from 1982 to 1994, focusing on a specific structure (1) without specifying the characteristics of the bonds and substituents. This search resulted in a total of 6621 results. A total of 831 papers and 386 patents were identified using a restricted search across three areas of chemical abstracts. Remarkably, there has been a noticeable absence of thorough review publications about thiadiazole chemistry since 1984. the 1,3,4-thiadiazole which include the aromatic 1,3,4-thiadiazoles (1), the non-aromatic Δ^2 -thiadiazolines (2), Δ^3 -thiadiazolines (3), and the thiadiazolidine (4). The systems, denoted as (5), exhibit aromaticity, but the tautomeric

forms, represented as (6) and (7), do not possess aromaticity. The mesoionic systems (8) can be classified as another group of thiadiazole. The process of benzene fusion in 1,3,4-thiadiazoles is deemed unattainable [57].

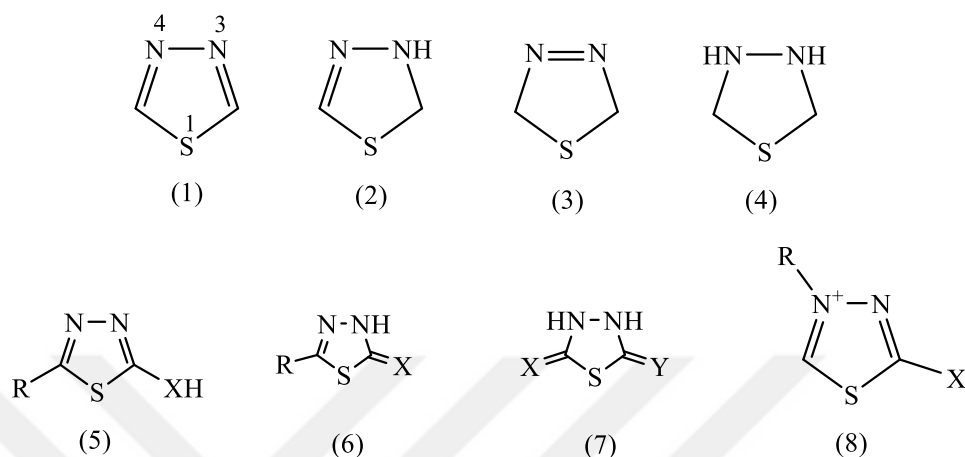


Figure 1.15. The compound 1,3,4-thiadiazole and derivatives (1-8).

1.3.1. Thiadiazole Derivatives

Numerous scholarly articles have been published on the efficacy of thiazole and thiadiazole derivatives in mitigating the corrosion of various metals, including mill steel, Cu⁺², and Al⁺³[58–60]. In recent years, there is a rising interest in the work of I.H. R. Tomi the thiazole and thiadiazole compounds provided were synthesized by the researchers and their colleagues (Figure1.16.) The inhibitory effects of these compounds on copper corrosion in acidic solutions were explored by experimental methods. The researchers determined that the corrosion inhibitory properties of these compounds exhibit a decreasing trend in relative strength, following a specific order. The hierarchy of inhibitory neurotransmitters can be described as follows: Inh5 is the highest level, followed by Inh4, Inh3, Inh2, and finally Inh1. The objective of this study is to examine the inhibitory properties of compounds synthesized by the researchers in relation to iron corrosion. This will be accomplished via the use of DFT and molecular dynamics simulation methodologies. The aim is to theoretically forecast the most efficient inhibitor among the synthesized molecules [61].

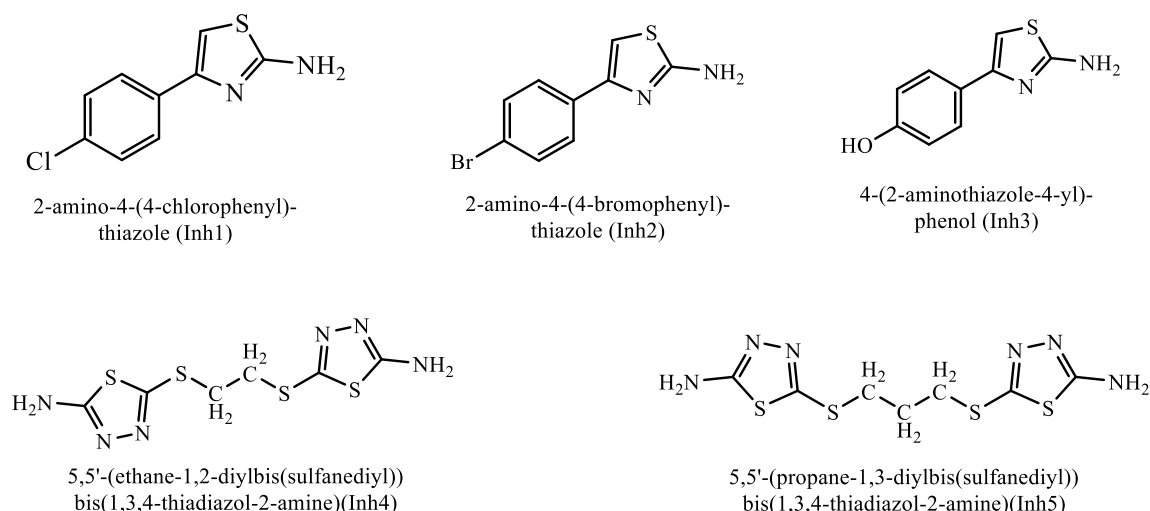


Figure 1.16. Some compound 1,3,4-thiadiazole derivatives.

Fused carbocyclic compounds of thiadiazole are present. Halogenated thiadiazoles have the capability to conduct both Stille and Suzuki reactions [62].

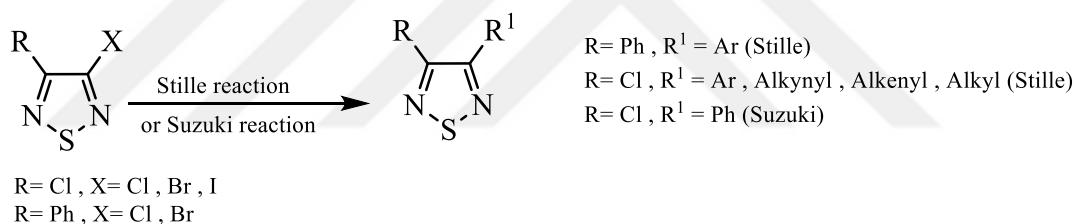


Figure 1.17. Steele and Suzuki reactions.

The contemporaneous degradation of the heterocyclic ring of 3,4-dichloro-1,2,5-thiadiazole occurred in the presence of triphenylphosphine (C₁₈H₁₅P) ligands, leading to side reactions.

The present study involved a reexamination of the chemical reactions involving 3,4-dichloro and 3-chloro-4-hydroxythiadiazoles (C₂H₃ClN₂OS) with different acetylene nucleophiles (NaC CNa, LiC C-TMS, and LiC C-SnMe₃). The results indicated that the initial thiadiazoles were consumed during the reactions, but no substantial formation of higher-molecular-weight products was seen.

Chloro-substituted thiadiazoles can be efficiently hydrolyzed to hydroxythiadiazoles by employing aqueous sodium or potassium hydroxide with dimethyl sulfoxide (DMSO) at 100 °C. Aryl ethers can be efficiently produced via Ullmann-type coupling using copper at high temperatures. Using phenols with electron-withdrawing groups like CF₃ or NO₂ inhibits the process. Benzyl, allyl, and alkyl ethers can be easily produced from their corresponding alcohols with different bases. 1,2,5-thiadiazole derivatives can be efficiently produced by utilizing various ethylene glycols and dihydroxy alkanes. Thiadiazole thiolate salts can be synthesized by reacting chlorothiadiazoles with alkali metal sulfides in solvents like DMF or ethanol. The nucleophilic sulfur source is believed to originate from the breakdown of thiadiazole. Nucleophilic displacement of halide from halo-1,2,5-thiadiazoles can be observed using ammonia, primary alkylamines, secondary alkylamines, arylamines, sulfonamides, and phthalimide. It is important to note that these reactions typically require elevated temperatures and an excess of the nucleophile [62].

Upon subjecting the thiadiazole derivative (**1**) to a range of isoselenocyanates, the resulting products were observed to be either (**2**) or (**3**), depending on the specific R group present on the isoselenocyanate. This information is presented in Figure 1:18. Tetracycles (**2**) are formed using alkyl isoselenocyanates. Compound **2d** exhibited a 1:1 clathrate formation with benzene, cyclohexane, toluene, and 1,2-dichloroethane. Additionally, it formed a 3 host:1 guest clathrate with diethyl ether (Et₂O) and a 4 host:3 guest clathrate with dichloromethane (DCM). The diazepine (**1**) underwent a reaction with aryl isoselenocyanates, resulting in the removal of MeCN. However, this reaction only led to the inclusion of a single molecule of isoselenocyanate, resulting in the formation of compound (**3**). The confirmation of the structures of compounds (**2**) and (**3**) was achieved using X-ray crystallography on select members of the series [63].

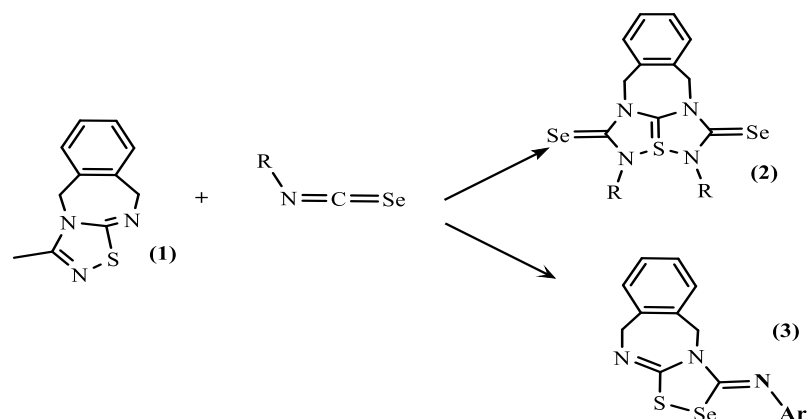


Figure 1.18. Subjecting the thiadiazole derivative (1) to a range of isoselenocyanates.

1.3.2. Uv Properties Of Thiadiazole Compounds

The compound 1,2,4-Thiadiazole exhibits an absorption peak at a wavelength of 229 nm. The incorporation of amino groups into the heteroaromatic nucleus leads to a redshift in the absorption spectrum. Consequently, the 1,2,4-thiadiazole ring induces a redshift, resulting in a maximum absorption wavelength of 247 nm in 5-amino and 256 nm in 3,5-diamino-1,2,4-thiadiazole (C₂H₄N₄S). There have been no recent papers pertaining to the ultraviolet (UV) spectra of 1,2,4-thiadiazoles after the publication [63].

1.3.3. Thiadiazole Synthesis

Compounds with thiadiazole rings, which consist of two nitrogen atoms and one sulfur atom, are widely utilized in many research investigations. The isomers of 1,3,4-thiadiazole are the predominant derivatives within the class of thiadiazoles, exhibiting notable pharmacological characteristics [64].

The present study outlines a comprehensive protocol for Synthesizing new 1,3,4-thiadiazole compounds. A mixture of 4,4'-benzophenonedicarboxylic acid, a thiosemicarbazide derivative, and POCl₃ was subjected to reflux for a duration of 4 hours at a temperature of 90 °C. The product was subjected to precipitation by cooling it with ice water. The combination that had been neutralized with ammonia solution was placed in the refrigerator for an extended period. The ultimate substance

underwent filtration and washing, followed by drying through the utilization of a vacuum oven. Subsequently, it was subjected to crystallization in a combination consisting of DMF and water in a ratio of 2:1. Additional substances were synthesized using an identical experimental technique. Thiosemicarbazide derivatives were acquired in accordance with the findings documented in the literature [65]. The synthesis scheme is given in Figure 1.19.

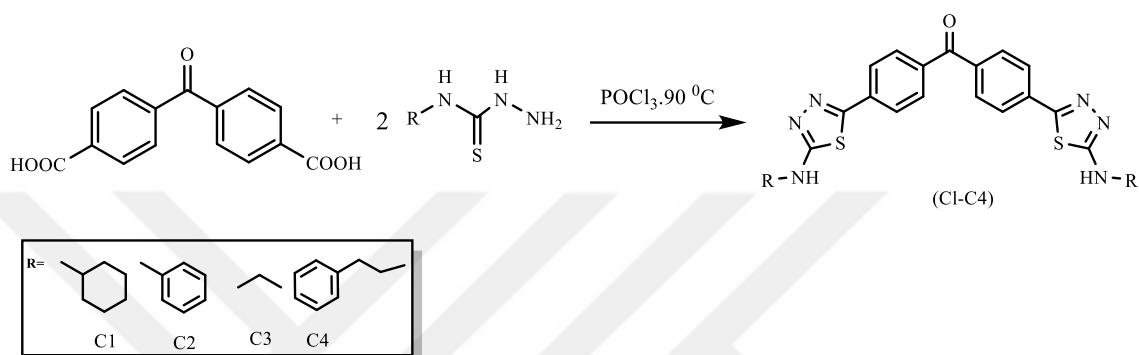


Figure 1.19. Synthesis of novel 1,3,4-thiadiazole derivatives.

1.3.4. Thiadiazole Applications

The chemical known as 1,3,4-thiadiazole is a heterocyclic complex consisting of five members and including three heteroatoms. This compound serves as a structural subunit in various bioactive compounds [66–68]. Molecules that contain the thiadiazole component have demonstrated anticancer [69,70], antimicrobial [71], antiepileptic [72], and many other properties. Cefazolin and azamulin are two often utilized antibiotics in clinical settings shown in Figure 1.20.

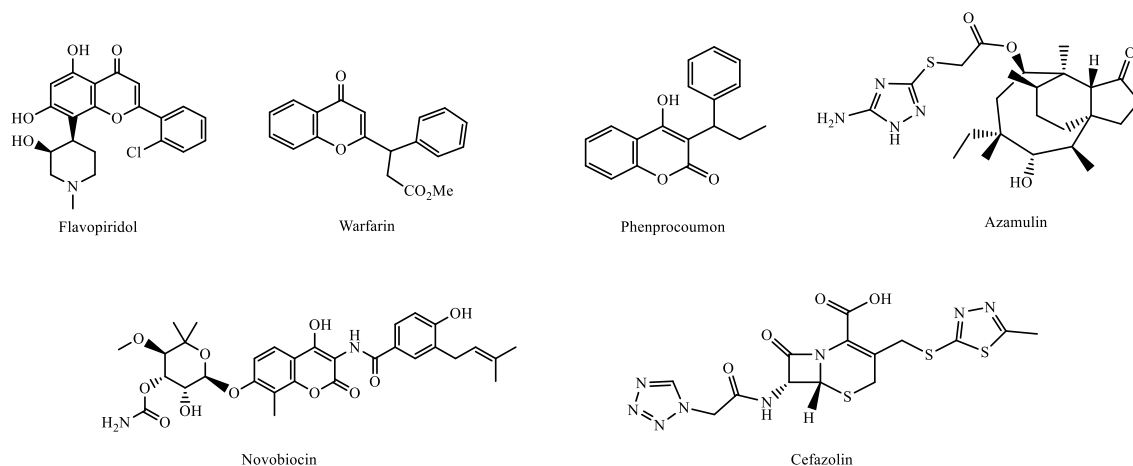


Figure 1.20. Different medical drug that contains thiazole.

In contrast to the extensive research conducted on coumarin and thiazole derivatives, there is a relative dearth of studies on molecules that incorporate both structural components within a single molecule. However, numerous instances have demonstrated a diverse range of biological activities, encompassing antibacterial properties [73], antifungal [74], anticancer [75,76], for treating Alzheimer's disease and neurodegenerative diseases for treating Alzheimer's disease and neurodegenerative diseases [77], suppressing allergic reactions agents [78], and many others medical conditions.

1.4. TRANSITION METAL COMPLEXES

Transition metal complexes are generated through the combination of transition metals with other elements or molecules. The arrangement of the ligands in relation to the metal plays a crucial role in determining the structure of the complex [79].

Transition metal complexes involve the coordination of a metal with a ligand, which might possess a positive, neutral, or negative charge [80].

1.4.1. Applications of The Transition Metal Complexes

Metal complex ions exhibit a diverse array of applications, encompassing the transportation and storage of oxygen, facilitation of electron transfer, catalytic functions in enzymes, and pharmaceutical applications [81].

Moreover, the remarkable electrical and structural characteristics exhibited by transition metal complexes render them highly valuable in a diverse range of applications. Several instances can be cited to demonstrate the utility of transition metal compounds.

Industrial operations: Transition metal complexes are utilized in a diverse range of industrial operations. Dyes and pigments derived from them are used in various sectors, such as textiles, printing, and paint. Transition metal complexes have been utilized as catalysts in the production of several compounds, including polyethylene and propylene oxide.

Environmental Applications: Transition metal complexes play a pivotal role in various environmental applications. Catalysts were employed for the purpose of facilitating environmental remediation endeavors, specifically the degradation of pollutants present in water and air. Transition metal complexes are also utilized in many applications, such as wastewater treatment, carbon dioxide capture and conversion, and the generation of renewable energy.

Numerous chemical processes heavily depend on the utilization of transition metal complexes as catalysts. These catalysts have the potential to decrease the energy required for activation, enhance the speed of reactions, and control the degree of selectivity, thereby facilitating the whole reaction process. Industrial processes such as ammonia synthesis, olefin polymerization, and oxidation reactions employ homogeneous transition metal catalysts, exemplified by the Haber-Bosch process.

Transition metal complexes are utilized in the fields of electronics and optoelectronics due to their inherent ability to exhibit diverse electrical and optical properties. Transition metal oxides play a significant role in the production of various technologically advanced products, such as electrochromic devices, solar cells, sensors, and organic light-emitting diodes. Transition metal complexes have been employed in the fields of molecular electronics and spintronics.

Transition metal complexes are commonly used as contrast agents in medical imaging methods like PET and MRI, detecting metal ions, gases, and biomolecules using fluorescent probes [82–86].



PART 2

LITERATURE REVIEW

In 2023, Redouane Kerkatou et al. stated that “two novel mononuclear Zn^{+2} coordination compounds, $\{Zn(MICO)_2Cl_2\}$ (I) and $\{Zn(MIPMO)_2Cl_2\}$ (II), were produced and identified using various techniques. The $Zn(II)$ cation in both complexes exhibits centrosymmetric properties, tetrahedral coordination, and stability through intermolecular hydrogen bonds. Analyzed the Hirshfeld surface to study intermolecular interactions in the crystal structure. The stability of the $Zn(II)$ complexes was assessed using their HOMO, LUMO, and energy gap” [87].

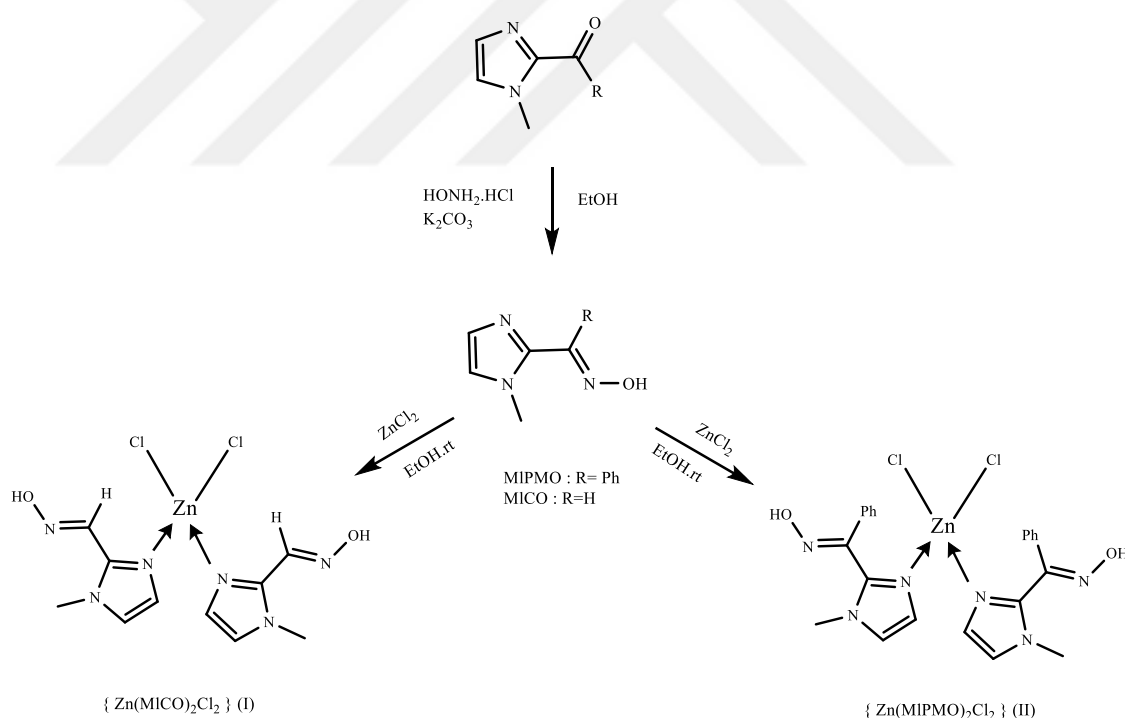


Figure 2.1. Synthesis of ligands MICO and MIPMO and their complexes $\{Zn(MICO)_2Cl_2\}$ (I) and $\{Zn(MIPMO)_2Cl_2\}$ (II).

In 2023, Mehdi Bouchouit et al. showed that “two new compounds, $Ni(L)_2Cl_2$ (I) and $Hg_2(L)_2Cl_4$, DMF (II), were created by utilizing L as the ligand. The complexes were identified by a hexa-coordinated molecule with a distorted octahedral shape,

containing a single Hg(II) atom, and a distorted tetrahedral geometry surrounding each mercury Centre metal. The techniques utilized were single-crystal diffraction, FT-IR, NMR, and UV-visible spectroscopy” [88].

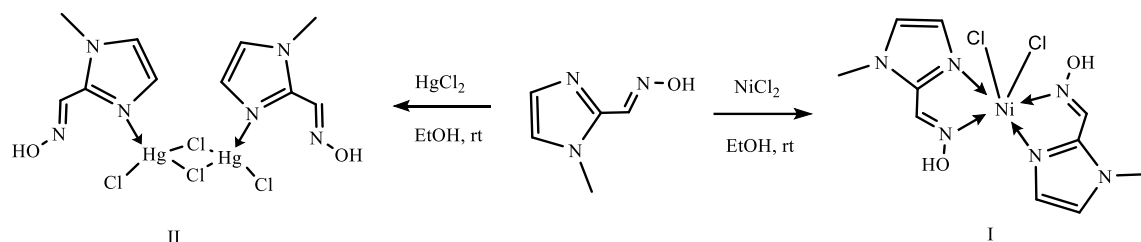


Figure 2.2. Synthesis of complexes I and II.

In 2022, Al-sabawi et al. explained that “salicyl-aldo-oxime, a nano-phenolic oxime complex, was synthesized with several transition metals such as Ni^{2+} , Cu^{2+} , Pd^{2+} , Zn^{2+} , and Hg^{2+} . The complexes underwent analysis using scanning electron microscopy (SEM), X-ray diffraction (XRD), (HNMR), and UV-visible spectroscopy to ascertain their geometric features. The biological activity of both ligands and complexes was tested against three distinct microorganisms. Complexes with Pt^{2+} ions showed the highest level of activity. MTT tests were performed on HepG-2 cell lines to evaluate their in vitro anticancer properties. The complexes produced by Zn^{2+} and Pt^{2+} ions exhibited notable activity, as indicated by their IC_{50} values. The copper (Cu) and nickel (Ni) complexes displayed the lowest activity when tested on the same cell” [84].

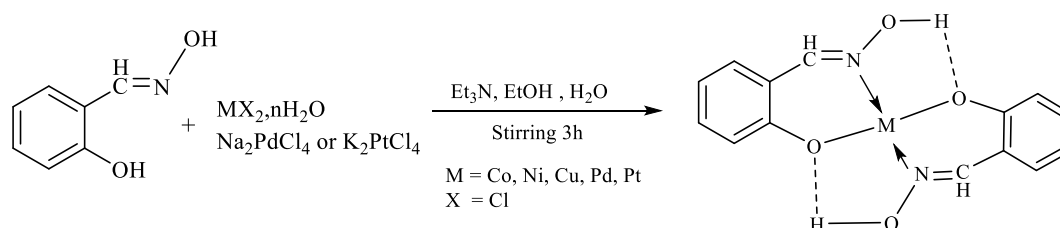


Figure 2.3. Synthesized nano-phenolic oxime complexes and transition metal complexes.

In 2022, Korkmaz et al. clarified that “an oxime ligand (HL) was synthesized by condensing 4-biphenylhydroxymoyl chloride with 2-amino-5-bromopyridine. Mixed-ligand complexes were synthesized by reacting ligands with metal (II) acetate salts of Co (II), Ni (II), and Cu (II). The ligand and its complexes were structurally analyzed

by elemental analysis, ^1H -, ^{13}C -NMR, FT-IR, ICP-OES, molar conductivity studies, and magnetic susceptibility tests. The compounds' thermal properties were evaluated by thermogravimetric and differential thermal studies. The compounds' antibacterial activity was evaluated using the resazurin-aided broth microdilution method. A molecular docking study was conducted to analyze the molecular interactions between the synthesized chemical and beta-ketoacyl-ACP synthase III (KAS III), an essential enzyme for bacterial survival. The Cu(II) complex exhibited higher antibacterial efficacy than other drugs, as shown by MIC values and binding energy scores obtained from both in vitro and in silico studies” [89].

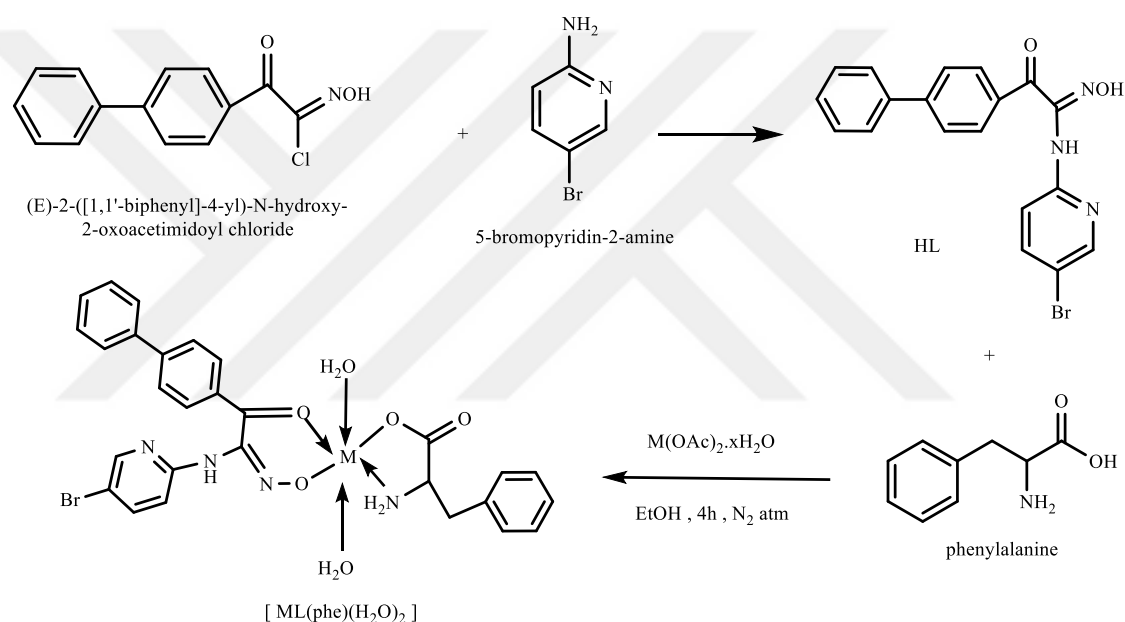


Figure 2.4. Synthesis of mixed ligand complexes $[\text{ML(phe)(H}_2\text{O)}_2]$ (M:Co(II), Ni(II), Cu(II)).

In 2011, Uysal and Coskun showed that “a set of trinuclear schiff base-oxime metal complexes was produced by reacting three equivalents of 4-hydroxybenzaldehyde with one equivalent of melamine. The compounds were identified using techniques such as FTIR spectroscopy, elemental analysis, ^1H NMR, and mass spectroscopy. The Schiff base ligand subsequently reacted with Cr^{3+} and Fe^{3+} ions, forming respective complexes. Verification of these complexes was done using FTIR spectroscopy and thermal analysis techniques. The complexes with low spin deformed octahedral Fe^{3+} and Cr^{3+} ions, connected by bridges containing keto-oxime groups, have been alternatively characterized in scientific literature. The identification of these

compounds was conducted using established techniques such as FTIR spectroscopy, elemental analysis, ^1H NMR, and mass spectroscopy” [90].

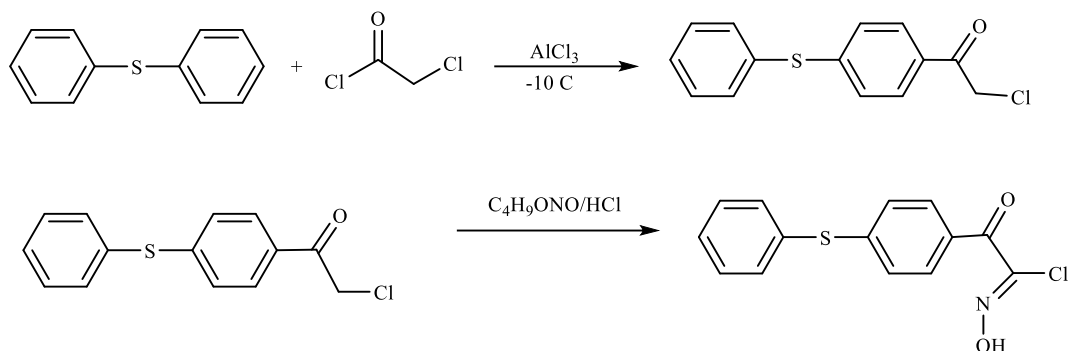


Figure 2.5. Synthesis of trinuclear Schiff Base-Oxime.

In 2006, Coskun clarified that “synthesized A set of keto oximes and glyoxime compounds were synthesized in the presence of transition metal ions, specifically Cu^{2+} , Co^{2+} , and Ni^{2+} . The starting materials used for the synthesis were acetyl chloride and diphenyl ether, with AlCl₃ serving as the catalyst. The verification of all produced complexes and ligands was conducted through the utilization of various analytical techniques, including ^1H - ^{13}C NMR, magnetic measurement, elemental analysis, and FTIR spectroscopy” [91].

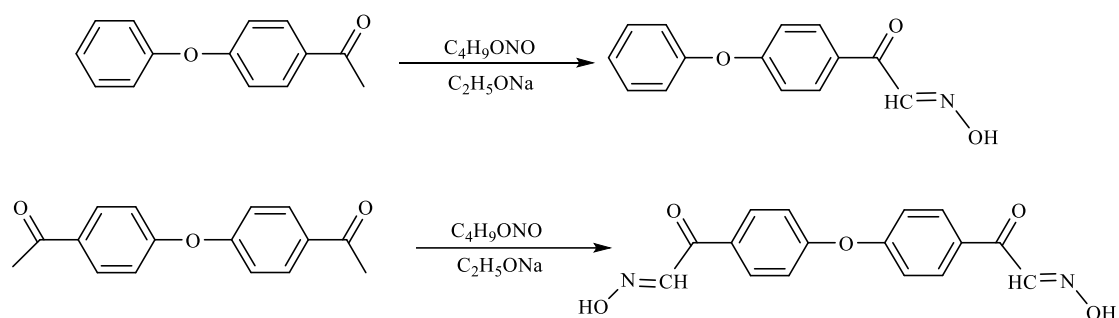


Figure 2.6. Synthesis of keto oxime and glyoxime with some transition metals.

In 2023, Topkaya et al. showed that “the compound being studied is the co-crystal [(aqua)2,2'-(propane-1,3-diylbis(azaneylylidene))bis(2-phenylacetaldehyde)dioximato]. Copper(II) chlorate, [Cu(HL1)ClO₄]₃, was synthesized by reacting 1,3-diaminopropane with isonitrosoacetophenone. The substance's molecular and crystal structures were determined using single-crystal X-

ray studies. Within the co-crystal's asymmetric unit are three copper complex molecules that have crystallized separately, together with three uncoordinated chloroperoxidase anions. The study evaluated the DNA binding ability of a Cu^{+2} complex by absorption spectrum measurements and fluorescence spectroscopy. The results indicated that the complex attaches to DNA via the minor groove. The study examined DNA cleavage by a gel electrophoresis experiment, demonstrating a high efficiency in cleaving supercoiled DNA. The combination showed strong inhibition against topoisomerase I and $\text{II}\alpha$ enzymes. The complex's cytotoxicity was tested on different human cell lines, such as A549, HT29, HepG2, MDA-MB-231, and LnCaP. The combination showed significant cytotoxicity in vitro against HepG2 and LnCaP cells” [92].

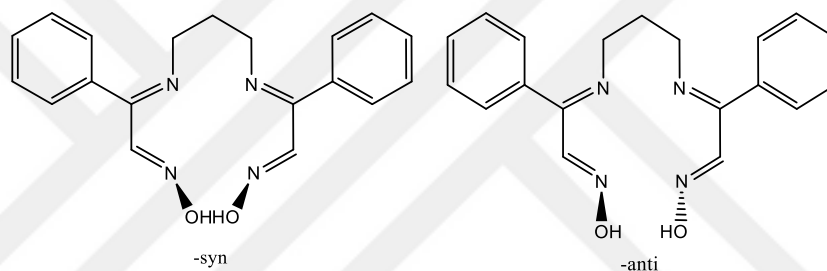


Figure 2.7. *Syn*- and *anti*- isomer forms of the synthesized ligands.

In 2023, Emirik et al. showed that “in contemporary research, there is a concerted effort to address the problem of toxicity linked to the use of approved platinum-based anticancer medications. This is being pursued through the implementation of diverse tactics that focus on the development of novel and very potent therapeutic candidates. This paper combines the current understanding of the cytotoxic effects of two active ligands that selectively bind to DNA with new experimental results. We aim to propose novel anticancer drugs and evaluate their efficacy using quantum mechanical computations. We specifically assess their hydrolysis and DNA binding capabilities, comparing them to traditional platinum medicines. We also examine the global reactivity characteristics and charge distribution to obtain more information. Our study's findings suggest that the newly proposed platinum complexes show promise as potential anticancer drugs with higher activity. The deadly effect of these complexes, particularly in terms of DNA platination, is more prominent compared to cisplatin, an extensively used anticancer drug in clinical practice” [93].

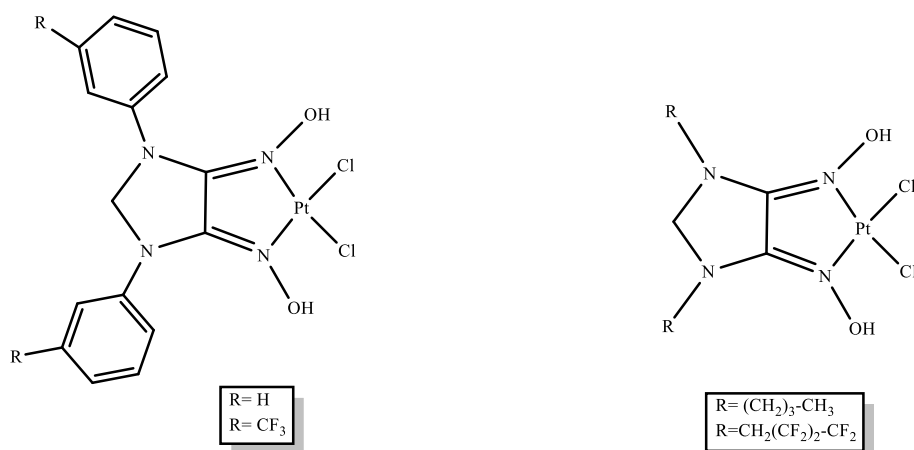


Figure 2.8. Structures of platinum complexes.

In 2022, Caliskan et al. they found that “the study investigated the interactions between synthesized compounds and two proteins: human epidermal growth factor protein kinase domain EGFR and cyclin-dependent kinase-2 CDK2. Quantum chemical calculations were conducted to examine energy levels in the Highest Occupied Molecular Orbital (HOMO) and Lowest Unoccupied Molecular Orbital (LUMO). The compounds' bioactivity characteristics were evaluated. The Ni(II) and Cu(II) complexes of ligands L¹H₂, L²H₂, and L³H₂ exhibited higher binding affinity towards EGFR and CDK2 proteins. The compounds [Cu(L¹H)₂] and [Cu(L²H)₂] exhibited promise as agents for selectively targeting CDK2 and EGFR, respectively. The ligands L¹H₂, L²H₂, and L³H₂ exhibited the lowest binding energy values in comparison to the metal complexes. The compounds [Ni(L²H)₂] and [Cu(L²H)₂] exhibited superior ligand efficiency and functional quality when binding to the EGFR. The [Cu(L³H)₂] combination exhibited a respectable FQ value but exceeded the allowed LE value. The chemicals show promise for further exploration in the creation of anti-cancer therapy because of their low toxicity and specific effects” [94].

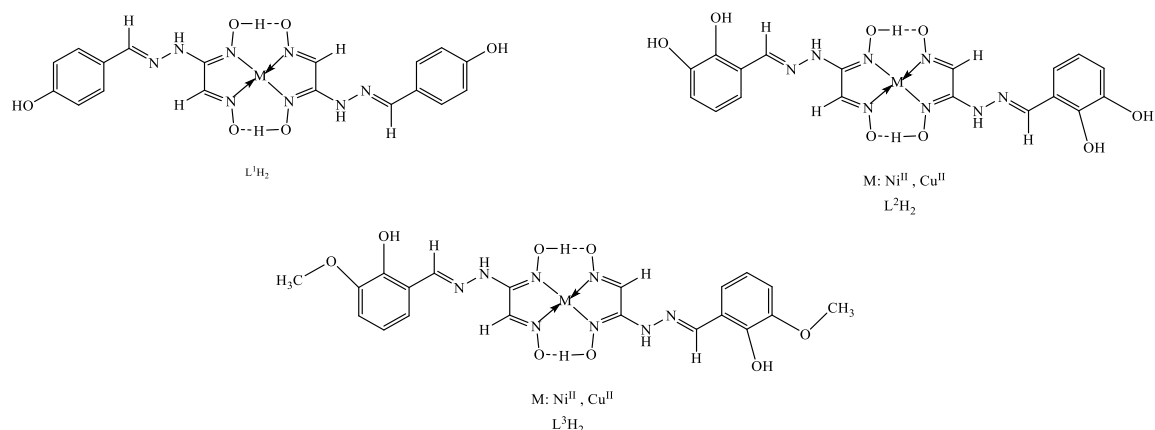


Figure 2.9. Expected ligand complexes with predetermined structures $[L^1H_2]$, $[L^2H_2]$, $[L^3H_2]$.

In 2022, Alhafez, et al. explained that “the study examines a recently created vic-dioxime ligand (LH_2) attached to the N4-oxime core structure. The study investigates compounds produced by LH_2 with Copper (II), Nickel (II), Titanium (IV), Vanadium (IV), and Zinc (II) salts. The ligand and its complexes were analyzed using NMR spectroscopy, LC/MS/MS, FT-IR, UV/VIS, melting point determination, and magnetic susceptibility studies for characterization. The ligand and its metal complexes were tested for their antibacterial and antioxidant activities in a laboratory setting. Compounds (1), (2), (3), and (6) exhibited notable effectiveness, with compound (2) displaying a superior ability to chelate metals because of the detachment of ligands from the created metal complexes. All medications showed effectiveness against *C. albicans* and *S. cerevisiae*, like antibiotics” [95].

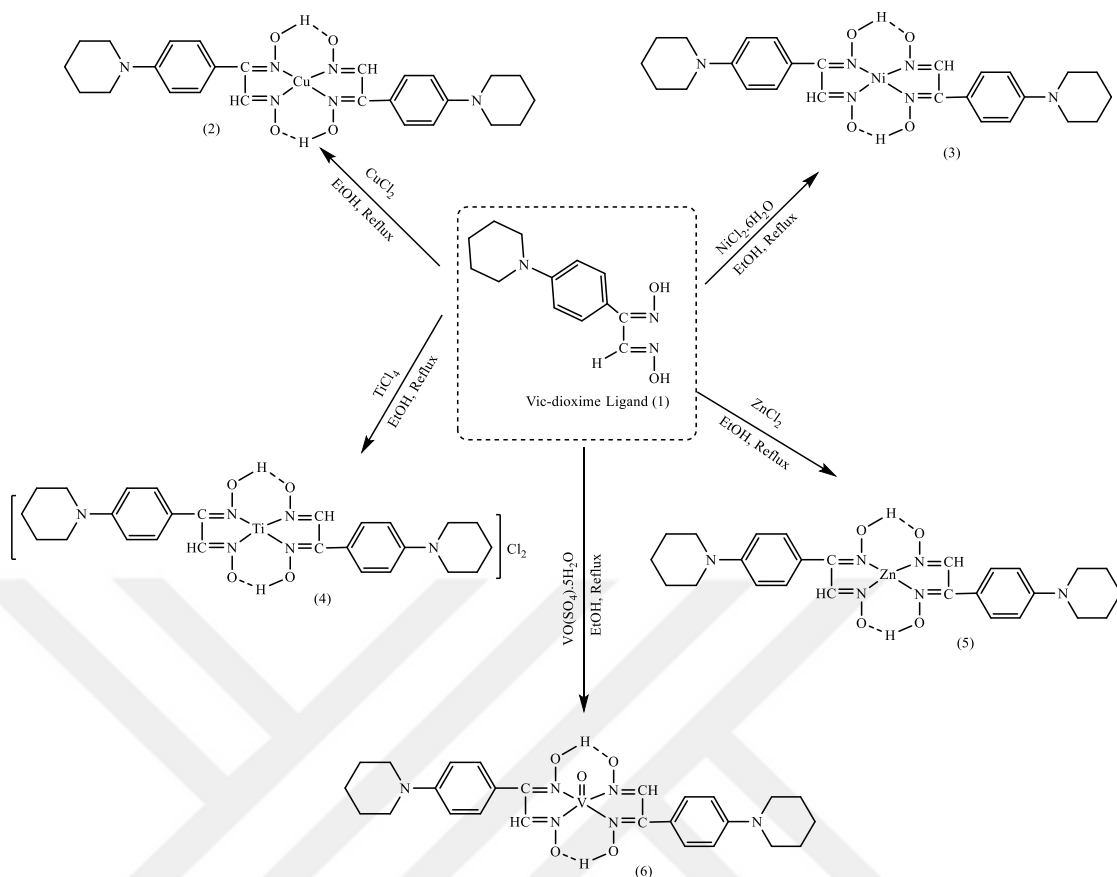


Figure 2.10. The configuration of the suggested *vic*-dioxime metal compounds $[\text{M}(\text{LH})_2]$.

In 2021, Ureche et al. explained that “*vic*-di-oximes are versatile compounds used in many industrial and scientific uses. Several coordination compounds have been synthesized with *vic*-di-oximes as a foundation. This work details the synthesis and thorough examination of two *vic*-di-oximes obtained from dichloroglyoxime: *p*-aminobenzoic acid and *p*-aminotoluene. Their structures were verified using IR, ^1H , ^{13}C , and ^{15}N NMR spectroscopic studies, along with Single crystal X-ray diffraction. One of the *vic*-di-oximes reported, bis(di-*p*-aminotoluene) glyoxime mono-*p*-aminotoluene trihydrate, showed notable antibacterial effects against several bacteria (including *Bacillus subtilis* and *Pseudomonas fluorescens*) and phytopathogenic microorganisms (such as *Xanthomonas campestris*), *Erwinia amylovora*, and *E. carotovora*), and fungi (*Candida utilis* and *Saccharomyces cerevisiae*) at a minimum inhibitory concentration (MIC) ranging from 70 to 150 $\mu\text{g}/\text{mL}$ ” [96].

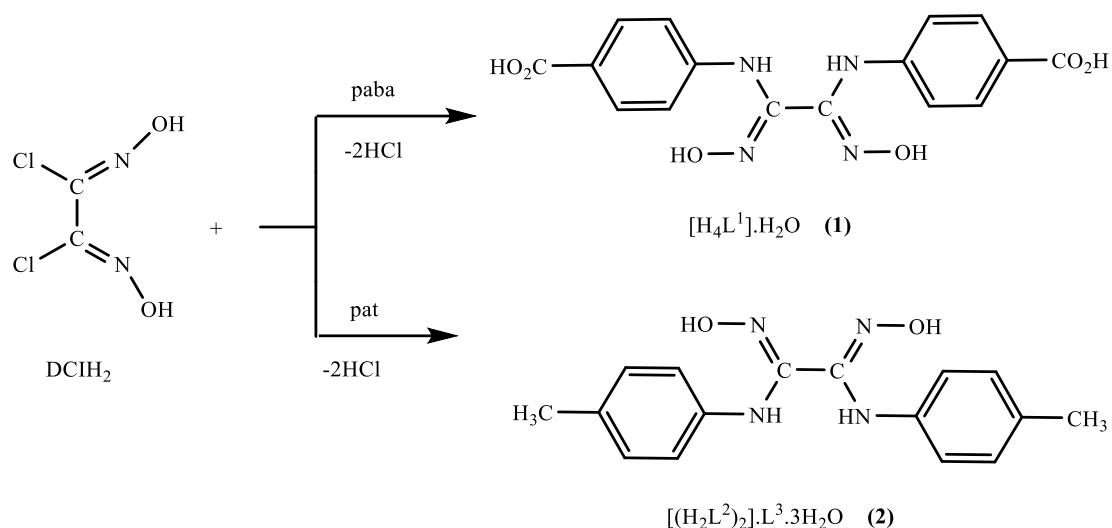


Figure 2.11. Synthesis of *vic*-dioximes **1** and **2**.

In 2019, Celik et al. clarified that “this study focused on creating and analyzing the Cu (II) and Ni (II) transition metal complexes of the *vic*-dioxime ligand, 2-(hydroxyimino)-N'-[(1E)-2-oxo-2-phenylethylidene]ethanehydroximohydrazide (LH₂), by analytical and spectroscopic methods. In vitro, the cytotoxic and apoptotic effects of the ligand and its complexes were evaluated on Caco-2 heterogeneous human epithelial colorectal cancer cells. The ligand and its complexes displayed varying cytotoxic and apoptotic effects based on the concentration. The ligand caused very few harmful effects on both Caco-2 cancer cells and lymphocytes, showing low cytotoxic and apoptotic effects. The Ni(II) complex of the ligand exhibited notable cytotoxic and apoptotic effects on both Caco2 cancer cells and lymphocytes. The Cu(II) combination of the ligand exhibited notable cytotoxic and apoptotic effects on Caco-2 cells, but only modest effects on lymphocytes. The ligand and its Ni(II) and Cu(II) complexes showed concentration-dependent cytotoxic and apoptotic effects, with increased concentrations leading to higher cytotoxicity. The findings indicate that the Cu(II) complex shows promise as a strong anti-cancer medication for targeting Caco-2 colon cancer cells” [97].

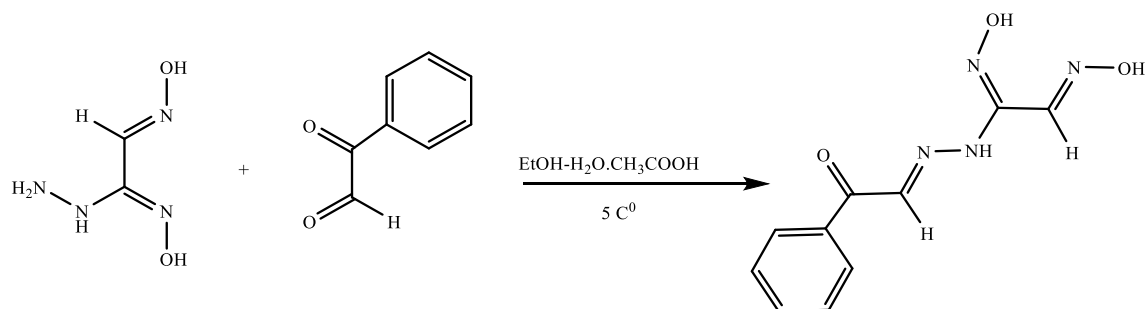


Figure 2.12. Synthesis of the ligand (LH2).

In 2008, Uysal et al. clarified that “compounds 1, 2, 3, and 4 were synthesized using the procedure described in the literature. The earliest complexes [Fe(III)(salen/saloph) dopaminephenylglyoxime] were synthesized by reacting dopaminophenylglyoxime with tetradentate Schiff bases containing dinuclear Fe⁺³ oxygen bridges. The Schiff bases utilized are N,N-bis(salicylidene)ethylenediamine (salenH₂) and bis(salicylidene)-o-phenylenediamine (salophH₂). Heterotrinnuclear complexes were synthesized by reacting initial compounds with Co⁺², Ni⁺², and Cu⁺² salts. Heterotrinnuclear vic-di-oxime complexes with BF²⁺ capping has been synthesized successfully. The complexes have been found to be Fe(III) complexes with a distorted octahedral structure, where the Fe(III) ions are linked by o-hydroxy phenolic groups and display low spin. The o-hydroxy phenolic groups act as linkers for weak antiferromagnetic intramolecular exchange. The structure of di-oxime and its complexes was determined using elemental analysis, ICP-AES, ¹H-NMR, and IR spectral data” [98].

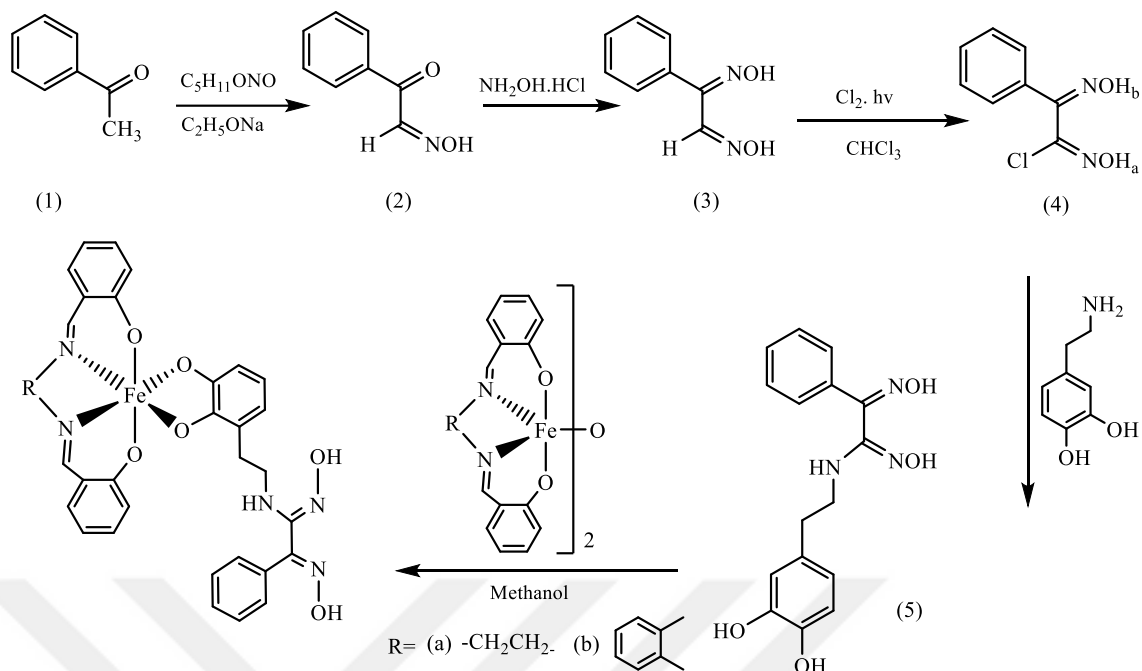


Figure 2.13. Synthesis protocol for Fe(III) complexes of [H2LSalen/Saloph].

In 2007, Uysal et al. showed that “acetophenone is the primary component in this investigation. ω Isonitrosoacetophenone was synthesized by reacting nitrosyl with amyl nitrite of acetophenone in the presence of sodium ethoxide. Anti-phenylglyoxime was synthesized by reacting ω -isonitrosoacetophenone with hydroxylamine and sodium acetate in an ethanolic solution later. Chlorophenyl glyoxime was synthesized by reacting with chlorine gases. Three aminophenylglyoxime ligands were produced by reacting chlorophenyl glyoxime with different amines. Ni(II), Co(II), and Cu(II) complexes containing a BF^{2+} bridge were synthesized by utilizing anilinophenylglyoxime and 2,4-dimethylanilinophenylglyoxime. Polymeric metal complexes with a BF^{2+} -bridge of dopamiophenylglyoxime were synthesized afterwards. The compounds structures were identified by FT-IR, ^1H NMR, and ICP-AES spectroscopic data, together with elemental studies and magnetic measurements” [38].

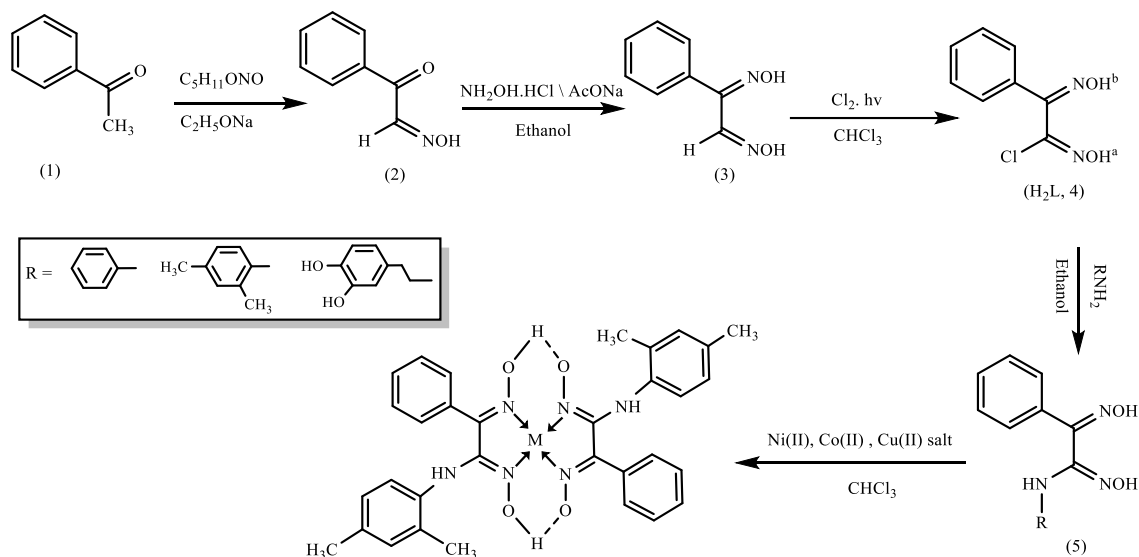


Figure 2.14. Synthesis of some complexes with *vic*-dioxime.

In 2022, Deswal et al. finished research containing “the researcher successfully synthesized a series of complexes consisting of thiadiazole derivatives and several transition metals, including Co^{2+} , Zn^{2+} , Cu^{2+} , and Ni^{2+} ions. Various analytical techniques were employed to characterize the synthesized compounds, including ^{13}C (NMR), ^1H NMR, (IR), (XRD), thermogravimetric analysis (TGA), scanning electron microscopy (SEM), energy-dispersive X-ray spectroscopy (EDAX), and electron spin resonance (ESR). The study made a prediction regarding the coordination geometry of the complexes, suggesting that they would exhibit a penta-coordinated structure. This coordination is achieved by the involvement of the nitrogen atom in the azomethine group, the deprotonated oxygen atom, and one of the nitrogen atoms in the thiadiazole heterocycle. These Schiff base ligands demonstrate tridentate behavior in this context. An *in vitro* experiment was conducted to assess the antidiabetic properties of the synthesized compounds by examining their effects on the α -amylase and α -glucosidase enzymes. The compounds had a noteworthy degree of biological activity, as seen by their "IC50" value, which closely resembled that of acarbose. The *in-silico* research provided confirmation that the synthesized compounds possess medical utility and can be employed as orally active pharmaceutical agents” [99].

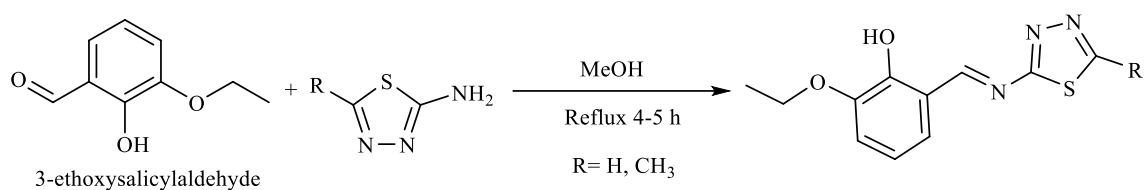


Figure 2.15. Synthesis of complexes of thiadiazole derivatives.

In 2021, Askin et al. showed that “a range of disubstituted imidazole and 1,3,4-thiadiazole derivatives, together with trisubstituted 1,3,4-thiadiazole and imidazole derivatives, were created and tested for their ability to inhibit human carbonic anhydrase (hCA) activity. The cytotoxicity of the produced compounds was evaluated using the L929 murine fibroblast cell line. Molecular docking simulations were used to investigate the potential binding interactions of these inhibitors with hCA I and II isoforms and AChE. The study's findings offer useful insights for improving and optimizing hCA and AChE inhibitors. The chemicals examined in this study show promise as interesting primary candidates” [100].

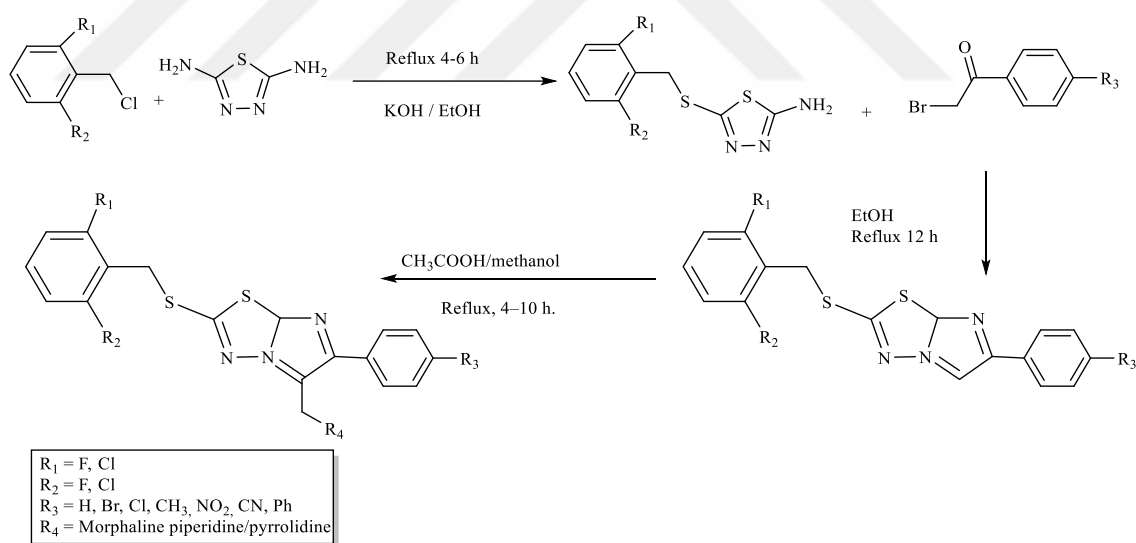


Figure 2.16. Synthesis of disubstituted Imidazole and 1,3,4-thiadiazole derivatives.

In 2021, Serbest et al. showed that “in this study, hetero-ligand complexes were synthesized by combining transition metals (M) such as Mn²⁺, Zn²⁺, and Ni²⁺ ions with ligands (L) in the formula [MHL]. The ligands used were (phen)(ClO₄) and 2-[(E)-(hydroxyamino)methyl], and they reacted in varying mole ratios. The synthesized complexes were classified based on various analytical techniques, including UV-

visible spectroscopy, (NMR), (FT-IR), thermal analysis, and matrix-assisted laser desorption/ionization time-of-flight (MALDI-TOF) mass spectrometry. The ligands used in the synthesis were referred to as mono-nuclear ligands. The complexes containing Ni^{2+} and Mn^{2+} ions exhibited distorted octahedral geometry, whereas the complexes containing Cu^{2+} and Zn^{2+} ions displayed distorted square-pyramidal geometry. The investigation also encompassed an examination of the complexes' capacity to scavenge superoxide, with subsequent determination of their IC_{50} values. Among the examined complexes, it was observed that the Cu^{2+} ion complex exhibited the highest activity and the lowest IC_{50} value" [101].

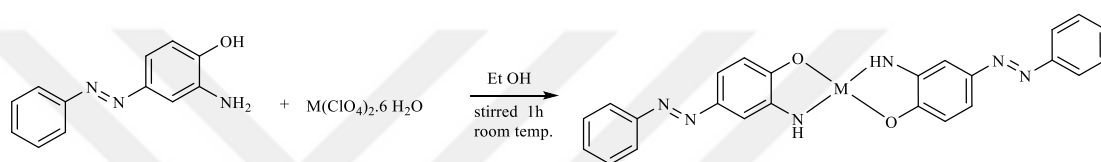


Figure 2.17. Synthesis of hetero-ligand complexes with some transition metal.

In 2021, Salman clarified that “a series of transition metal complexes were synthesized by incorporating several transition metal ions, namely Cr^{3+} , Ni^{2+} , Cu^{2+} , Co^{3+} , and Fe^{3+} , with 1,3,4-thiadiazole moiety ligands. The synthesized complexes were characterized using elemental analysis, ^1H NMR, mass spectroscopy, and IR techniques. Based on these analyses, it was seen that the complexes containing Cu^{2+} and Ni^{3+} ions exhibited a tetrahedral geometry, while the complexes containing Cr^{3+} , Co^{3+} , and Fe^{3+} ions displayed an octahedral geometry. The synthesized compounds were subjected to testing for antibacterial activity through the determination of inhibitory zones against *Staphylococcus aureus* and *E. coli* bacteria. Dimethyl sulfoxide (DMSO) was employed as the solvent for these experiments” [102].

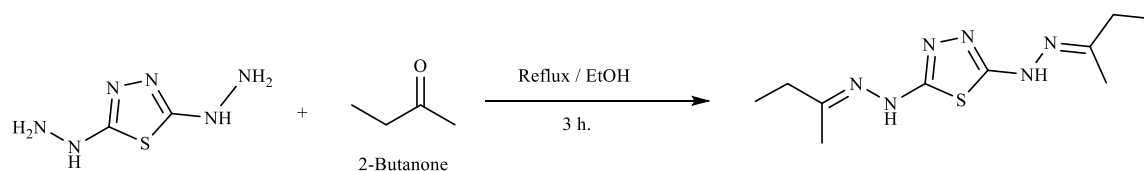


Figure 2:18 Synthesis of a complex ligand with some transition metal.

In 2021, Erdogan et al. clarified that “in this study, a series of metal ion complexes were synthesized by employing transition metals, specifically nickel (Ni^{2+}) and cobalt

(Co²⁺), along with 1,3,4-thiadiazole derivatives. The synthesis process used the reaction of acyl halide derivatives with a compound known as "2-(5-amino-1,3,4-thiadiazol-2-yl) thio)-1-(3,4-dichlorophenyl) ethanone". The identification of all produced complexes and ligands was accomplished by the utilization of various analytical techniques, including ¹³C NMR, FTIR, ¹H NMR, and mass spectroscopy. The complex produced by the Ni²⁺ ion and Co²⁺ ion exhibited an octahedral geometry that deviated from the ideal shape” [103].

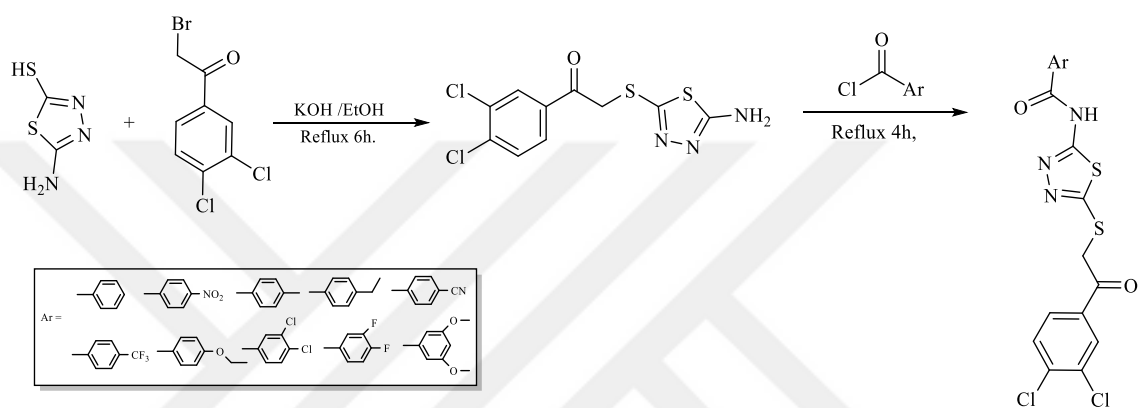


Figure 2.19. Preparation of 1,3,4-thiadiazole derivatives and their complexes with some transition metal.

In 2020, Freitas et al. explained that “a series of 1,3,4-thiadiazole derivatives were synthesized and developed utilizing N-arylhydrazone or N-aminobenzyl compounds as starting materials. The trypanomastigote stage of *Trypanosoma cruzi* was subjected to comprehensive testing across all derivatives, and the resulting IC₅₀ values were subsequently presented. The imine portion of the hydrazine moiety, which is connected to the 2-pyridinyl segment, demonstrated pharmacophoric properties that suggest potential trypanocidal activity within this series” [104].

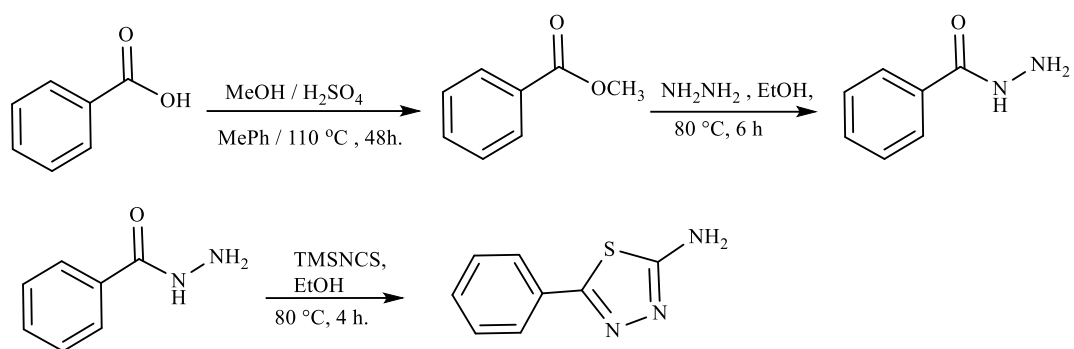


Figure 2.20. 1,3,4-thiadiazole synthesis.

PART 3

EXPERIMENTAL SECTION

3.1. DEVICES USED IN THIS STUDY

The ligands synthesized in this work were analyzed using $^1\text{H-NMR}$ at the laboratory of the Necmettin Erbakan University Science and Technology Research and Application Centre (BİTAM) using a Bruker Avance Core NMR spectrometer (400 MHz). The ligands $^1\text{H-NMR}$ spectra were recorded in a DMSO- d_6 solvent. Elemental studies of the substances were conducted using the LECO 932 CHNS equipment from St. Joseph, MI, USA. The FT-IR spectra of the synthesized complex compounds were analyzed using the ID7 model ATR apparatus on the Thermo Nicolet IS5 model FT-IR device in the Department of Chemistry, Faculty of Science, Karabuk University. The complexes' magnetic susceptibility was measured at Selçuk University Faculty of Science using the Gouy method with $\text{Hg}[\text{Co}(\text{SCN})_4]$ as the calibrant on the Sherwood Scientific MX Gouy apparatus. The compounds were analyzed using a HITACHI brand STA7300 model Thermal Analysis System instrument at Karabuk University MARGEM, including TGA and pH-meter measurements. Milwaukee, Karabuk University, Faculty of Science, Department of Chemistry, specialized in electrothermal and UV-vis analysis using Genesys 10s.

3.2. CHEMICALS USED IN THIS STUDY

We used in this study: Diphenyl Ether (Merck), chloroacetyl chloride (Merck), Aluminum chloride (Merck), Dichloro Methane (Merck), Butyl nitrite (Merck), Concentrated Sulphuric Acid (Sigma), N,N-Diisopropylethylamine (Merck), Methanol (Sigma), Ethanol (Sigma), Acetone (Sigma), Diethyl ether (Merck), Sodium Bicarbonate (Merck), Sodium Chloride (Merck), hydroxylamine hydrochloride (Merck). Substituents “(5-(4-chlorobenzyl)-1,3,4-thiadiazol-2-amine, 5-(3,4-dichlorobenzyl)-1,3,4-thiadiazol-2-amine and 5-(4-bromobenzyl)-1,3,4-thiadiazol-2-amine” used in this study were synthesized according to literature [65], by

Mojahid Salah Ibrahim ALI, a PhD student of Prof. Dr. Şaban UYSAL, who is also the advisor of this thesis.

3.3. THE FORMULA OF SYNTHESIZED LIGANDS IN THIS STUDY

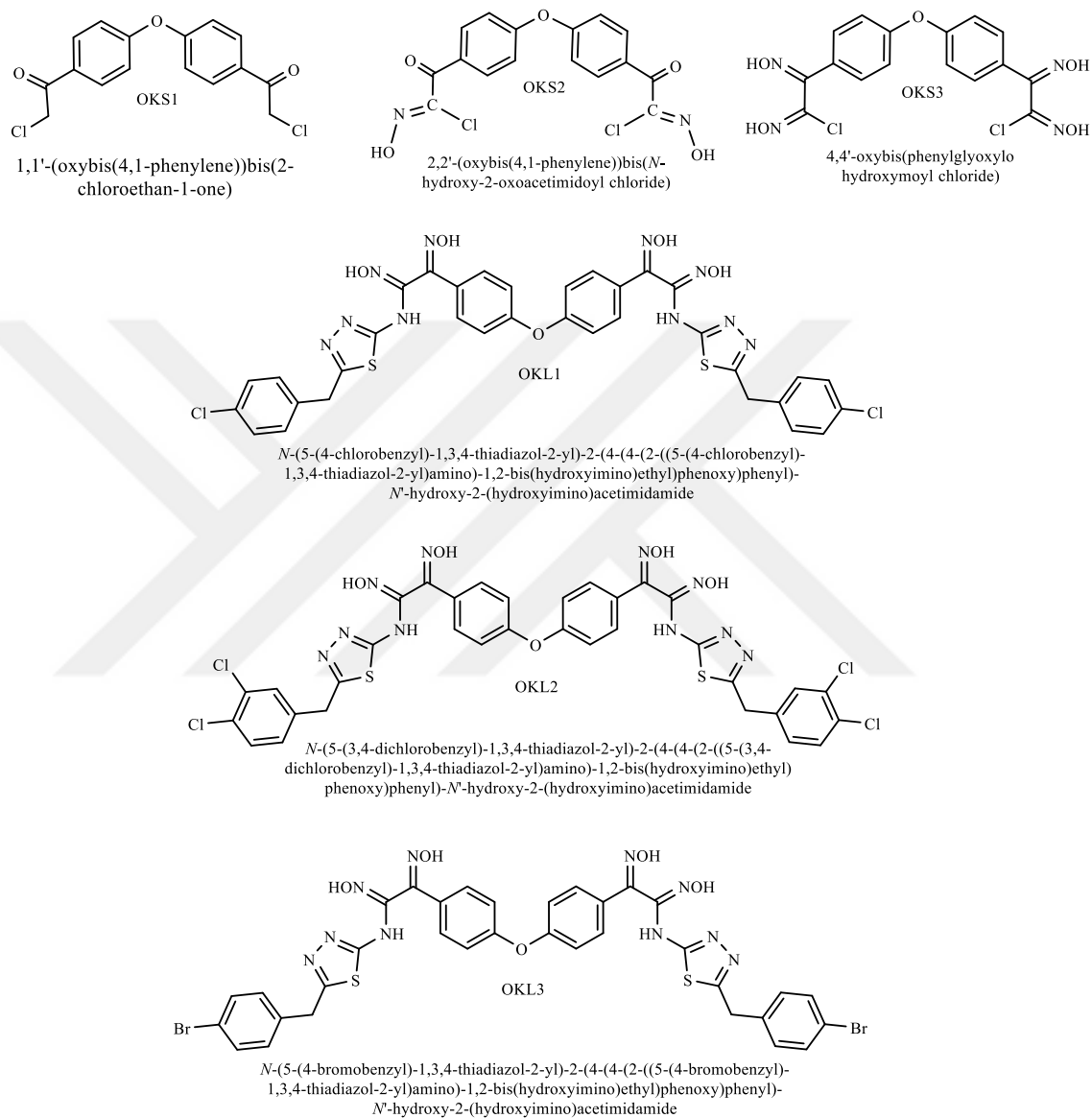


Figure 3.1. The formula of synthesized ligands in this study.

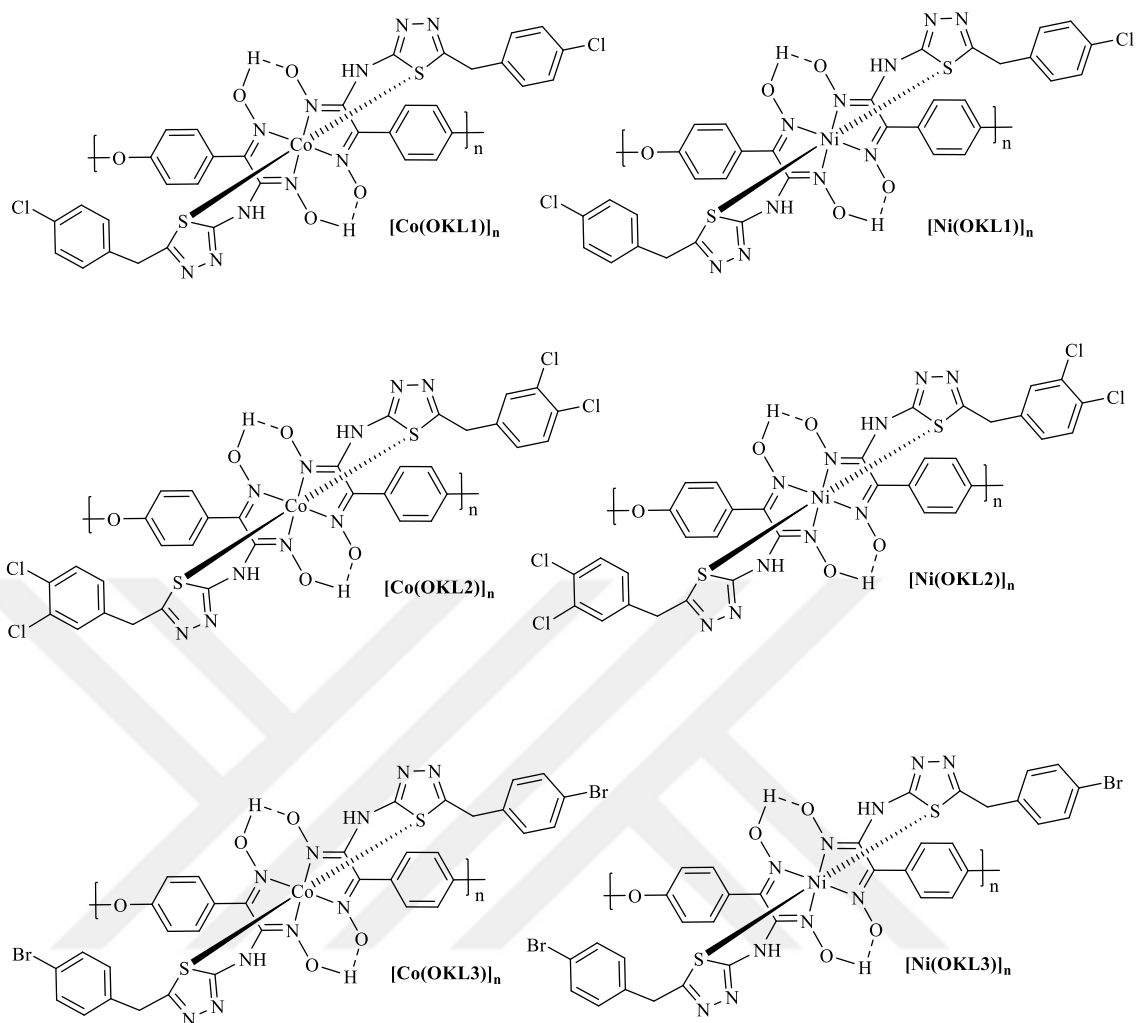


Figure 3.2. The formula of synthesized complexes in this study.

3.4. SYNTHESIS METHODS OF ALL COMPOUNDS

3.4.1. Synthesis Methods of Starting Compound

3.4.1.1. Synthesis of 1,1'-(Oxybis(4,1-phenylene))bis(2-chloroethane) [OKS1]

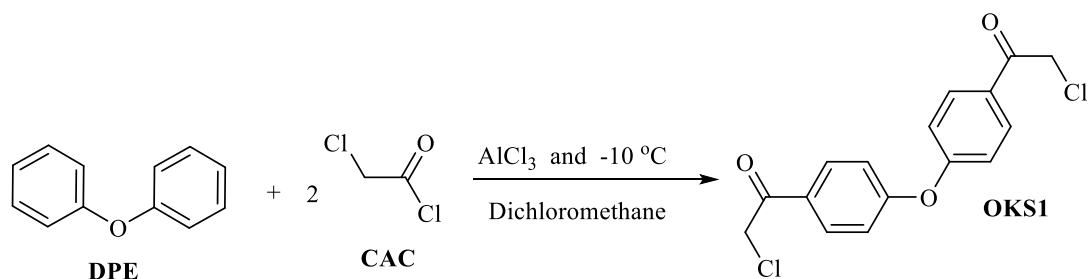


Figure 3.3. Synthesis reaction of “OKS1” coded compound.

of concentrated sulfuric acid is placed in a dropping funnel, the acid is dropwise onto a round glass containing sodium chloride to release hydrochloric acid gas, and the gas is passed over the above mixture for 30 min. After 30 min, added 3 mL (22 mmol) of butyl nitrite in a dropping funnel, dissolved in 21 mL of chloroform, and drop the mixture for 90 min. Hydrochloric acid gas is continued after the end of the butyl nitrite dropping on the mixture for 3 h. Leave the mixture at room temperature to dry for 24 hr. The sample is evaporated and then recrystallized using ether and N-hexane to obtain a yellowish white substance, the substance is highly soluble in diethyl ether, ethyl alcohol, dimethylformamide, dimethyl sulfoxide and acetone and slightly soluble in dichloromethane.

3.4.1.3. Synthesis Methods of 4,4'-Oxybis (phenylglyoxylohydroxymoyl Chloride) (OKS3)

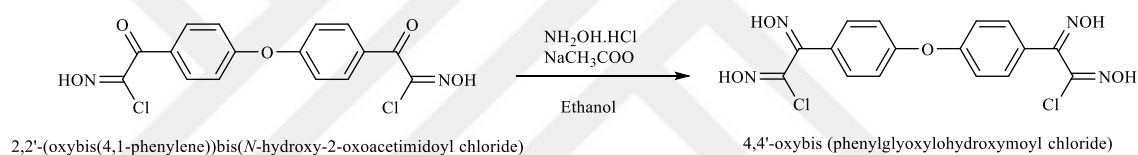


Figure 3.5. Synthesis reaction of “OKS3” coded compound.

OKS3: M.W.= 411.20, Color: white; Produce: (50%); M.P.: 229-232 °C. This substance was synthesized according to literature [91]. 7.62 g (20 mmol) of 4,4'-oxybis (phenylglyoxylohydroxymoylchloride) was dissolved in 25 mL of ethanol, followed by 3.06 g (44 mmol) of NH_2OH . The minimum water solution of HCl was added. This solution was mixed at 40 °C for 6 h and then left to stand on its own for 5 days. The white precipitate was filtered and crystallized with ethanol. The substance is very soluble in dimethylformamide, dimethyl sulfoxide, and acetone and slightly soluble in diethyl ether, ethyl alcohol, chloroform, and dichloromethane.

3.4.1.4. General Synthesis Procedure of Ligands (OKL1-OKL3)

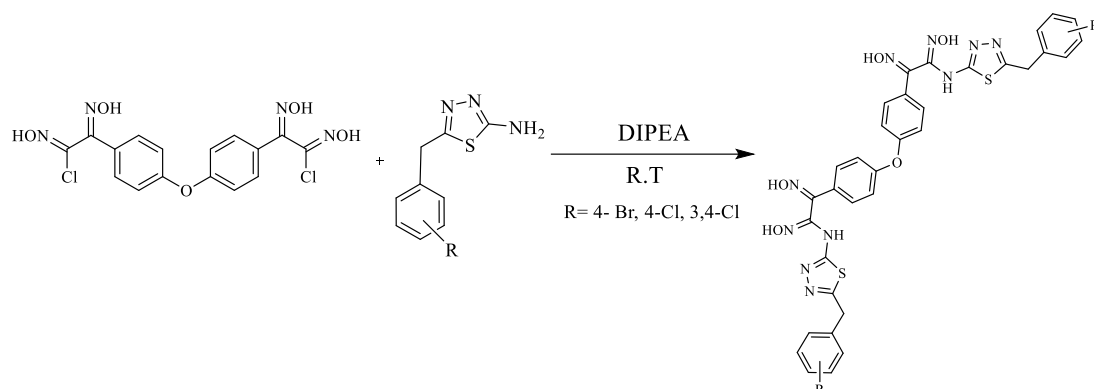


Figure 3.6. General synthesis reaction of target ligands (OKL1-OKL3).

This substance, which is not available in the literature, was synthesized according to similar literature [91]. 0.2055 g (0.5 mmol) of 4,4'-oxybis(chlorophenylglyoxime) was dissolved in 25 mL of ethanol alcohol. The 1,3,4-thiadiazol compounds (5-(4-chlorobenzyl)-1,3,4-thiadiazol-2-amine, 5-(3,4-dichlorobenzyl)-1,3,4-thiadiazol-2-amine or 5-(4-bromobenzyl)-1,3,4-thiadiazol-2-amine) were added (1mmol) and dissolved with the smallest possible amount of ethanol alcohol in the form of a drop by drop at room temperature. The reactions were left for 3 hours to move until the color of the solution became yellow. After that, water was added to the solutions for the substance to precipitate and they were left. Until they dry, then they are recrystallized with a mixture of alcohol and water.

OKL1: M.W.= 789.67, Color: Yellow; Produce: 2.8 g (67%); M.P.: 153-156 °C. FT-IR(ATR, cm^{-1}): 2848, 2990 (C-H_{aliph.}), 3175 (C-H_{arom.}), 1638 (C=N_{th}), 1593 (C=N_{ox}), 1412,1455,1493 (C-C_{arom.}), 1168 (DFE), 3336 (N-H_{sec.}), 973,1013 (N-O_{ox}); ¹H NMR (400 Mhz, DMSO-d₆): 4.13 ppm (s, 4H for H_d), 7.04 ppm (s, 2H for H_c), 12.76 ppm (s, 2H for H_g), 11.31 ppm (s, 2H for H_h), 7.22,7.28,7.33,7.38 ppm (d, 4H for H_a,H_e,H_f,H_b) ; ¹³C NMR (100 MHz, DMSO-d₆): 137.50 ppm 2C for C1; 128.56 ppm 4C for C2; 129.02 ppm 4C for C3; 128.70 ppm 2C for C4; 169.35 ppm 2C for C5; 131.81 ppm 2C for C6; 131.94 ppm 2C for C7; 157.35 ppm 2C for C8; 35.08 ppm 2C for C9; 131.53 ppm 2C for C10; 131.06 ppm 4C for C11; 128.80ppm 4C for C12; 130.98 ppm 2C for C13; Anal. Calculated/Found: C: 51.71/51.67, N: 17.74/17.69, H: 3.32/3.28, S: 8.12/8.09.

OKL2: M.W.= 858.55, Color: Yellow; Produce: 3.1 g (69%); M.P.: 134-137 °C. FT-IR(ATR, cm^{-1}): 2849, 2919, 2977 (C-H_{aliph.}), 3104 (C-H_{arom.}), 1638 (C=N_{th}), 1594 (C=N_{ox}), 3291 (O-H), 1416,1469,1496 (C-C_{arom.}), 3324 (N-H_{sec.}), 1170 (DFE) 975,1011 (N-O_{ox}); ¹H NMR (400 Mhz, DMSO-d₆): 4.16 ppm (s, 4H for H_d), 7.07 ppm (s, 2H for H_c), 11.34 ppm (s, 2H for H_i), 13.01 ppm (s, 2H for H_h), 7.25,7.38 ppm (d, 4H for H_a,H_b), and 7.16,7.55 ppm (d, 2H for H_g,H_f) 7.58 (s, 2H for H_e); ¹³C NMR (100 MHz, DMSO-d₆): 139.58 ppm 2C for C1; 119.12 ppm 4C for C2; 129.60 ppm 4C for C3; 128.65 ppm 2C for C4; 131.33 ppm 2C for C5; 169.40 ppm 2C for C6; 131.48 ppm 2C for C7; 156.60 ppm 2C for C8; 34.59 ppm 2C for C9; 131.19 ppm 2C for C10; 129.72 ppm 2C for C11; 129.95 ppm 2C for C12; 130.82 ppm 2C for C13; 131.13 ppm 2C for C14; 130.14 ppm 2C for C15; Anal. Calculated/Found: C: 49.55/49.48, N: 17.00/16.95, H: 3.06/3.05, S: 7.78/7.75.

OKL3: M.W.= 878.58, Color: Yellow; Produce: 3.3 g (72%); M.P.:115-120 °C. FT-IR(ATR, cm^{-1}): 2991 (C-H_{aliph.}), 3099 (C-H_{arom.}), 1638 (C=N_{th}), 1594 (C=N_{ox}), 3269 (O-H), 1404, 1421, 1486 (C-C_{arom.}), 3321 (N-H_{sec.}), 1071 (DFE) 973,1011 (N-O_{ox}); ¹H NMR (400 MHz, DMSO-d₆): 4.13 ppm (s, 4H for H_d), 7.06 ppm (s, 2H for H_c), 13.01 ppm (s, 2H for H_g), 11.34 ppm (s, 2H for H_h), 7.16,7.26,7.48,7.53 ppm (d, 4H for H_a,H_e,H_b,H_f); ¹³C NMR (100 MHz, DMSO-d₆): 137.93 ppm 2C for C1; 120.42 ppm 4C for C2; 131.42 ppm 4C for C3; 131.36 ppm 2C for C4; 131.94 ppm 2C for C5; 169.33 ppm 2C for C6; 132.20 ppm 2C for C7; 157.25 ppm 2C for C8; 35.15 ppm 2C for C9; 131.71 ppm 2C for C10; 131.62 ppm 4C for C11; 131.49 ppm 4C for C12; 128.72 ppm 2C for C13; Anal. Calculated/Found: C: 46.48/46.45, N: 15.94/15.92, H: 2.98/2.97, S: 7.30/7.26.

3.4.1.5. General Synthesis Procedure of Co(II) and Ni(II) Complexes of The Ligands (OKL1-OKL)

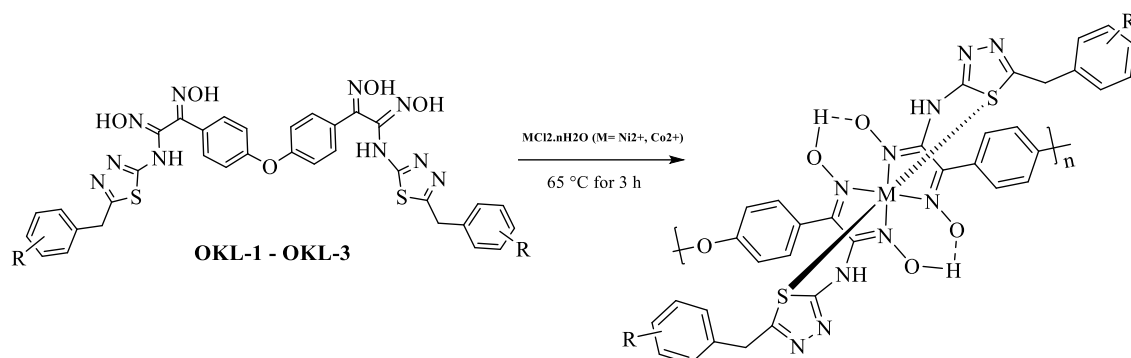


Figure 3.7. General synthesis reaction of Co(II) and Ni(II) complexes of target ligands.

(5.0 mmol) of (OKL1-OKL3) dissolved in 25 mL of ethanol, and a solution of (5.0 mmol) of $MCl_2 \cdot nH_2O$ ($M = Ni^{2+}, Co^{2+}$) in the minimum possible amount of the same solvent was added. The mixture was stirred at 65 °C for 3 h. pH was 2.5-3.0 in the end of the reaction. pH was adjusted to 5.5-6.0. After that, precipitate was formed, then was left in the water bath at 50 °C for 2 h to mature. The precipitate was filtered and dried under vacuum.

[Co(OKL1)]*n*: M.W.= 876.56, Color: Brown solid; D.P.: 178-183 °C; $\mu_{eff} = 1.79$ B.M.; FT-IR(ATR, cm^{-1}): 2980 (C-H_{aliph.}), 3168 (C-H_{arom.}), 1670 (C=N_{th}), 1595 (C=N_{ox}), 3525 (H-O...H), 1407, 1490 (C-C_{arom.}), 3392 (N-H_{sec.}), 1169 (DFE), 1015, 1048 (N-O_{ox}); 515 (Co-N), 486 (Co-O) Anal. Calculated/Found: C: 49.32/49.28, N: 15.98/15.95, H: 3.45/3.42, S: 7.31/7.30, Co: 6.72/6.70

[Ni(OKL1)]*n*: M.W.= 876.41, Color: Brown solid; D.P.: 195-200 °C; $\mu_{eff} = 2.85$ B.M.; FT-IR(ATR, cm^{-1}): 2980 (C-H_{aliph.}), 3113, 3174 (C-H_{arom.}), 1646 (C=N_{th}), 1603 (C=N_{ox}), 3513 (H-O...H), 1408, 1466, 1490, 1530 (C-C_{arom.}), 3421(N-H_{sec.}), 1171 (DFE), 991,1015 (N-O_{ox}); 512 (Ni-N), 443 (Ni-O) Anal. Calculated/Found: C: 49.34/49.31, N: 15.98/15.96, H: 3.45/3.44, S: 7.32/7.30, Ni: 6.70/6.67

[Co(OKL2)]*n*: M.W.= 945.54, Color: Brown solid; D.P.: 165-170 °C; $\mu_{eff} = 1.77$ B.M.; FT-IR(ATR, cm^{-1}): 3089 (C-H_{arom.}), 1666 (C=N_{th}), 1595 (C=N_{ox}), 1420, 1468, 1495, 1517 (C-C_{arom.}), 3270 (O-H), 3400 (N-H_{sec.}), 3521 (H-O...H), 1169 (DFE),

1013,1031 (N-O_{ox}); 515 (Co-N), 462 (Co-O) Anal. Calculated/Found: C: 45.73/45.70, N: 11.81/11.78, H: 2.98/2.97, S: 6.78/6.76, Co: 6.23/6.20

[Ni(OKL2)]n: M.W.= 945.30, Color: Brown solid; D.P.: 180-185 °C; $\mu_{\text{eff}}=2.84$ B.M.; FT-IR(ATR, cm⁻¹): 2931, 2976 (C-H_{aliph.}), 3094, 3152 (C-H_{arom.}), 1670 (C=N_{th}), 1595 (C=N_{ox}), 3506 (H-O...H), 1420, 1467, 1495 (C-C_{arom.}), 3270 (N-H.) and (O-H) broad, 1170 (DFE), 1011, 1031 (N-O_{ox}); 512 (Ni-N), 462 (Ni-O) Anal. Calculated/Found: C: 45.74/45.71, N: 14.82/14.80, H: 2.99/2.98, S: 6.78/6.75, Ni: 6.21/6.19

[Co(OKL3)]n: M.W.= 965.56, Color: Brown solid; D.P.: 153-159 °C; $\mu_{\text{eff}}=1.78$ B.M.; FT-IR(ATR, cm⁻¹): 2927, 2982 (C-H_{aliph.}), 3098 (C-H_{arom.}), 1666 (C=N_{th}), 1594 (C=N_{ox}), 3521 (H-O...H), 3273 (O-H), 1405, 1417, 1486, 1515 (C-C_{arom.}), 1169 (DFE), 3323 (N-H_{sec.}), 1012, 1043 (N-O_{ox}); 509 (Co-N), 477 (Co-O) Anal. Calculated/Found: C: 44.78/44.76, N: 14.51/14.48, H: 3.13/3.11, S: 6.64/6.61, Co: 6.10/6.08

[Ni(OKL3)]n: M.W.= 965.32, Color: Brown solid; D.P.: 178-184 °C; $\mu_{\text{eff}}=2.85$ B.M.; FT-IR(ATR, cm⁻¹): 2988 (C-H_{aliph.}), 3056, 3161 (C-H_{arom.}), 1675 (C=N_{th}), 1594 (C=N_{ox}), 1169 (DFE), 1405, 1454, 1487 (C-C_{arom.}), 3335 (N-H.) and (O-H) broad, 1011,1032 (N-O); 514 (Ni-N), 477 (Ni-O) Anal. Calculated/Found: C: 44.79/44.77, N: 14.51/14.49, H: 3.13/3.11, S: 6.64/6.61, Ni: 6.08/6.06

PART 4

RESULTS AND DISCUSSION

4.1. CHEMICAL EVALUATION OF ALL COMPOUNDS

In this study, diphenyl ether (DPE) was used as the main starting material. 4,4'-bis(chloroacetyl)diphenyl ether (C₁₆H₁₂Cl₂O₃) (OKS1) was produced through the reaction of diphenyl ether and chloroacetylchloride in chloroform media according to literature [91]. Then, (Z)-2-(4-(4-((E)-2-chloro-2-(hydroxyimino)acetyl)phenoxy)phenyl)-N-hydroxy-2-oxoacetimidoyl chloride (OKS2) was synthesized from the reaction of “OKS1” and butyl nitrite at 0 °C in a chloroform medium, catalyzed by hydrogen chloride gas. And then, (1Z,2E)-2-(4-(4-((1E,2E)-2-chloro-1,2-bis(hydroxyimino)ethyl)phenoxy)phenyl)-N-hydroxy-2-(hydroxyimino)acetimidoyl chloride (OKS3) synthesized from the reaction of “OKS2” and hydroxylaminehydrochloride at 40 °C in an ethanol media. To characterize the products obtained, melting point determination, ¹H and ¹³C NMR, and FTIR analyses were performed and confirmed the structure. The stretching bands at 1600 cm⁻¹ for C=N_{oxime}, 989 and 1032 cm⁻¹ for N-O_{oxime} in the FTIR spectrum, the signal 13.64 and 11.30 ppm for NOH protons, and range of 7.11-7.93 ppm for aromatic C-H protons in the ¹H NMR spectrum confirmed that the OKS3-encoded starting compound was successfully synthesized [91]. It was seen that the spectral data obtained from the starting compounds are in good harmony with the literature. These target ligands were synthesized from the reaction of “OKS3” and 2-amino-1,3,4-thiadiazole derivatives at room temperature in an ethanol media. To characterize the functional group structures of the obtained target ligands FTIR analyses were performed.

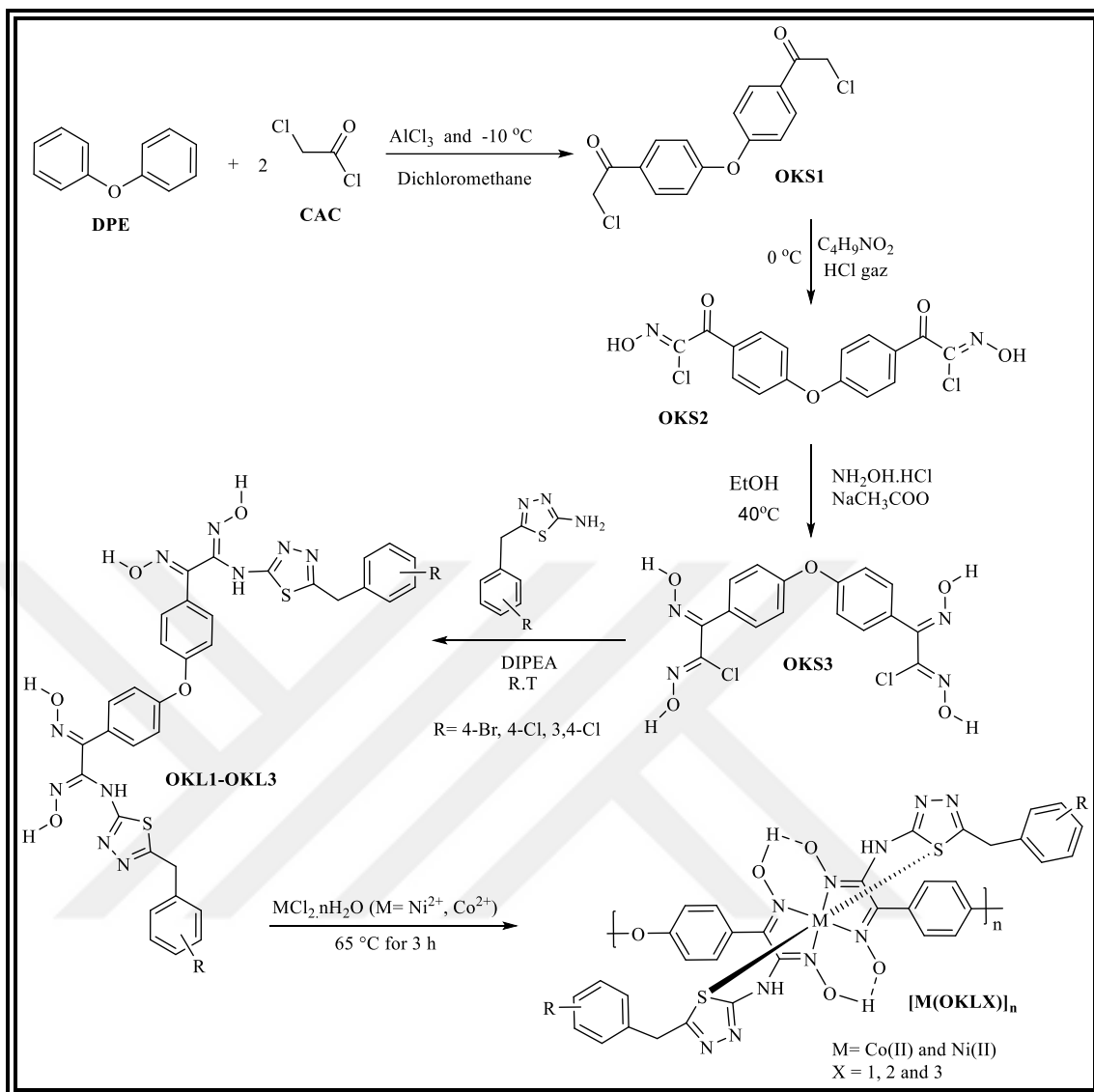


Figure 4.1. Synthetic route of all ligands and complexes.

In the ^1H NMR spectra of target ligand (OKL1), observation of the singlet signals at 4.13 ppm (4 H_d) for $-\text{CH}_2\text{-Ph}$, the singlet signal at 7.04 ppm (2 H_c) for $-\text{NH-Th}$, the singlet signal at 12.76 ppm (2 H_g) and 11.31 ppm (2 H_h) for OH_{oxime} groups, and the doublet signals at 7.22 ppm (4 H_a), 7.28 ppm (4 H_e), 7.33 ppm (4 H_f), 7.38 ppm (4 H_b) for aromatic C-H proved that the OKL1-encoded ligand was successfully synthesized (Figure 4.2). In the ^{13}C NMR spectrum of OKL1, The signals are observed at 137.50 ppm 2C for C1; 128.56 ppm 4C for C2; 129.02 ppm 4C for C3; 128.70 ppm 2C for C4; 169.35 ppm 2C for C5; 131.81 ppm 2C for C6; 131.94 ppm 2C for C7; 157.35 ppm 2C for C8; 35.08 ppm 2C for C9; 131.53 ppm 2C for C10; 131.06 ppm 4C for C11; 128.80 ppm 4C for C12; 130.98 ppm 2C for C13. The identification of these

chemical shift values serves as compelling evidence substantiating the successful synthesis of the original OKL1 coded target ligand (Figure 4.3) [6, 38, 65, 88, 90-95, 98-103].

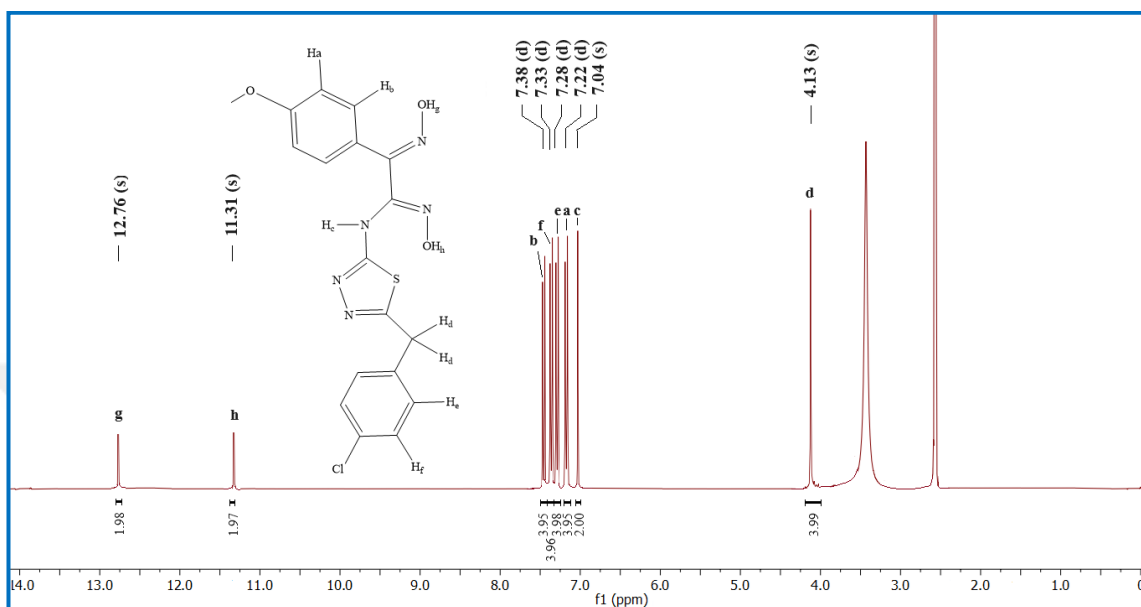


Figure 4.2. ^1H NMR Spectrum of OKL1.

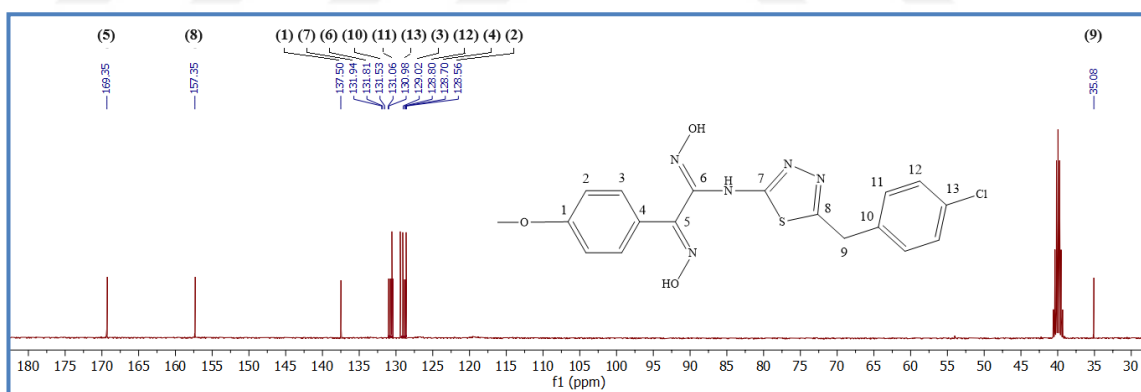


Figure 4.3. ^{13}C NMR Spectrum of OKL1.

In the ^1H NMR spectra of target ligand (OKL2), observation of the singlet signals at 4.16 ppm (4 H_d) for $-\text{CH}_2\text{-Ph}$, the singlet signal at 7.07 ppm (2 H_c) for $-\text{NH-Th}$, the singlet signal at 11.34 ppm (2 H_i) and 13.01 ppm (2 H_h) for OH_{oxime} groups, and the doublet signals at 7.16 ppm (2 H_g), 7.25 ppm (4 H_a), 7.38 ppm (4 H_b), 7.55 ppm (2 H_f) for aromatic C-H, and the singlet signal at 7.58 ppm (2 H_e) for aromatic C-H proved that the OKL2-encoded ligand was successfully synthesized (Figure 4.4). In the ^{13}C

NMR spectrum of OKL2, the signals are observed at 139.58 ppm 2C for C1; 119.12 ppm 4C for C2; 129.60 ppm 4C for C3; 128.65 ppm 2C for C4; 131.33 ppm 2C for C5; 169.40 ppm 2C for C6; 131.48 ppm 2C for C7; 156.60 ppm 2C for C8; 34.59 ppm 2C for C9; 131.19 ppm 2C for C10; 129.72 ppm 2C for C11; 129.95 ppm 2C for C12; 130.82 ppm 2C for C13; 131.13 ppm 2C for C14; 130.14 ppm 2C for C15. The identification of these chemical shift values serves as compelling evidence substantiating the successful synthesis of the original OKL2 coded target ligand (Figure 4.5) [6, 38, 65, 88, 90-95, 98-103].

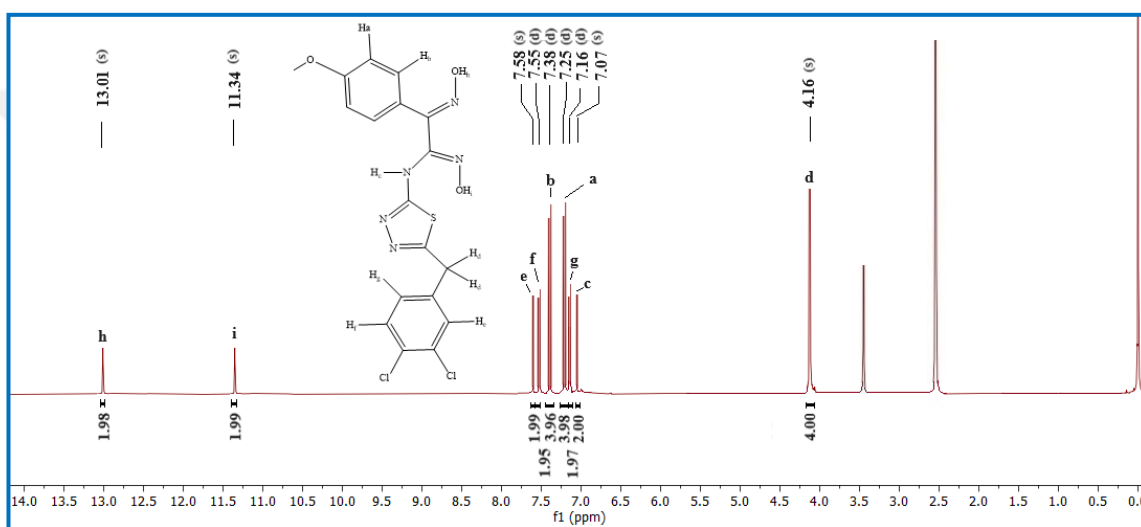


Figure 4.4. ^1H NMR Spectrum of OKL2.

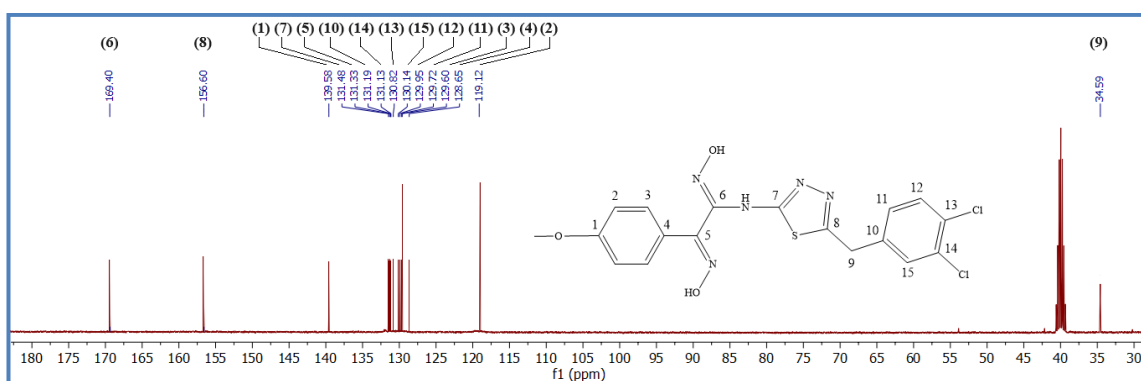


Figure 4.5. ^{13}C NMR Spectrum of OKL2.

As for evaluating the ^1H NMR spectra of target ligand (OKL3), observation of the singlet signals at 4.13 ppm (4H_d) for $-\text{CH}_2\text{-Ph}$, the singlet signal at 7.06 ppm (2H_c) for $-\text{NH-Th}$, the singlet signal at 13.01 ppm (2H_g) and 11.34 ppm (2H_h) for OH_{oxime}

groups, and the doublet signals at 7.16 ppm (4H_a), 7.26 ppm (4H_e), 7.48 ppm (4H_b), 7.53 ppm (4H_f), for aromatic C-H proved that the OKL3-encoded ligand was successfully synthesized (Figure 4.6). In the ¹³C NMR spectrum of OKL3, the signals are observed at 137.93 ppm 2C for C1; 120.42 ppm 4C for C2; 131.42 ppm 4C for C3; 131.36 ppm 2C for C4; 131.94 ppm 2C for C5; 169.33 ppm 2C for C6; 132.20 ppm 2C for C7; 157.25 ppm 2C for C8; 35.15 ppm 2C for C9; 131.71 ppm 2C for C10; 131.62 ppm 4C for C11; 131.49 ppm 4C for C12; 128.72 ppm 2C for C13. The identification of these chemical shift values serves as compelling evidence substantiating the successful synthesis of the original OKL3 coded target ligand (Figure 4.7) [6, 38, 65, 88, 90-95, 98-103].

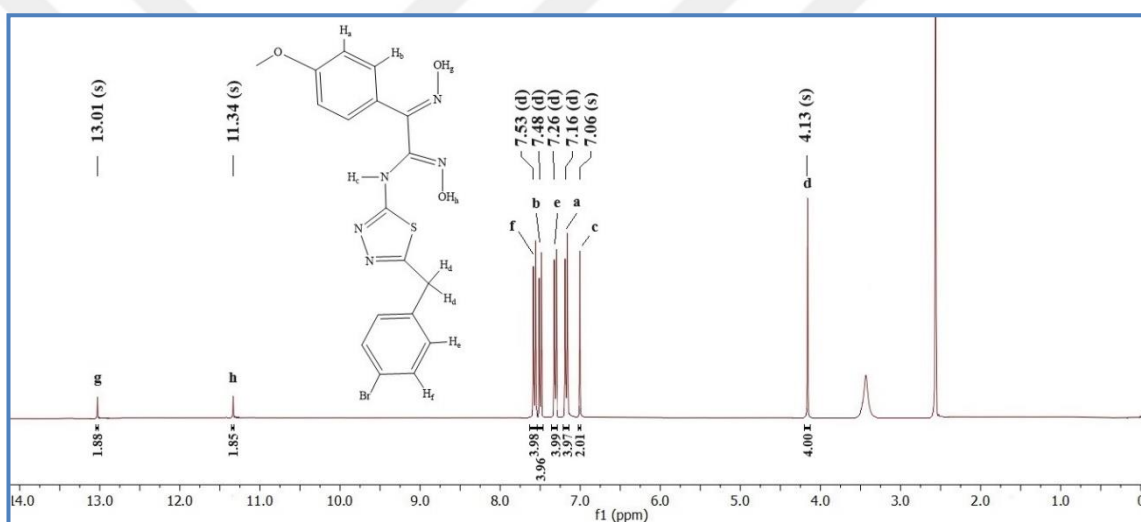


Figure 4.6. ¹H NMR Spectrum of OKL3.

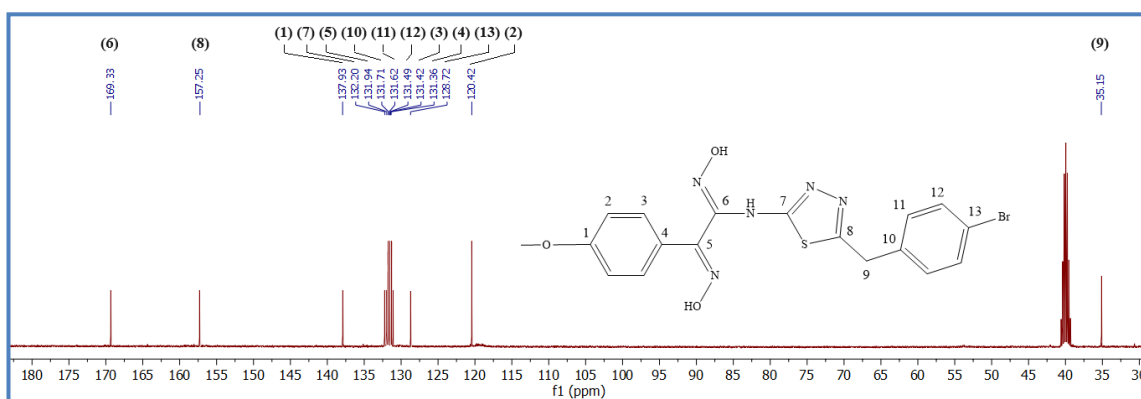


Figure 4.7. ¹³C NMR Spectrum of OKL3.

When we evaluate the FTIR spectra of target ligands, the band Noticed at 1594 cm^{-1} for the $\text{C}=\text{N}_{\text{oxime}}$ group of the starting compound was Noticed at an average of 5 cm^{-1} lower frequency for the target ligands. In addition, the thiadiazole ring stretching bands were observed at $1636, 1635, 1638\text{ cm}^{-1}$, and N-O stretching bands were observed at $973, 1013; 975, 1011; 973, 1011\text{ cm}^{-1}$ for OKL1, OKL2 and OKL3 encoded ligands, respectively, verified that the compounds were successfully synthesized (Figure 4.8- Figure 4.10) [6, 38, 65, 88, 90-95, 98-103].

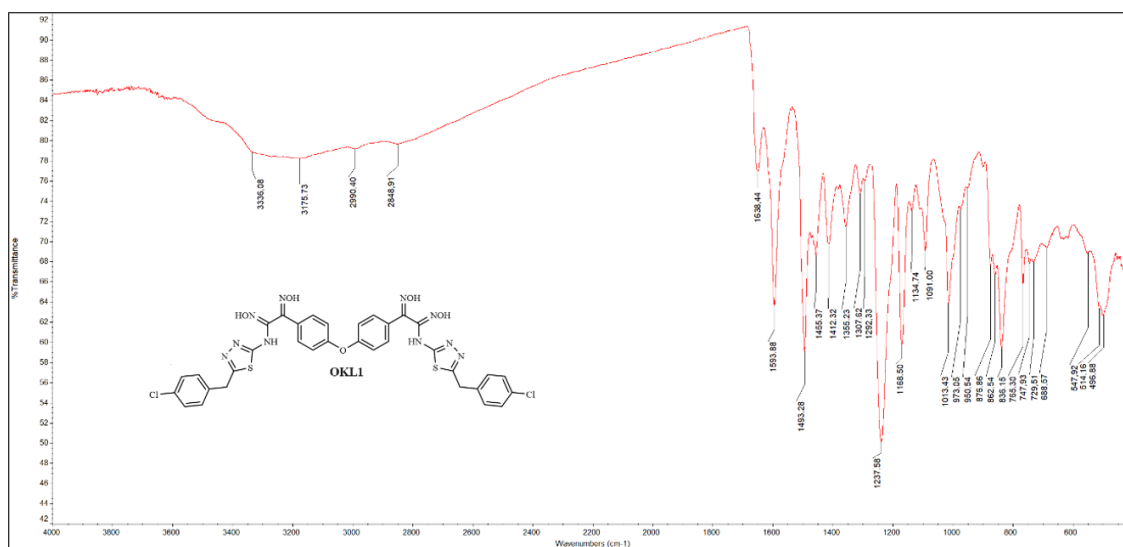


Figure 4.8. FTIR Spectrum of OKL1.

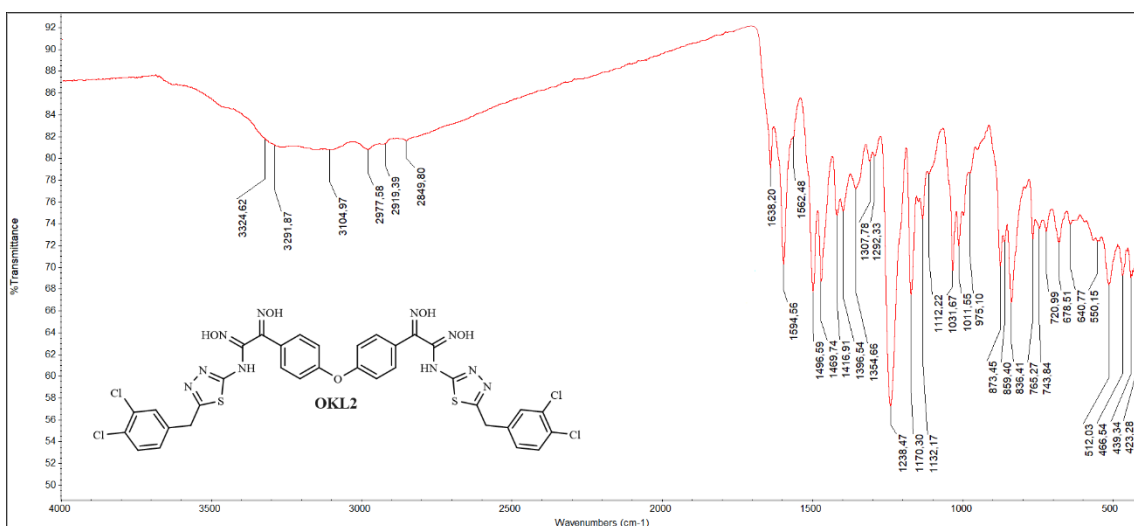


Figure 4.9. FTIR Spectrum of OKL2.

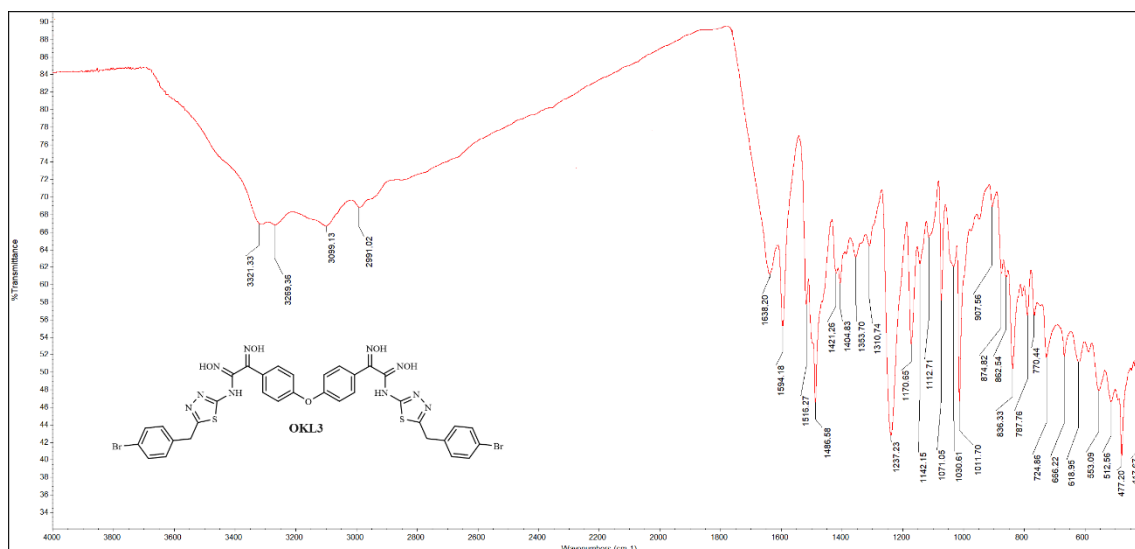


Figure 4.10. FTIR Spectrum of OKL3.

Finally, Co(II) and Ni(II) complexes of all ligands were obtained from the reaction of $\text{CoCl}_2 \cdot 6\text{H}_2\text{O}$ or $\text{NiCl}_2 \cdot 6\text{H}_2\text{O}$ and target ligands in an ethanol media at 65°C . When we evaluate the FTIR spectra of target complexes of the ligands, observation of the bands at the range of $3513\text{-}3523\text{ cm}^{-1}$ for O-H-O groups, observation of the bands at the range of $1011\text{-}1015\text{ cm}^{-1}$ and $1032\text{-}1050\text{ cm}^{-1}$ for N-O groups, and observation of the bands at the range of $1632\text{-}1636$ and $1594\text{-}1603\text{ cm}^{-1}$ for C=N groups, shift of N-O and C=N stretching bands to higher frequency by approximately $40\text{-}45\text{ cm}^{-1}$ and $30\text{-}35\text{ cm}^{-1}$, respectively, verified that the complexes were successfully synthesized (Figure A.1-Figure A.6) [6, 38, 65, 88, 90-95, 98-103].

4.2. PHYSICAL EVALUATION OF ALL COMPOUNDS

4.2.1. Evaluation of Magnetic Susceptibility Data

To elucidate the electronic structures and confirm the spin states of the synthesized complexes, molar magnetic susceptibilities (μ_{eff}) were measured at room temperature using a Gouy balance from Sherwood Scientific. Details of the experimental procedure are provided in the Experimental Section. The magnetic susceptibility measurements revealed low-spin configurations for all Co(II) and Ni(II) complexes, indicative of paramagnetic behavior. Co(II) complexes: $[\text{Co}(\text{OKL1})]_n$, $[\text{Co}(\text{OKL2})]_n$, $[\text{Co}(\text{OKL3})]_n$ exhibited magnetic moments of 1.79, 1.77, and 1.78 BM, respectively, consistent with the $t_{2g}^6 e_g^0$ configuration and outer-orbital complexation. These measured values can

be explained by the delocalization of an excess electron remaining on the Co^{2+} ion because of complexation onto the entire molecule via resonance. Ni(II) complexes: $[\text{Co}(\text{OKL1})]_n$, $[\text{Co}(\text{OKL2})]_n$, $[\text{Co}(\text{OKL3})]_n$ exhibited magnetic moments of exhibited high-spin configurations with magnetic moments of 2.85, 2.84, and 2.85 BM, respectively, corresponding to the $t_{2g}^6 e_g^2$ configuration [6, 38, 65, 88, 90-95, 98-103].

The observed μ_{eff} values can be attributed to octahedral coordination geometries around the metal centers. Slightly higher experimental values compared to theoretical calculations suggest paramagnetic ion spin interaction tendencies (magnetic coupling) between metal centers within the polymeric chains. These findings support the polymeric structures proposed for complexes [65, 91, 103].

4.2.2. Evaluation of Electrospray Ionization Mass Spectrometry (ESI-MS) Data of All Ligands

Electrospray ionization mass spectrometry (ESI-MS) confirmed the successful synthesis of the ligands. The experimental M/Z values for OKL1 were 788.08 (100%), 310.11 (25%), 275.11 (53%), 214.21(42%); for OKL2 were 858.55 (100%), 343.99 (57%), 275.11 (53%), 214.28 (37%); and for OKL3 were 877.99 (100%), 356.03 (8%), 295.27 (56%), 275.11(43%), respectively, which agreed well with their calculated molecular weights (Figure 4.11- Figure 4.13).

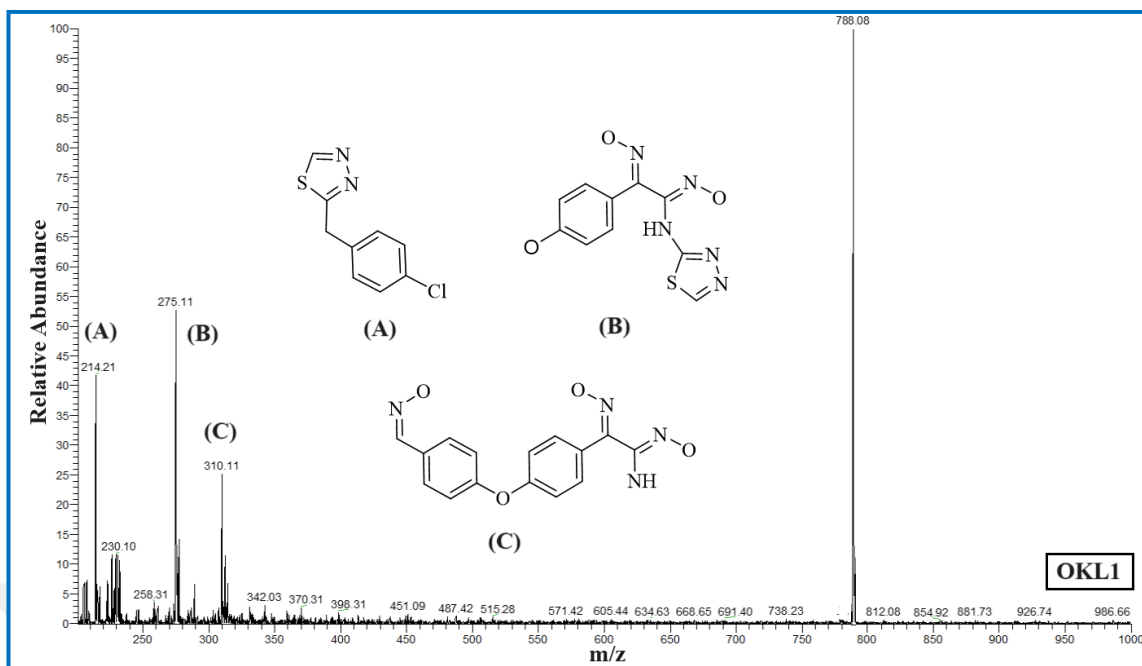


Figure 4.11: ESI-MS spectrum of OKL1.

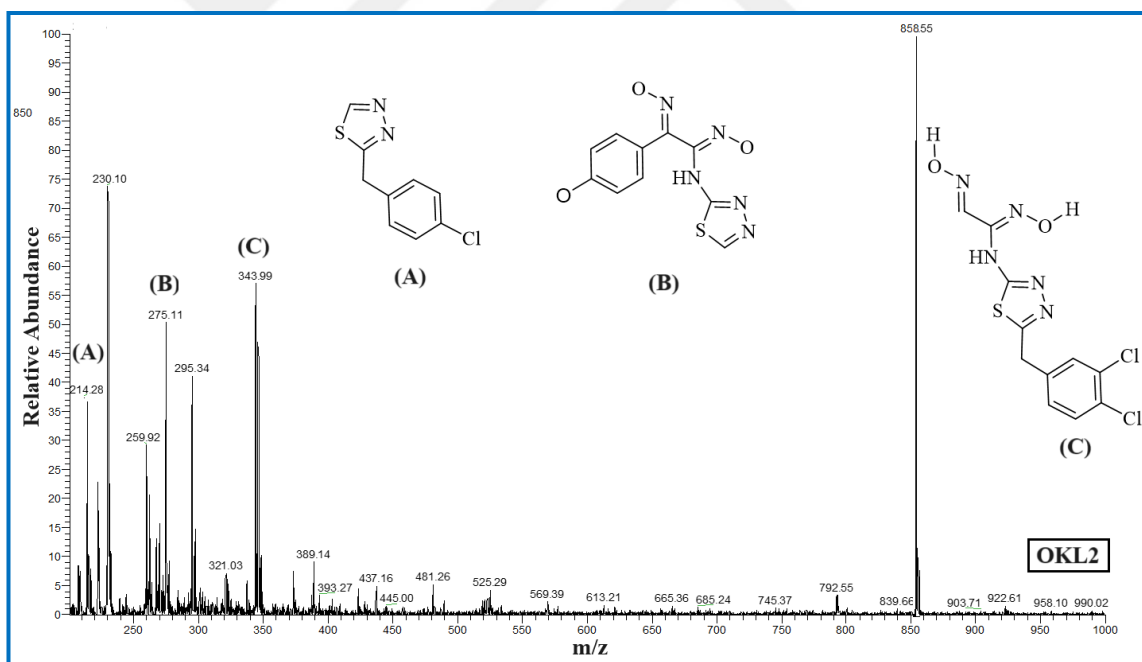


Figure 4.12: ESI-MS spectrum of OKL2.

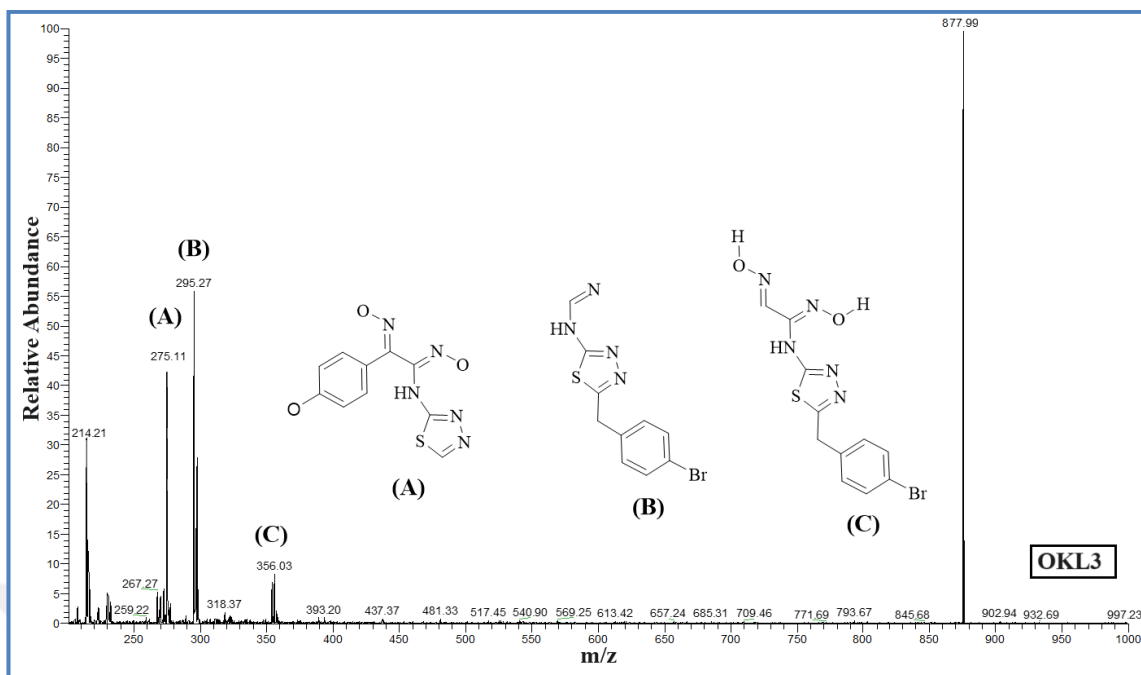


Figure 4.13: ESI-MS spectrum of OKL3.

4.2.3. Evaluation of Thermogravimetric Analysis Results

In this study, the thermal decomposition behavior and substituted functional groups of Ni(II) complexes of OKL1 and OKL3 ligands namely $[\text{Ni}(\text{OKL1})]_n$ and $[\text{Ni}(\text{OKL3})]_n$ were investigated. (TGA) Thermogravimetric analysis and (DTA) differential thermal analysis were conducted in a controlled N_2 environment at a heating rate of $10^\circ\text{C}/\text{min}$ from 25°C to 800°C . Before analysis, all samples were dried under vacuum at 60°C for 4 hours.

Upon examination of the TGA curve of the $[\text{Ni}(\text{OKL1})]_n$ complex, it can be observed that degradation occurred in four steps. The first degradation step occurred between $140\text{-}230^\circ\text{C}$ with a reduction in mass of 28.00%. The calculated theoretical reduction in mass for this step is 28.66%. The calculated and measured reduction in mass correspond to the mass of the 4-chlorobenzyl group, which separates from the main molecule. The second degradation step occurred between $250\text{-}340^\circ\text{C}$ with a reduction in mass of 21.95%. The calculated theoretical reduction in mass for this step is 22.62%. The calculated and measured reduction in mass corresponds to the mass of the 2-amino, 1,3,4-thiadiazole group, which separates from the main molecule. The third degradation step occurred between $390\text{-}495^\circ\text{C}$ with a reduction in mass of 19.00%.

The calculated theoretical reduction in mass for this step is 19.19%. The calculated and measured reduction in mass corresponds to the mass of the diphenyl ether group, which forms the polymer chain. The polymer chain is broken in this step. The final degradation step occurred between 510-600 °C with a reduction in mass of 17.00%. The calculated theoretical reduction in mass for this step is 17.57%. The calculated and measured reduction in mass corresponds to the mass of the oxime groups, which separate from the main molecule. In this step, the entire organic structure decomposes, and the remaining solid mass corresponds to the mass of NiO. These results demonstrate a strong correlation between the computed values and empirical observations. Therefore, these findings support the proposed structure of our target complex (Figure 4.14) [65, 91].

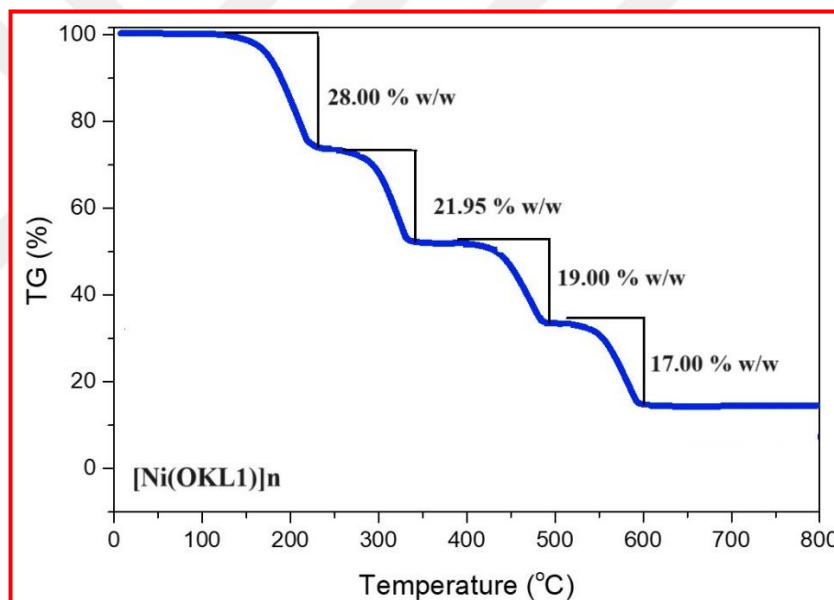


Figure 4.14. TGA-DTA curve of [Ni(OKL1)]_n complex.

Also if we examining the TGA curve of [Ni(OKL3)]_n complex, it can be observed that degradation occurred in four steps. The first degradation step occurred between 125-220 °C with a reduction in mass of 34.10%. The calculated theoretical reduction in mass for this step is 35.22%. The calculated and measured reduction in mass corresponds to the mass of the 4-bromobenzyl group, which separates from the main molecule. The second degradation step occurred between 240-325 °C with a reduction in mass of 20.21%. The calculated theoretical reduction in mass for this step is 20.53%. The calculated and measured reduction in mass corresponds to the mass of the 2-

amino-1,3,4-thiadiazole group, which separates from the main molecule. The third degradation step occurred between 405-480 °C with a reduction in mass of 17.10%. The calculated theoretical reduction in mass for this step is 17.42%. The calculated and measured reduction in mass corresponds to the mass of the diphenyl ether group, which forms the polymer chain. The polymer chain is broken in this step. The final degradation step occurred between 520-600 °C with a reduction in mass of 21.29%. The calculated theoretical reduction in mass for this step is 19.09%. The calculated and measured reduction in mass corresponds to the mass of the oxime groups, which separate from the main molecule. In this step, the entire organic structure decomposes, and the remaining solid mass corresponds to the mass of NiO. These results demonstrate a strong correlation between the computed values and empirical observations. Therefore, these findings support the proposed structure of our target complex (Figure 4.15) [65, 91].

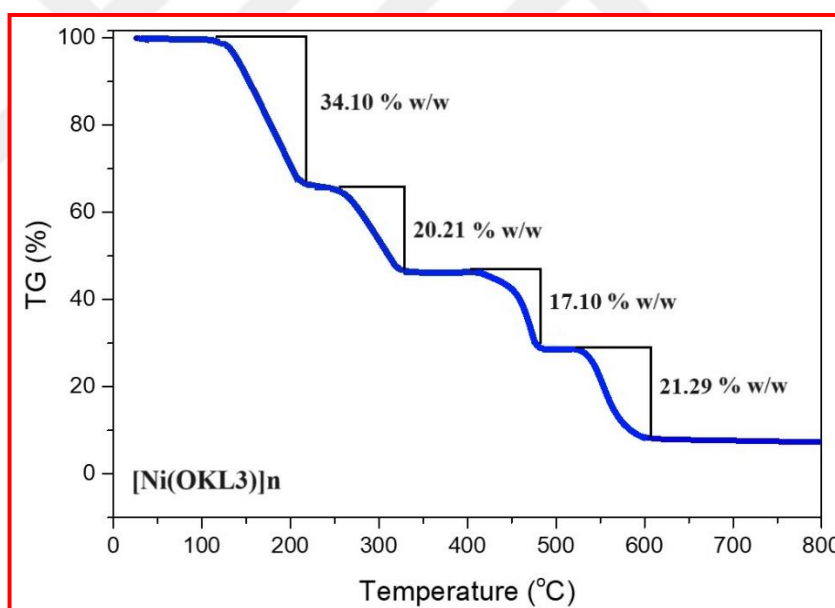


Figure 4.15. TGA-DTA curve of [Ni(OKL3)]_n complex.

PART5

CONCLUSION AND RECOMMENDATIONS

In this thesis work, three novel thiadiazole-substituted *vic*-dioxime ligands (OKL1, OKL2, and OKL3) were adeptly synthesized and meticulously characterized through the application of elemental analysis, (¹HNMR) and (¹³CNMR) spectroscopy, FTIR spectroscopy, ESI-MS spectroscopy, and thermogravimetric analysis methods. The Co⁺² and Ni⁺² complexes of these *vic*-dioxime ligands were synthesized in ethanol media. Their structures were characterized using FTIR spectroscopy and thermogravimetric analysis. The metal concentrations in all complexes were analyzed using ICP-AES spectroscopy. Their molecular geometries were judged by using magnetic susceptibility data. Thermal stabilities of some complexes were determined by using thermogravimetric analysis. It was understood that the resulting complexes showed high thermal stability. All Co⁺² complexes were found to be paramagnetic with 1 unpaired electron with low spin, and each Co²⁺ ion was characterized as an inner orbital complex with a $t_{2g}^6e_g^0$ electron configuration. The measured values can be elucidated by the delocalization of the excess electron remaining on the Co²⁺ ion because of complexation on the entire molecule through resonance. The magnetic susceptibility values were measured in the range of 1.77-1.79 BM. Similarly, the Ni(II) complexes were also paramagnetic with a high-spin 2 unpaired electron, and each Ni²⁺ ion formed an outer orbital complex with a $t_{2g}^6e_g^2$ electron configuration. The magnetic susceptibility values were measured in the range of 2.84-2.85 BM.

ESI-MS spectra were performed for all ligands. M/Z values of molecular ion peaks for ligands and their fragments obtained from these spectra were determined as 788.08 (100%), 310.11 (25%), 275.11 (53%), 214.21(42%) for OKL1; 858.55 (100%), 343.99 (57%), 275.11 (53%), 214.28 (37%) for OKL2; and 877.99 (100%), 356.03 (8%), 295.27 (56%), 275.11(43%) for OKL3, respectively. The agreement between the calculated molecular weights of the ligands and the results obtained from the mass spectra confirms the successful synthesis of the ligands.

The anticancer, antibacterial, and antifungal activities of the obtained ligands can be investigated in the future, and new ligands can be synthesized by binding other functional groups that may show anticancer, antibacterial, and antifungal activity to the central *vic*-dioxime ligands, and their antibiotic activities can be investigated.



REFERENCES

1. Chakravorty, A., "Structural chemistry of transition metal complexes of oximes", *Coordination Chemistry Reviews*, 13(1), 1-46 (1974).
2. Kukushkin, V. Y. and Pombeiro, A. J. L., "Oxime and oximate metal complexes: Unconventional synthesis and reactivity", *Coordination Chemistry Reviews*, 181(1), 147-175 (1999).
3. Krylov, I.B., Segida, O.O., Budnikov, A.S., Terent'ev, A. "Oxime-Derived Iminyl Radicals in Selective Processes of Hydrogen Atom Transfer and Addition to Carbon-Carbon π -Bonds." *Advanced Synthesis & Catalysis*, 363(10), 2502-2528 (2021).
4. Karakurt, A., Aytemir, M. D., Stables, J. P., Ozalp, M., Betul Kaynak, F., Ozbey, S., Dalkara, S. "Synthesis of some Oxime ether derivatives of 1-(2-Naphthyl)-2-(1,2,4-triazol-1-yl) ethanone and their anticonvulsant and antimicrobial activities." *Archiv der Pharmazie: An International Journal Pharmaceutical and Medicinal Chemistry*, 339(9), 513-520 (2006).
5. March, J. *Advanced organic chemistry: reactions, mechanisms, and structure* (p. 825). New York: McGraw-Hill (1977).
6. Karipcin, F., Arabali, F. "Synthesis and characterization of 4-arylamino-biphenylglyoximes and their complexes." *Journal of the Chilean Chemical Society*, 51(3), 982-985 (2006).
7. Al-Sha'alan, N.H. "Antimicrobial activity and spectral, magnetic and thermal studies of some transition metal complexes of a Schiff base hydrazone containing a quinoline moiety." *Molecules*, 12(5), 1080-1091 (2007).
8. Yaul, S.R., Yaul, A.R., Pethe, G.B., Aswar, A.S. "Synthesis and characterization of transition metal complexes with N, O-chelating hydrazone Schiff base ligand." *Am-Euras. J. Sci. Res*, 4(4), 229-234 (2009).
9. Tyler, L. J. *Ketoxime Dangers*. Chemischer Informationsdienst, 5(50), (1974).
10. Babahan, I., Poyrazolu, E., Ozmen, A., Biyik, H., and Iman, B., "Synthesis, characterization and biological activity of vic-dioxime derivatives containing benzaldehydehydrazone groups and their metal complexes", *African Journal of Microbiology Research*, 5(3), 271-283 (2011).
11. Topal, T., Kart, H. H., Tunay Taslı, P., and Karapınar, E., "Synthesis and structural study on (1E,2E,1'E,2'E)-3,3'-bis[(4-bromophenyl)-3,3'-(4-methy-

- 1,2-phenylene diimine)] acetaldehyde dioxime: A combined experimental and theoretical study", *Optics And Spectroscopy (English Translation Of Optika I Spektroskopiya)*, 118(6), 865-881 (2015).
12. Kukushkin, V.Y., Tudela, D., Pombeiro, A.J. "Metal-ion assisted reactions of oximes and reactivity of oxime-containing metal complexes." *Coordination Chemistry Reviews*, 156, 333-362 (1996).
 13. Paterson, B.M., Donnelly, P.S., "Copper complexes of bis(thiosemicarbazones): From chemotherapeutics to diagnostic and therapeutic radiopharmaceuticals", *Chemical Society Reviews*, 40(5) (2011).
 14. Bakir, M., "Electrochemical properties of the first Re(I)-carbonyl compound of di-2-pyridyl ketone.oxime (dpk.oxime), fac-Re(CO)₃(dpk.oxime)Cl, in non-aqueous media", *Journal of Electroanalytical Chemistry*, 466(1), 60-66 (1999).
 15. Dilworth, J. R., Parrott, S. J., "The biomedical chemistry of technetium and rhenium", *Chemical Society Reviews*, 27(1), 43-55 (1998).
 16. Brink, A., Jacobs, F. J., Helliwell, J. R. "Trends in coordination of rhenium organometallic complexes in the Protein Data Bank." *IUCrJ*, 9(2), 180-193 (2022).
 17. Kandaz, M., Ylmaz, I., Keskin, S., and Koca, A., "Synthesis, spectroscopy and redox properties of a novel (E-E) vic-dioxime and its mono-, di- and trinuclear complexes bearing an 18-membered N₂O₂S₂ macrocyle", *Polyhedron*, 21(8), 825-834 (2002).
 18. Yoshida, M., Kitamura, M., Narasaka, K. "Synthesis of dihydropyrrole and pyrrole derivatives by radical cyclization of γ,δ -unsaturated ketone O-acetyloximes." *Bulletin of the Chemical Society of Japan*, 76(10), 2003-2008 (2003).
 19. Abele, E. and Lukevics, E., "Recent advances in the chemistry of oximes", *Organic Preparations and Procedures International*, 32(3), 235-264 (2000).
 20. Kukushkin, V.Y., Pombeiro, A. J. L., "ChemInform Abstract: Oxime and Oximate Metal Complexes: Unconventional Synthesis and Reactivity", *ChemInform*, 30(15), 147-175 (1999).
 21. Sander, S. R., Karo, W. "Organic functional groups preparation. by AT Blomquist" 2, 268-284 (1989).
 22. Scheinbaum, M. L. "1, 2-Hydroxylamino oximes and pyrazine N, N-dioxides." *The Journal of Organic Chemistry*, 35(8), 2790-2792 (1970).
 23. Sundararajan, G., Rajaraman, D., Srinivasan, T., Velmurugan, D., Krishnasamy, K., "Synthesis, characterization, computational calculation and biological

- studies of some 2,6-diaryl-1-(prop-2-yn-1-yl) piperidin-4-one oxime derivatives", *Spectrochimica Acta - Part A: Molecular and Biomolecular Spectroscopy*, 139(1), 108-118 (2015).
24. Ladenburg, A. "Ueber die Einwirkung des Hydroxylamins auf Aldehyde und Ketone." *Berichte der deutschen chemischen Gesellschaft*, 16(2), 1406-1412 (1883).
 25. Ramalingam, S., Karabacak, M., Periandy, S., Puviarasan, N., Tanuja, D., "Spectroscopic (infrared, Raman, UV and NMR) analysis, Gaussian hybrid computational investigation (MEP maps/HOMO and LUMO) on cyclohexanone oxime", *Spectrochimica Acta - Part A: Molecular and Biomolecular Spectroscopy*, 96, 207-220 (2012).
 26. Pasca, R.D., Moldovan, A., Horovitz, O., Lupan, A., "Thermodynamic investigation of tautomerism in triazine oximes", *Journal of Mathematical Chemistry*, 55(9), 1857-1868 (2017).
 27. Li, Q., Cai, B. G., Li, L., Xuan, J., "Oxime Ether Synthesis through O-H Functionalization of Oximes with Diazo Esters under Blue LED Irradiation", *Organic Letters*, 23(17), 6951-6955 (2021).
 28. Latif, A. D., Gonda, T., Vagvolgyi, M., Kusz, N., Kulmany, A., Ocsovszki, I., Zomborszki, Z. P., Zupko, I., Hunyadi, A., "Synthesis and in vitro antitumor activity of naringenin oxime and oxime ether derivatives", *International Journal of Molecular Sciences*, 20(9), 2184 (2019).
 29. Yagnam, S., Trivedi, R., Krishna, S., Giribabu, L., Praveena, G., and Prakasham, R. S., "Bioactive isatin (oxime)-triazole-thiazolidinedione ferrocene molecular conjugates: Design, synthesis and antimicrobial activities", *Journal of Organometallic Chemistry*, 937, 121716 (2021).
 30. Finnin, M. S., Donigian, J. R., Cohen, A., Richon, V. M., Rifkind, R. A., Marks, P. A., Breslow, R., Pavletich, N. P., "Structures of a histone deacetylase homologue bound to the TSA and SAHA inhibitors", *Nature*, 401, 6749 (1999).
 31. Gomes, R. F. A., Isca, V. M. S., Andrade, K., Rijo, P., Afonso, C. A. M., "Functionalized Cyclopentenones and an Oxime Ether as Antimicrobial Agents", *ChemMedChem*, 16(18), 2781-2785 (2021).
 32. Zou, B., Zhang, S., Sun, P., Zhao, Q., Zhang, W., Zhang, X., Ran, L., Zhou, L., Ye, Z., "Synthesis of a novel Poly-chloromethyl styrene chelating resin containing Tri-pyridine aniline groups and its efficient adsorption of heavy metal ions and catalytic degradation of bisphenol A", *Separation and Purification Technology*, 275, 119-234 (2021).
 33. Peng, X., Liu, Y., Shen, Q., Chen, D., Chen, X., Fu, Y., Wang, J., Zhang, X., Jiang, H., Li, J., "BODIPY Photocatalyzed Beckmann Rearrangement and Hydrolysis of Oximes under Visible Light", *Journal of Organic Chemistry*, 87 (18), 11958-11967 (2022).

34. Sharma, R., Gupta, B., Singh, N., Acharya, J. R., Musilek, K., Kuca, K., Ghosh, K., "Development and Structural Modifications of Cholinesterase Reactivators against Chemical Warfare Agents in Last Decade: A Review", *Mini-Reviews In Medicinal Chemistry*, 15(1), 58-72 (2014).
35. Yuan, M. C., Yeh, T. K., Chen, C. T., Song, J. S., Huang, Y. C., Hsieh, T. C., Huang, C. Y., Huang, Y. L., Wang, M. H., Wu, S. H., Yao, C. H., Chao, Y. S., Lee, J. C., "Identification of an oxime-containing C-glucosylarene as a potential inhibitor of sodium-dependent glucose co-transporter 2", *European Journal of Medicinal Chemistry*, 143, 611-620 (2018).
36. Smith, J. P. "Bis and Tris Dioxime Complexes of Cobalt". The University of Manchester (United Kingdom), (1999).
37. Nag, K. and Chakravorty, A., "Monovalent, trivalent and tetravalent nickel", *Coordination Chemistry Reviews*, 33(2), 87-147 (1980).
38. Uysal, S., Coskun, A., Koc, Z. E., Ucan, M., Ucan, H. I., "Synthesis and characterization of some vic-dioxime and its mononuclear complexes", *Russian Journal of Coordination Chemistry*, 33(5), 351-357 (2007).
39. Sen, Z., Gurol, I., Gumus, G., Musluoglu, E., Harbeck, M., Ahsen, V., Ozturk, Z. Z., "Organophosphate sensing with Vic-dioximes using QCM sensors", 2127-2130 (2010).
40. J. Kassa, "Review of oximes in the antidotal treatment of poisoning by organophosphorus nerve agents," *Journal of Toxicology - Clinical Toxicology*, 40(6), 803-816 (2002).
41. Harries, C., Haga, T., "Ueber die beiden inactiven 2.4-Diaminopentane", *Berichte Der Deutschen Chemischen Gesellschaft*, 31(1), 550-551 (1898).
42. Stephanidou-Stephanatou, J., "Oxidative cyclization of some 1,3-dioximes with lead tetraacetate", *Journal of Heterocyclic Chemistry*, 22(2), 293-295 (1985).
43. Manning, D.T., Coleman, H.A., "Reaction of Hydroxylamine with 3,3-Disubstituted 2,4-Pentanediones. Formation of Novel Isoxazole Derivatives", *Journal of Organic Chemistry*, 34(11), 3248-3252 (1969).
44. Gnichtel, H. and Schönherr, H.-J., "Uber Pyrazol-N-oxide aus 1.3-Dioximen", *Chemische Berichte*, 99(2), 618-624 (1966).
45. Su, Z.F., Ballinger, J.R., Rauth, A.M., Abrams, D.N., Billingham, M.W., "A novel amine-dioxime chelator for technetium-99m: Synthesis and evaluation of 2-nitroimidazole-containing analogues as markers for hypoxic cells", *Bioconjugate Chemistry*, 11(5), 652-653 (2000).
46. Kotali, A., Papageorgiou, V. P., "The chemistry of 1,3-dioximes. A brief review", *Organic Preparations and Procedures International*, 23(5), 593-610 (1991).

47. Treibs, A., Dinelli, D., "Über einige Pyrrolderivate mit angegliedertem isocyclischem Ring. Bz-Tetrahydrindole und Cyclopentenopyrrole", *Justus Liebigs Annalen Der Chemie*, 517(1), 152-169 (1935).
48. Treibs, A., Kuhn, A., "Über Isonitroso-Ketone", *Chemische Berichte*, 90(8), 1691-1696 (1957).
49. Ferris, A. F., Johnson, G. S., Gould, F. E., Latourette, H. K., "α-Oximinoketones. V. The Synthesis of 5-Cyano-2-oximinovaleric Acid and DL-Lysine from 2,6-Dioximinocyclohexanone", *Journal of Organic Chemistry*, 25(4), 492-495 (1960).
50. Archer, C. M., Burke, J. F., Canning, L. R., Edwards, B., King, A. C. U.S. Patent No. 5,997,843. Washington, DC: U.S. Patent and Trademark Office.", (1999).
51. Lynde-Kernell, T., Schlemper, E. O., "Preparation, characterization and crystal structures of two amine-oxime rhodium complexes", *Journal of Coordination Chemistry*, 16 (4), 347-356 (1988).
52. Soldi, R., Horrigan, S.K., Cholody, M.W., Padia, J., Sorna, V., Bearss, J., Gilcrease, G., Bhalla, K., Verma, A., Vankayalapati, H., Sharma, S., "Design, Synthesis, and Biological Evaluation of a Series of Anthracene-9,10-dione Dioxime β-Catenin Pathway Inhibitors", *Journal of Medicinal Chemistry*, 58(15), 5854-5862 (2015).
53. Motaleb M.A., Selim, A.A. "Dioximes: Synthesis and biomedical applications," *Bioorganic Chemistry*, 82, 145-155 (2019).
54. Konidaris, K.F., Giouli, M., Raptopoulou, C.P., Psycharis, V., Verginadis, I.I., Vasiliadis, A., Afendra, A.S., Karkabounas, S., Manessi-Zoupa, E., Stamatatos, T. C., "Employment of pyridyl oximes and dioximes in zinc(II) chemistry: Synthesis, structural and spectroscopic characterization, and biological evaluation", *Inorganica Chimica Acta*, 396, 49-59 (2013).
55. Gonzalez, G., Kvasnica, M., Svrckova, K., Stepankova, S., Santos, J.R.C., Perina, M., Jorda, R., Lopes, S.M.M., Melo, T.M.V.D.P., "Ring-fused 3β-acetoxyandrost-5-enes as novel neuroprotective agents with cholinesterase inhibitory properties", *Journal of Steroid Biochemistry and Molecular Biology*, 225, 106194 (2023).
56. Di Tuoro, D., Portaccio, M., Lepore, M., Arduini, F., Moscone, D., Bencivenga, U., and Mita, D. G., "An acetylcholinesterase biosensor for determination of low concentrations of Paraoxon and Dichlorvos", *New Biotechnology*, 29(1), 132-138 (2011).
57. StC Black, D., Cossy, J., Stevens, C.V., "Comprehensive Heterocyclic Chemistry IV", *Comprehensive Heterocyclic Chemistry IV*, 285-471 (2021).

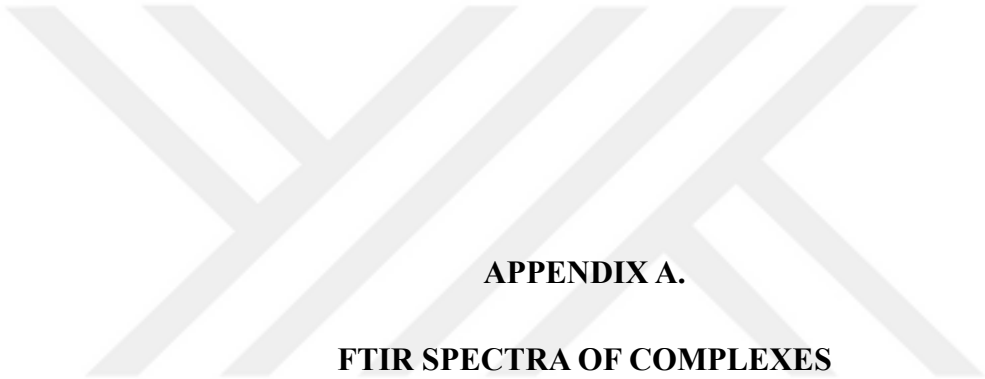
58. Doner, A., Solmaz, R., Ozcan, M., Kardas, G., "Experimental and theoretical studies of thiazoles as corrosion inhibitors for mild steel in sulphuric acid solution", *Corrosion Science*, 53(9), 2902-2913 (2011).
59. Quraishi, M. A., Wajid Khan, M., Ajmal, M., Muralidharan, S., and Venkatakrishna Iyer, S., "Influence of some thiazole derivatives on the corrosion of mild steel in hydrochloric acid", *Anti-Corrosion Methods and Materials*, 43(2), 5-8 (1996).
60. Tian, H., Li, W., Cao, K., and Hou, B., "Potent inhibition of copper corrosion in neutral chloride media by novel non-toxic thiadiazole derivatives", *Corrosion Science*, 73, 281-291 (2013).
61. Kaya, S., Kaya, C., Guo, L., Kandemirli, F., Tuzun, B., Ugurlu, I., Madkour, L. H., and Saracoglu, M., "Quantum chemical and molecular dynamics simulation studies on inhibition performances of some thiazole and thiadiazole derivatives against corrosion of iron", *Journal of Molecular Liquids*, 219, 497-504 (2016).
62. Rakitin, O.A., "1,2,5-Thiadiazoles", *Comprehensive Heterocyclic Chemistry IV*, 152230 (2021).
63. Katritzky, A.R., Ramsden, C.A., Scriven, E.F.V., Taylor, R.J.K., "Comprehensive Heterocyclic Chemistry III", *Comprehensive Heterocyclic Chemistry III*, 1-13718 (2008).
64. Janowska, S., Paneth, A., Wujec, M. "Cytotoxic properties of 1,3,4-Thiadiazole derivatives—A review," *Molecules*, 25(18), 4309 (2020).
65. Gur, M., Zurnaci, M., Altinoz, E., Sener, N., Sahin, C., Senturan, M., Sener, İ., Cavus, M., Altuner, E.M., "Novel 1,3,4-Thiadiazole Derivatives as Antibiofilm, Antimicrobial, Efflux Pump Inhibiting Agents and Their ADMET Characterizations", *Hittite Journal of Science and Engineering*, 99116 (2023).
66. A. K. Jain, S. Sharma, A. Vaidya, V. Ravichandran, and R. K. Agrawal, "1,3,4-thiadiazole and its derivatives: A review on recent progress in biological activities," *Chemical Biology and Drug Design*, 81(5), 557-576 (2013).
67. Hu, Y., Li, C.Y., Wang, X.M., Yang, Y.H., Zhu, H.L. "1,3,4-Thiadiazole: Synthesis, reactions, and applications in medicinal, agricultural, and materials chemistry," *Chemical Reviews*, 5572-5610 (2014).
68. Matysiak, J., "Biological and Pharmacological Activities of 1,3,4-Thiadiazole Based Compounds", *Mini-Reviews in Medicinal Chemistry*, 15(9), 762-775 (2015).
69. Aliabadi, A., "1,3,4-Thiadiazole Based Anticancer Agents", *Anti-Cancer Agents in Medicinal Chemistry*, 16(10), 1301-1314 (2016).

70. Raj, V., Rai, A., Saha, S., "Human Cancer Cell Line Based Approach of 1,3,4-thiadiazole and its Fused Ring: A Comprehensive Review", *Anti-Cancer Agents in Medicinal Chemistry*, 17(4), 500-523 (2016).
71. Serban, G., Stanasel, O., Serban, E., Bota, S. "2-Amino-1,3,4-thiadiazole as a potential scaffold for promising antimicrobial agents," *Drug Design, Development and Therapy*, 12, 1545-1566 (2018).
72. Anthwal, T., Nain, S. "1,3,4-Thiadiazole Scaffold: As Anti-Epileptic Agents," *Frontiers in Chemistry*, 9, 671212 (2022).
73. Karcz, D., Starzak, K., Ciszkowicz, E., Lecka-Szlachta, K., Kamiński, D., Creaven, B., Jenkins, H., Radomski, P., Miłoś, A., Ślusarczyk, L., Matwijczuk, A., "Novel coumarin-thiadiazole hybrids and their Cu(II) and Zn(II) complexes as potential antimicrobial agents and acetylcholinesterase inhibitors", *International Journal of Molecular Sciences*, 22(18), 9709 (2021).
74. Sabt, A., Abdelrahman, M.T., Abdelraof, M., Rashdan, H.R.M., "Investigation of Novel Mucorales Fungal Inhibitors: Synthesis, In-Silico Study and Anti-Fungal Potency of Novel Class of Coumarin-6-Sulfonamides-Thiazole and Thiadiazole Hybrids", *Chemistry Select*, 7(17) (2022).
75. Morsy, S.A., Farahat, A.A., Nasr, M.N.A., Tantawy, A.S., "Synthesis, molecular modeling and anticancer activity of new coumarin containing compounds", *Saudi Pharmaceutical Journal*, 25(6), 873-883 (2017).
76. Ngoc Toan, V., Dinh Thanh, N., Minh Tri, N., "1,3,4-Thiadiazoline–coumarin hybrid compounds containing D-glucose/D-galactose moieties: Synthesis and evaluation of their antiproliferative activity", *Arabian Journal of Chemistry*, 14(4), 103053 (2021).
77. Ujan, R., Saeed, A., Channar, P.A., Larik, F.A., Abbas, Q., Alajmi, M.F., El-Seedi, H. R., Rind, M. A., Hassan, M., Raza, H., Seo, S. Y., "Drug-1,3,4-thiadiazole conjugates as novel mixed-type inhibitors of acetylcholinesterase: Synthesis, molecular docking, pharmacokinetics, and ADMET evaluation", *Molecules*, 24(5), 860 (2019).
78. Gareau, Y., Juteau, H., MacKay, D. B., Friesen, R., Grimm, E. L., Blouin, M., Laliberte, S. U.S. Patent No. 7,439,260. Washington, DC: U.S. Patent and Trademark Office. " (2008).
79. Theil, E.C., Raymond, K.N., "Transition-metal storage, transport, and biomineralization", *Bioinorganic*, 1-35 (1994).
80. Noolvi, M.N., Patel, H.M. Kamboj, S., Kaur, A., Mann, V. "2,6-Disubstituted imidazo[2,1-b][1,3,4]thiadiazoles: Search for anticancer agents," *Eur J Med Chem*, 56-69 (2012).

81. Ma, D.L., He, H.Z., Leung, K.H., Chan, D.S. H., Leung, C.H. "Bioactive luminescent transition-metal complexes for biomedical applications." *Angewandte Chemie International Edition*, 52(30), 7666-7682 (2013).
82. Tian, F., Yan, G., Yu, J., "Recent advances in the synthesis and applications of α -(trifluoromethyl) styrenes in organic synthesis", *Chemical Communications*, 55 (90), 13486-13505 (2019).
83. Jacques, P. A., Artero, V., Pecautb, J., Fontecave, M., "Cobalt and nickel diimine-dioxime complexes as molecular electrocatalysts for hydrogen evolution with low overvoltages", *Proceedings of The National Academy of Sciences of The United States of America*, 106 (49), 20627-20632 (2009).
84. Al-Sabawi, E. N., Al-Janabi, A. S. M., Jerjis, H. M., Khairy, M., Alduaij, O. K., Yousef, T. A., "Synthesis, characterization, antibacterial, anticancer, and density-functional theory studies of nano-metal (II) oxime complexes", *Applied Organometallic Chemistry*, 36 (5), e6654 (2022).
85. Estevao, B. M., Vilela, R. R. C., Geremias, I. P., Zanoni, K. P. S., de Camargo, A. S. S., Zucolotto, V., "Mesoporous silica nanoparticles incorporated with Ir(III) complexes: From photophysics to photodynamic therapy", *Photodiagnosis and Photodynamic Therapy*, 40, 103052 (2022).
86. Pereira, A. L. da C., "Síntese, elucidacao estrutural e estudos in silico de novos compostos 2-amino-tiofenicos imidicos candidatos a farmacos antifungicos, antileishmanicida e antitumorais", (2019).
87. Kerkatou, R., Belahlou, H., Bouchouit, M., Berrah, F., Bouacida, S., Bouchouit, K., and Bouraiou, A., "Synthesis, characterization and structural study of two imidazole oxime ligand and their ZnII mononuclear coordination compounds", *Journal of Molecular Structure*, 1294, 136545 (2023).
88. Bouchouit, M., Belahlou, H., Guergouri, M., Bensegueni, R., Bouacida, S., Bendeif, E. E., Bouchouit, K., and Bouraiou, A., "Synthesis, characterization and structural study of new nickel (II) and mercury (II) complexes with imidazole oxime ligand", *Journal of Molecular Structure*, 1287, 135674 (2023).
89. Korkmaz, U., Findik, B. T., Dede, B., and Karipcin, F., "Synthesis, structural elucidation, in vitro antibacterial activity, DFT calculations, and molecular docking aspects of mixed-ligand complexes of a novel oxime and phenylalanine", *Bioorganic Chemistry*, 121, 105685 (2022).
90. Uysal, S. and Coskun, A., "The novel triazine cored tripodal and trinuclear Schiff base-oxime metal complexes: Their magnetic properties and thermal decompositions", *Journal of Heterocyclic Chemistry*, 48(4), 936-941 (2011).
91. Coskun, A., "The synthesis of 4-phenoxyphenylglyoxime and 4,4'-oxybis(phenylglyoxime) and their complexes with Cu(II), Ni(II) and Co(II)", *Turkish Journal of Chemistry*, 30(4), 461-469 (2006).

92. Topkaya, C.G., Cetin, E.S., Gokturk, T., Kincal, S., Hokelek, T., Gup, R. "Synthesis, spectroscopic characterization, crystal structure and biological properties of novel co-crystal copper (II) complex containing dioxime ligand". *Inorganic Chemistry Communications*, 111040 (2023).
93. Emirik, O. F., Sanlı, C., Ahsen, V., Gurek, A. G., Dedeoglu, B., "Theoretical investigation of the hydrolysis and DNA binding of platinum (II) complexes of imidazolidine dioximes", *Molecular Physics*, 121(22), e2236244 (2023).
94. Caliskan, S. G., Genc, O., Erol, F., Sarikavakli, N., "Molecular Docking, HOMO-LUMO, Quantum Chemical Computation and Bioactivity Analysis of vic-Dioxim Derivatives Bearing Hydrazone Group Ligand and Their NiII and CuII Complexes", *Gazi University Journal of Science Part A: Engineering and Innovation*, 9, 3, 299-313 (2022).
95. Alhafez, A., Savci, A., Alan, Y., Soylemez, R., and Kilic, A., "Preparation of Cu(II), Ni(II), Ti(IV), VO(IV), and Zn(II) Metal Complexes Derived from Novel vic-Dioxime and Investigation of Their Antioxidant and Antibacterial Activities", *Chemistry and Biodiversity*, 19(3), 1-13 (2022).
96. Ureche, D., Bulhac, I., Ciocarlan, A., Roshca, D., Lupascu, L., and Bourosh, P., "Novel vic-dioximes: synthesis, structure characterization, and antimicrobial activity evaluation", *Turkish Journal of Chemistry*, 45(6), 1873–1881 (2021).
97. Celik, T. A., Sarikavakli, N., Aslanturk, O. S. In vitro cytotoxic and apoptotic effect of vic-dioxime ligand and its metal complexes. *Applied Organometallic Chemistry*, 33(4), e4818 (2019).
98. Uysal, S., Coskun, A., Koc, Z.E., Ucan, H.I., "Synthesis and characterization of a new dioxime and its heterotrinnuclear BF_2^+ capped complexes", *Journal of Macromolecular Science, Part A: Pure and Applied Chemistry*, 45(9), 727–732 (2008).
99. Deswal, Y., Asija, S., Dubey, A., Deswal, L., Kumar, D., Jindal, D. K., Devi, J. Cobalt(II), Nickel(II), Copper(II) and Zinc(II) complexes of thiadiazole based Schiff base ligands: Synthesis, structural characterization, DFT, antidiabetic and molecular docking studies. *Journal of Molecular Structure*, 1253, 132266 (2022).
100. Askin, S., Tahtaci, H., Turkes, C., Demir, Y., Ece, A., Ciftci, G. A., Beydemir, S. "Design, synthesis, characterization, in vitro and in silico evaluation of novel imidazo [2,1-b][1,3,4] thiadiazoles as highly potent acetylcholinesterase and non-classical carbonic anhydrase inhibitors." *Bioorganic Chemistry*, 113, 105009 (2021).
101. Serbest, K., Dural, T., Emirik, M., Zengin, A., Faiz, O. "Heteroligand bivalent transition metal complexes with an azo-oxime ligand and 1, 10-phenanthroline: Synthesis, spectroscopy, thermal analysis, DFT calculations and SOD-mimetic activities." *Journal of Molecular Structure*, 1229, 129579 (2021).

102. Salman, W.A., "Synthesis, characterization, and biological activity for a new ligand 2,5-bis[(Butan-2-ylidene)hydrazinyl]-1,3,4-thiadiazole with some transition metal complexes", *International Journal of Drug Delivery Technology*, 11(3), 711-715 (2021).
103. Erdogan, M., Kiyamaz, K., Tahtaci, H., Uysal, S., "Synthesis and characterization of the Co(II) and Ni(II) complexes of 1,3,4-thiadiazole-derived ketones and secondary alcohols: thermal and magnetic properties", *Journal of Coordination Chemistry*, 74(15), 2508-2533 (2021).
104. Freitas, R.H.C.N., Barbosa, J.M.C., Bernardino, P., Sueth-Santiago, V., Wardell, S.M.S.V., Wardell, J.L., Decoté-Ricardo, D., Melo, T.G., da Silva, E.F., Salomão, K., Fraga, C.A.M., "Synthesis and trypanocidal activity of novel pyridinyl-1,3,4-thiadiazole derivatives", *Biomedicine and Pharmacotherapy*, 127, 110162 (2020).
105. Coskun, A. Yilmaz, F., "Synthesis and characterization of 4-(alkylaminoiso nitrosoacetyl)diphenyl ether and some of their metal complexes", *Turkish Journal of Chemistry*, 32(3), 305-312 (2008).



APPENDIX A.
FTIR SPECTRA OF COMPLEXES

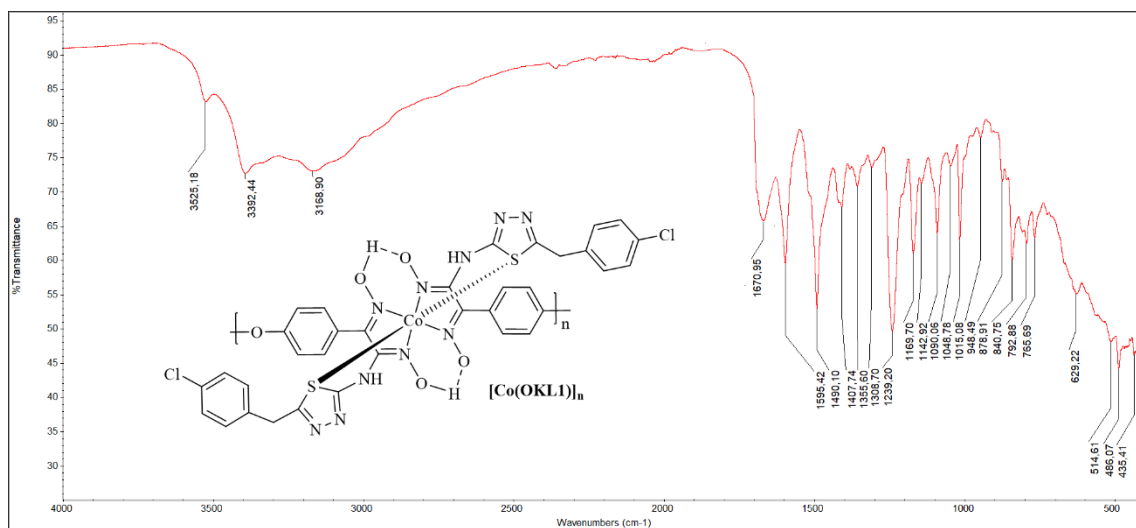


Figure A.1. FTIR Spectrum of $[\text{Co}(\text{OKL1})]_n$ complex.

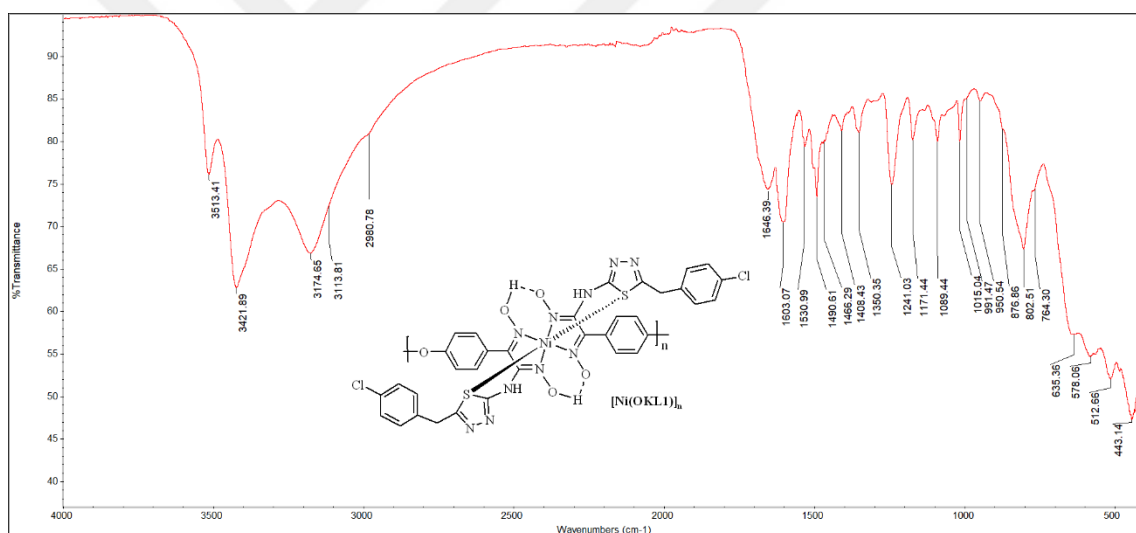


Figure A.2. FTIR Spectrum of $[\text{Ni}(\text{OKL1})]_n$ complex.

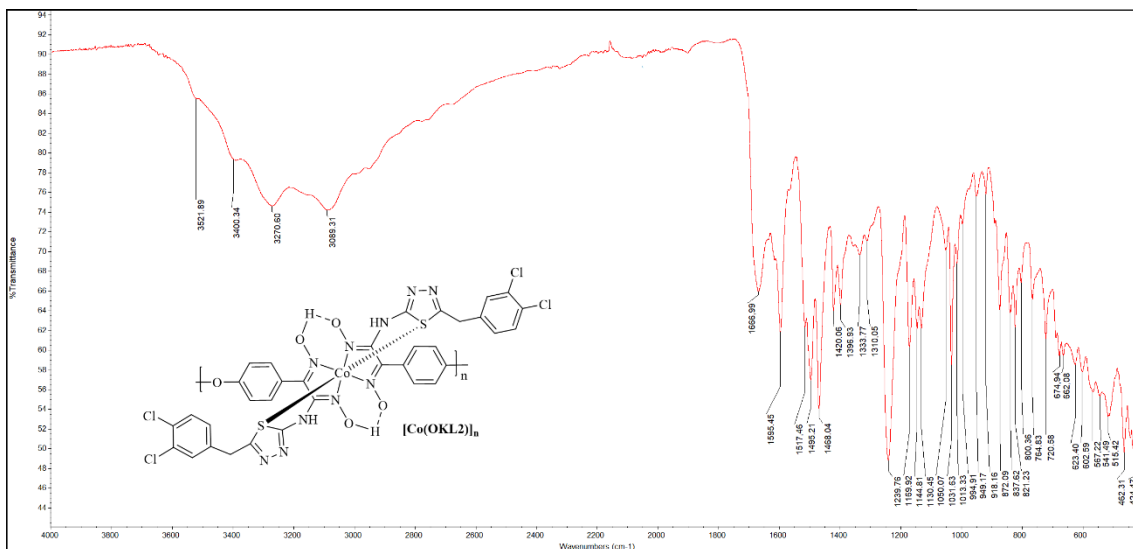


Figure A.3. FTIR Spectrum of $[\text{Co}(\text{OKL}2)]_n$ complex.

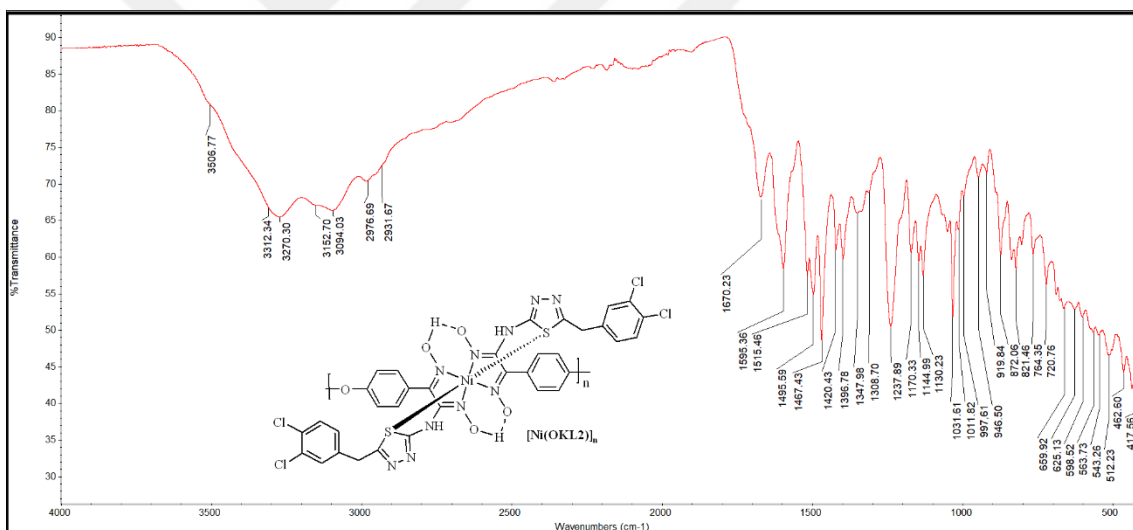


Figure A.4. FTIR Spectrum of $[\text{Ni}(\text{OKL}2)]_n$ complex.

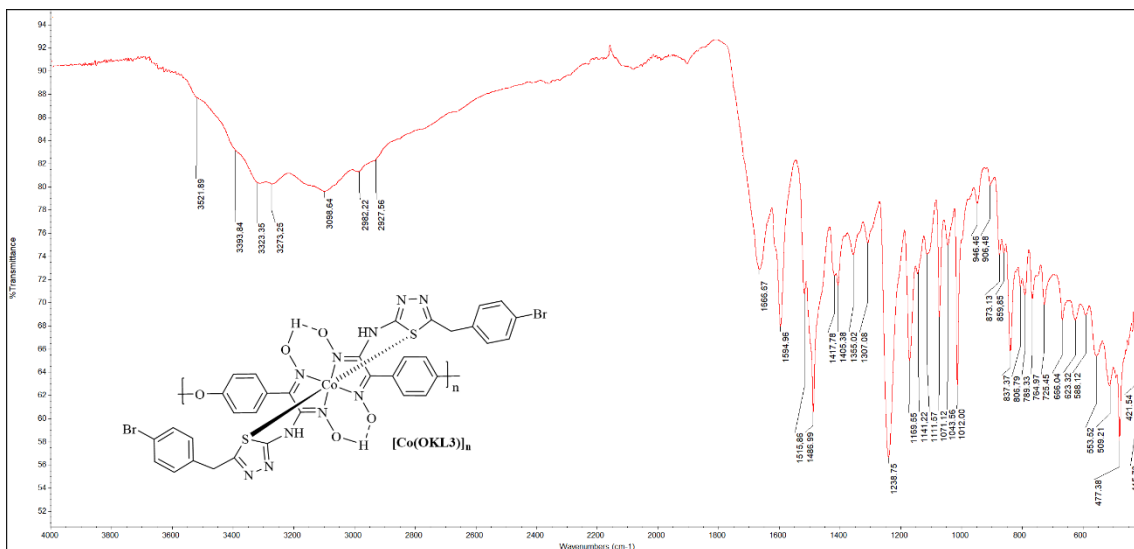


Figure A.5. FTIR Spectrum of $[\text{Co}(\text{OKL3})]_n$ complex.

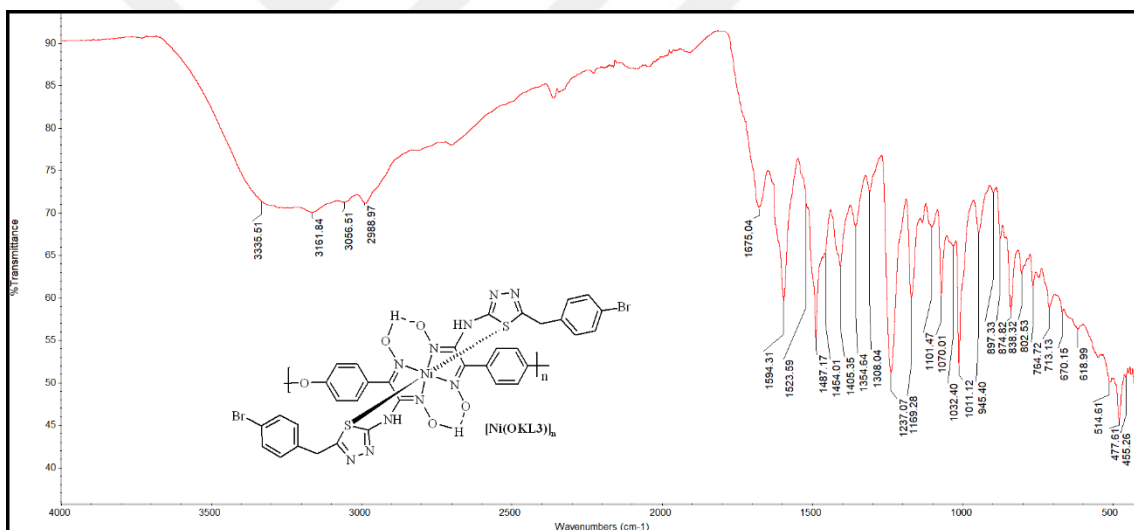


Figure A.6. FTIR Spectrum of $[\text{Ni}(\text{OKL3})]_n$ complex.

RESUME

Omar Khalid Abdulkareem AL-QARAGHULI graduated from Al-Markaziya High School for Boys, Baghdad in 2010. I started my undergraduate studies at the Faculty of Education at Al-Iraqia University, Department of Chemistry, in 2011 and graduated in 2015. I work as a teacher at Sahib Al-Buraq High School. I started my master's studies at the Department of Chemistry at Karabuk University, Turkey, in 2022.

